CR 137548
AVAILABLE TO THE PUBLIC

(NASA-CR-137548) A METHOD FOR DETECTING STRUCTURAL DETERIORATION IN BRIDGES (Nielsen Engineering and Research, Inc.) 94 p HC $7.75 CSCL 13F

N74-32346

Unclas
G3/32 46693

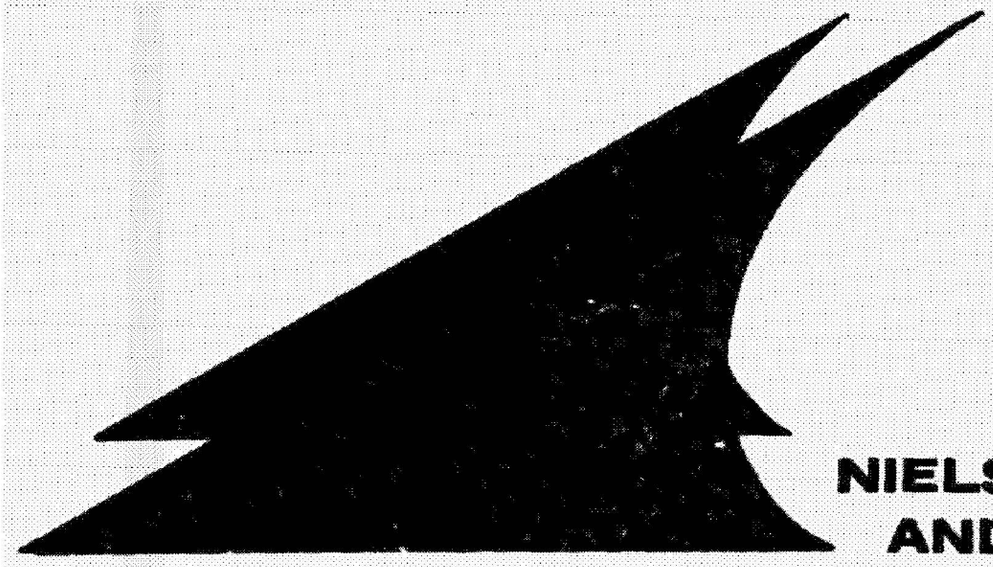

NIELSEN ENGINEERING AND RESEARCH, INC.

OFFICES: 510 CLYDE AVENUE / MOUNTAIN VIEW, CALIFORNIA 94043 / TELEPHONE (415) 968-9457

COPY NO. 14
CR 137548
AVAILABLE TO THE PUBLIC

A METHOD FOR DETECTING STRUCTURAL DETERIORATION IN BRIDGES

by

H. A. Cole, Jr. and R. E. Reed, Jr.

NEAR TR 71

July 1974

Prepared under Contract NAS2-7695

by

NIELSEN ENGINEERING & RESEARCH, INC.
Mountain View, California

for

Ames Research Center

NATIONAL AERONAUTICS AND SPACE ADMINISTRATION

and

Offices of Research and Development

FEDERAL HIGHWAY ADMINISTRATION

ACKNOWLEDGEMENT

The authors would like to acknowledge the contributions to this program made by both FHWA and NASA personnel. The laboratory study which produced the recorded time histories of fatigue tested beams was conducted by Dr. Karl H. Frank at the FHWA Fairbank Highway Research Station at McLean, Virginia. Dr. Frank contributed many useful suggestions throughout the project. Also, NASA-Ames personnel under the technical monitor, Mr. David H. Brocker, were most cooperative in providing access to computer facilities and field instrumentation.

DING PAGE BLANK NOT FILMED

TABLE OF CONTENTS

Section	Page No.
SUMMARY	1
INTRODUCTION	1
SIGNATURE CONCEPTS	2
MEASUREMENT OF SIGNATURES	3
Field Test	4
Time histories	4
Frequency content	5
Randomdec signatures	5
Fairbank Laboratory Test	6
Beam No. 1	6
Crack detection on Beam No. 1	7
Beam No. 2	8
Crack detection on Beam No. 2	9
Crack history of Beam No. 2	9
Signature differences	10
CONCLUSIONS	12
APPENDIX A - ANALYSIS PROCEDURE	14
APPENDIX B - INSTRUMENTATION	17
APPENDIX C - AUXILIARY OBSERVATIONS	19
REFERENCES	21
TABLES I THROUGH III	22
FIGURES 1 THROUGH 60	25

A METHOD FOR DETECTING STRUCTURAL DETERIORATION IN BRIDGES

By H. A. Cole, Jr. and R. E. Reed, Jr.
Nielsen Engineering & Research, Inc.

SUMMARY

The problem of detecting deterioration in bridge structures is studied with the use of Randomdec analysis. Randomdec signatures, derived from the ambient bridge vibrations in the acoustic range, were obtained for a girder bridge over a period of a year to show the insensitivity of the signatures to environmental changes. A laboratory study was also conducted to show the sensitivity of signatures to fatigue cracks on the order of a centimeter in length in steel beams.

INTRODUCTION

A problem receiving increasing attention among bridge engineers is the detection of failure producing flaws in bridges. Some types of flaws become quite large and visible before serious trouble occurs. However, other types can cause catastrophic failure or lead to costly repairs after reaching, over a period of years, a critical size which is small enough to have escaped detection. For example, the Tacoma Narrows bridge had an overall design "flaw" that was spectacularly apparent before actual failure occurred. On the other hand, the Point Pleasant bridge in West Virginia suddenly collapsed, killing 46 people, after an undetected crack had grown to its critical length of about one quarter of an inch. It is the detection of these small flaws during their slow growth stage that is of interest here. Except for isolated cases, the only method of detection currently being used is visual inspection. Obviously, many flaws that are hidden by paint, overlapping members, inaccessible locations, etc., escape detection. There are sophisticated methods for detecting flaws such as x-rays, ultrasonics, etc., but no method has been developed to the point where it is economically and physically practical to use on large structures such as bridges.

A possible solution to the bridge inspection problem, called "Randomdec" analysis, has been under study in a one-year program jointly sponsored by FHWA and NASA. In this program the ambient variations of the bridge

structure due to random forces of traffic and wind are analyzed by a special purpose computer to obtain a signature. This signature is then used as a standard of comparison for detecting deterioration in the bridge structure. For such a method to be practical, the variations in the signature due to changes in environmental conditions must be much smaller than those due to cracks and structural degradation. In order to see if "Randomdec" analysis could fulfill this requirement, two parallel test programs were conducted; a field study to test the effects of environmental changes on signatures, and a laboratory study to test the sensitivity of signatures to fatigue cracks.

In the present report a short section on the concept of Randomdec analysis is given first, followed by a section on the field tests, a section on the laboratory tests, and finally, conclusions and recommendations. Details of analysis and instrumentation are given in appendices.

SIGNATURE CONCEPTS

It is well known that the ambient forces applied to a bridge are statistical in nature and that the resulting vibrations are random. Examples of the randomness (i.e., arrival times of traffic, roadway roughness and vehicle noise) are given in references 1, 2, and 3. If the vibration of a point on a bridge is measured with an accelerometer, a curve such as shown in figure 1(a) is obtained. This curve is random, which infers that, no matter how many times the measurement is repeated, the same curve will not be obtained again. Hence, it cannot be used as a "signature" for detecting changes in the bridge.

The problem of making sense out of random signals has been explored to great depth in communications theory, and as explained in references 4 and 5, random time histories such as figure 1(a) may be transformed into a meaningful signature by plotting the absolute squared amplitudes of the sinusoidal components versus frequency. This signature, called power spectral density, as shown on figure 1(b) has peaks which correspond to the natural frequencies of the structural modes and bandwidths which are related to the structural damping. This technique has been applied to suspension bridges in reference 6 to obtain natural frequencies and damping of the lower structural modes. Small flaws have little or no effect on the lower structural modes, and hence, this information is not of much use

for failure detection. If the power spectral density is extended into acoustical frequency ranges, where flaw effects would be expected, the peaks become very close together and many spurious peaks appear so that detection of any change due to a flaw becomes extremely difficult.

Another signature which can be extracted from the random data is called Randomdec (fig. 1(c)) and was developed in wind-tunnel tests of dynamic models for on-line measurement of damping in a random turbulent airflow. As described in reference 7, this signature was found to be quite repeatable in the acoustic frequency range as well as very sensitive to flaws. It was observed that flaws caused large changes in the shape of the signatures in the acoustic frequency range as shown in figure 1(c). The signature is obtained by bandpass filtering the time history and then averaging all time segments which start at a given constant initial value, y_s (or $\ddot{y}_s$ if the time history is acceleration). This gives a signature which has the same dimensions as the original time history and which can be interpreted as the free vibration curve of the structure with an initial value, y_s (or $\ddot{y}_s$), at the measurement point. Details of analysis are given in Appendix A.

Of course, there are many other possible signatures which could be extracted from random data. For the present purpose, detection of a flaw in a structure, the Randomdec signature appears to have the properties needed.

MEASUREMENT OF SIGNATURES

In this section measurements taken in field tests and the laboratory are described. The general procedure followed is shown on figure 2. Excitation in the field test was provided by the normal traffic flow, wind and ambient noise. In the laboratory, random excitation was simulated by an electrodynamic shaker. As shown in figure 2, data handling was the same in both cases. The outputs from accelerometers were recorded on magnetic tape and then were analyzed either on a standard digital computer using software or on a special purpose computer. Discussions of the two methods is given in Appendix A.

Field Test

A typical highway girder bridge was instrumented in the field to determine if the magnitude and frequency of the vibrations were sufficient for analysis and to determine if standard signatures were subject to change due to effects other than cracking, such as environmental variations. With permission of the California State Division of Highways, one girder of a 5-span bridge located at the intersection of Highway 85 and 101, see figure 3, was instrumented with accelerometers and monitored periodically for a year. Figure 4 shows the span selected. One interior girder of the four comprising the span as well as a diaphragm was instrumented as shown in figure 4 and described in Table I. The span of the welded girder is 17 meters and its depth 2.28 meters. It is of noncomposite design and fabricated of A36 steel.

The accelerometers were attached to the girder by first gluing a cementing stud to the girder and then screwing the accelerometer onto the stud. The studs were left in place throughout the contract and the rest of the field equipment was removed after each test. Each transducer measured acceleration normal to its mounting surface. Details of the field instrumentation are given in Appendix B.

Records were obtained about once a month with a total of eleven tests being conducted. Table II gives a summary of the individual test conditions. Record lengths were determined by counting 100 vehicles. This gave 4 to 10 minutes of record which was sufficient for analysis. The average vehicle speed was 50 mph and about 5 percent of the traffic was trucks.

Time histories.- Some 20 millisecond samples of typical data are shown on figure 5. The random nature of the data created by traffic inputs is apparent. These data differ from the laboratory data in that the vibrations occur in bursts followed by quiet periods as compared to the more stationary level of the laboratory outputs. Because of this, the field data presents a more difficult problem in recording and analysis. With heavy trucks the accelerometer peak output voltage was as high as 6 volts and in quiet periods peak voltages were typically as low as 5 millivolts giving a dynamic range exceeding 60 decibels. Since the magnetic tape recording saturates at 1.4 volts, data were also recorded on a channel attenuated by a factor of 10. Several factors may contribute to the extreme nonstationary behavior of these data. First, the traffic is one way and often of low

density so that the direction and frequency of inputs is limited. Second, the bridge has simple spans and primary inputs only occur when vehicles are on the span being measured. It might be expected that data on bridges with more sources of inputs (i.e., two-way traffic, continuous spans, wind excitation, etc.) would be of a more constant level.

Frequency content.- Typical power spectral densities of the field data are shown on figure 6. The level of signal at web locations such as Station 6 was generally about 7 db higher than the level at flange locations such as Station 8. The multiple peaks mentioned in the section on "Signature Concepts" are apparent. Before taking Randomdec signatures it is useful to examine the spectra to decide on the frequency range to be filtered for Randomdec signatures. Generally, filter settings are selected to remove the frequency ranges in which the flaw is expected to have little effect. In the present test, the low frequency modes were removed by a high-pass filter set at 1 KHz and high frequency instrumentation noise was removed by a low-pass filter set at 10 KHz which was the upper limit of the FM tape recording. More details on filtering are given in Appendix A.

Randomdec signatures.- The signatures taken throughout the year are shown on figure 7 for each station, and all the environmental conditions are given in Table II. Examination of the signatures shows that each station has a characteristic form which is easily recognized. All signatures have the same time scale (horizontal axis) and the length of each signature is 0.01 second. Repeatability of the signatures appears quite good and the variations over the year are sufficiently small to allow detection of flaws. A possible exception is Station 2, (fig. 7(b)), which was located on the flange which bears on the concrete deck. The signal obtained from this station was lower than the others and as may be seen, the signature was much less oscillatory. The lack of oscillations in the signature may be a result of the damping of the flange by the concrete deck. The variability over the year may be due to variations in the friction between deck and flange or cracks opening in the deck.

The only significant difference in signatures which occurred was in Test No. 6 which was taken during the heavy commute traffic in the morning. Some of the data were taken with the traffic bumper to bumper and the signatures obtained from these are marked with an asterisk. For this condition the signal levels were much lower than usual and amplification

during analysis had to be increased by a factor of 10, to reach the y_s level of the Randomdec. This raised the noise level which resulted in some noisy signatures, particularly Station 7, figure 7(g). These problems could probably be overcome by using amplifiers with lower noise levels or by averaging the signatures over a longer period of time, but it would be sounder practice to reject the signature if the excitation level were not high enough to give the same initial value of y_s. By holding y_s constant for all signatures, changes in the signature due to amplitude are avoided.

No effect on any signature is apparent from changes in temperature or for a wet versus dry concrete deck. However, more severe climate variations should be studied. Also, a 4.5 magnitude earthquake on the San Andreas Fault occurred in November with no apparent effect. The mounting stud at Station 2 came loose at the beginning of the January test. The accelerometer was hand held for that test and the stud was then reglued. This signature is marked by a double asterisk.

Fairbank Laboratory Test

The purpose of the laboratory test was to determine the sensitivity of Randomdec signatures to fatigue cracks. To accomplish this, Dr. Karl Frank at the Federal Highway Administration Fairbank Research Station near Washington, D. C. tested two 10-foot simply supported (12WF40) beams. Each beam was cyclically loaded as shown on figure 8 to produce fatigue cracks (see ref. 8). At various stages before and during crack formation, accelerometer records were taken and sent for analysis as was shown on figure 2. On Beam No. 1, a crack was started by a sawcut in the flange near the accelerometer in order to find out effects of crack length on detection. Beam No. 2 differed from Beam No. 1 in that it had welded coverplates and cracks were not started, but were allowed to develop naturally. The crack growth was documented, but was not revealed until after the Randomdec analysis was complete in order to test the ability of the method to detect an unknown crack from the random data. Results and discussion of the two beam tests follows.

Beam No. 1.- Figure 9 shows the beam configuration, location of accelerometers, the sawcut which started the crack, and two shaker locations. All tests were run with the shaker at the centerline on the coverplate and at the image in order to excite symmetrical as well as antisymmetrical

modes. This was done to insure that the crack region would be excited by one location or the other. Even with random vibrations, it has been shown, see reference 9, that a single point excitation of a plate produces regions of low excitation in patterns similar to Chladni's patterns for sinusoidal vibration. Of course, on a real bridge the inputs occur at many different points so a crack zone would almost certainly be excited.

Excitation of the stations with the shaker at the image and centerline were checked by calculating power spectral densities as shown on figures 10 and 11. The image point provided response distributed over a somewhat wider bandwidth than the centerline point. Spectra for response at Stations 3 and 4 are shown on figures 12 and 13 and it may be seen that response up to 12 KHz was provided at all stations. It may be noted that the spectra in the laboratory test differ in appearance from those shown for the field test. The reason for this is that the field data have a much higher content at low frequencies than the laboratory data and a logarithmic scale (decibels) had to be used to cover the dynamic range. The laboratory data on figures 10 to 13 are plotted on linear scales to show the structural mode peaks more clearly. For comparison purposes it may be noted that on figure 10 the peak to valley range of the highest peak is about 10 db which is comparable to the highest peaks to valley ranges on figure 6. Since the low frequency content is filtered out when signatures are obtained, it was felt that the laboratory excitation was a reasonable approximation to field excitation.

Crack detection on Beam No. 1.- Signatures of the random data for the following conditions of the beam were taken.

Test No.	Fatigue Cycles	Crack Length (Including Sawcut)
1	0	No Crack
2	0	0.54 cm
3	669,420	1.35 cm
4	777,000	2.41 cm
5	837,000	3.91 cm
6	881,000	10.0 cm (1/2 of flange width)

To show the effect of the crack only, Test No. 2 with the sawcut was selected for a standard. On figure 14, results from tests Nos. 3, 4, and 6

are shown superimposed on the standard. The filter used in this case was 10,250 to 15,000 Hz which only looked at the very highest frequencies contained in the spectra. The length of the signatures for Beam No. 1 is 0.00125 second. To judge these results, it should be remembered that the standard obtained from Test No. 2 could be almost exactly repeated, even though different time intervals were used (see Appendix A). It may be seen that the 1.35 cm crack caused an easily measurable change in the signature at this station, and that the 10 cm crack caused a very large change. The 2.4 cm crack, on the other hand, although larger than the 1.35 cm crack, showed much less change in the signature. These results seem to indicate that the sensitivity of the signature to a crack depends on more than the crack length.

In discussion with Dr. Karl Frank on these results, it turned out that for the 2.41 crack, the crack had apparently closed up, due to local stress changes when the beam was unloaded for the random test. Although these observations are based on a limited sample, it may be tentatively stated that the state of stress at the crack is a factor in the sensitivity of the signature. The fact that the 10 cm signature played such a large change is not necessarily significant because the accelerometer was mounted so close to the crack.

Signatures obtained with a wider filter bandwidth for all of the stations are shown on figures 15, 16, 17, and 18. A clip gage (an 8 gram transducer to measure crack length) added to the beam produced a change in the signature so the clip gage plus sawcut should be used as a standard of comparison. Comparison of this standard with the cracked conditions shows rather small changes in all cases except the 10.0 cm crack which shows large changes for all stations. Stations 3 and 4, which were across the crack from the shaker, show more change than Stations 1 and 2 for the 1.35 to 3.9 cm cracks. As mentioned above, there were indications that the 2.41 and 3.91 cm cracks closed up when the fatigue load was removed. A closed crack with compressive stress across it would probably only effect a signature if there was a slippage in shear on the crack surface. Instead of pursuing these effects further, testing of Beam No. 2, a more realistic test, was begun.

Beam No. 2.- As shown on figure 19, Beam No. 2 differed from Beam No. 1 in that it had welded coverplates. The test procedure was the same

except that the cracks were allowed to develop naturally from the cyclic loading. For the random excitation, three loading locations, A, B, and C, were selected to give adequate excitation to the crack regions which were expected to be near the welds. Stations 1 through 6 were selected for accelerometer measurements to provide both near and far measurements. As mentioned previously, the knowledge of the time, size, and location of cracks was kept separate from the analysis to provide an unbiased test of the method. Of course, the location of the cracks was expected to occur at the toe of the welds.

Crack detection on Beam No. 2.- Standards were first established for all accelerometer locations and shaker inputs using a filter bandwidth setting of 8,000 to 15,000 Hz with only 2,000 load cycles on the beam and no cracks. The length of the signatures shown for Beam No. 2 is 0.00125 second. Comparisons of the standards with signatures taken after 300,000 load cycles are shown on figure 20, for Station 2 near the weld and on figure 21 for Station 6 away from the weld. The large change in signatures is apparent. The decision to predict a crack from a signature change is much more difficult when the crack history is unknown, and especially, as in this case, when a crack was not expected at 300,000 cycles. Before predicting a crack from the results on figures 20 and 21, the standard was repeated to make sure that a change had not occurred in the electronics. When this checked out, it was concluded that a crack had developed in the beam. As will be seen below, for this condition, it turned out that there was a 1.9 cm crack at the toe of the welds near Station 4, and 0.5 cm cracks near Stations 1 and 2.

Crack history of Beam No. 2.- Although most of the analysis and predictions given below were completed without knowledge of the crack history, definition of the cracks at the various stages of fatigue loading are given here so that comparison of signature changes and crack changes can be made. Crack sizes are as shown on the following page. Impressions taken after Test No. 5 are shown on figure 22.

TEST	FATIGUE CYCLES	CRACK SIZE, CENTIMETERS STATION NO. 1*	STATION NO. 2	STATION NO. 3	STATION NO. 4
1	2,000	None	None	None	None
2	300,000	0.5	None	0.5	1.90
3	400,000	0.8	0.3	0.8	2.2 (thru flange)
4	433,000	1.5	0.6	1.9	6.6
5	442,000	2.1	1.37	2.5	11.4

Signatures were obtained for each station, each shaker location and each test for a total of 120 signatures. For documentation purposes, these are shown in figures 23 through 49 where each figure shows one station, one shaker location and all five tests. It is difficult to see variations in signatures so examples of pairs of successive tests superposed are shown in figures 47 through 49 for Stations 1, 4, and 6 with the shaker at A. Of Stations 1 to 4, which are close to the cracks, Station 1 showed the least change and Station 4 showed the most change. Station 6 is an example of a station some distance from the cracks.

Signature differences.- In order to numerically evaluate the difference between signatures, the differences between peaks and valleys of superposed signatures were measured and summed to give a numerical value. This method, was used to develop Table III. Although this procedure seemed satisfactory for the present illustrative purposes, it remains to develop a reliable method for numerically evaluating differences between signatures. Another way to compare them would be to compare the standard to each succeeding test. Comparison of successive pairs of tests was used here because the influence of incremental changes in crack lengths was of interest. The histogram in figure 50 shows the distribution of difference factors for the three shaker locations. Although differences can depend on shaker location, there is no significant trend apparent between the locations.

Before the crack history was known, the signatures were studied to see what could be predicted about the cracks. The following preliminary observations were stated.

*The location refers to fillet weld toe adjacent to accelerometer with corresponding number. The size refers to length on outside flange surface along weld toe.

1. The change in signatures depends on the shaker location. This emphasizes the advantage of using ambient excitation which is supplied through many points.

2. Shaker location A produced slightly more change although the difference (about 10 percent) between A, B, and C is probably not statistically significant.

3. The comparisons that showed the largest changes, considering all the stations, were the standard to 300,000 and 400,000 to 433,000 cycle comparisons. The 300,000 to 400,000 cycle comparison showed the smallest change.

4. The station showing the largest change, considering all comparisons, was Station 4 and the largest single change occurred at Station 4, shaker location A, comparison 400,000 to 433,000 cycles. Among the four stations close to the coverplate (Sta. 1 to Sta. 4), Station 1 showed the least change.

5. All stations show changes which indicates that flaws can be detected at least a meter away.

When the crack history became available, considerable study was done and the resulting conclusions were:

1. It is difficult to say which step represented the largest change but certainly the least change occurred during the 300,000 to 400,000 cycle period. Each crack grew about 0.25 cm and this produced changes at all stations although some of the changes were quite small. For this configuration, therefore, a crack at least 0.25 cm in length can be detected.

2. Station 2 had the smallest final crack with Station 1 next. It is surprising that a large difference was registered at Station 2 at 300 K without a crack nearby. Station 4 had the largest crack which was apparent from the signatures. However, except for possibly an accelerometer very close to a crack, no correlation could be found which would indicate the location or size of cracks. Clearly, this is an area in which important work can be done.

3. Signature changes were registered at all stations indicating that cracks could be detected at any location within distance of a meter. The variation of signature change with distance was not sufficient to estimate the maximum distance versus flaw size relationship.

4. Cracks induce changes in signatures over a wide frequency bandwidth and at generally lower frequencies than first suspected.

In order to explain the above statements, the mechanism by which cracks influence signatures must be understood. Originally, the hypothesis was that a crack introduced new degrees of freedom and produced a local resonance that would decrease in frequency as the flaw grew in size. However, the frequency of such a resonance for a crack of, say, 0.25 cm in length would be much higher than 15 KHz and would not be detectable with the record being low-pass filtered. In order to explain the sensitivity of the method, an additional mechanism must be present. The fact that cracks are detected 100 or more crack lengths away suggest that traveling waves are emitted from the crack in a repeatable sequence following the time the bias level, y_s, occurs. One hypothesis is that opening and closing or rubbing in shear of the crack surface emits signals that are related in phase and frequency to the vibration of the crack region. These signals (acoustic waves) are transmitted with low dissipation throughout the beam and, therefore, are detectable over a widespread area.

Once the actual mechanism, be it the above hypothesis or another, is understood; perhaps the changes in signatures can be deciphered to give information on locating cracks and determining their size.

CONCLUSIONS

This study has yielded positive results and considerably advanced the level of understanding and confidence of Randomdec analysis. The main conclusions are the following.

1. Changes in crack length as small as 0.3 cm in a coverplated girder can be detected at distances of at least a meter at frequencies less than 15 KHz.

2. The frequency content of the response of bridges to wind and traffic, as measured on a typical girder bridge, appears to be sufficient for crack detection.

3. The signatures of the girder bridge with normal traffic remained stable with no significant changes over a period of a year. Temperature and weather conditions at the time records were obtained varied from 40°F to 80°F and rainy to clear weather.

4. The main purpose of this study, to demonstrate the feasibility of Randomdec analysis, was accomplished. However, the application of Randomdec as an economical, practical flaw detection method remains to be demonstrated. A variety of bridge structures with actual and simulated flaws, must be studied to determine the sensitivity of the method; analytical and experimental work have to be done to understand the mechanism of crack detection; and procedural guidelines and costs have to be established for potential users.

APPENDIX A

ANALYSIS PROCEDURE

The basic idea of Randomdec analysis is straightforward. The time history is divided into short equal length segments, each of which begins at the same amplitude y_s and an alternating positive or negative initial slope as shown in figure 51. These segments are averaged to give the signature which is a plot of the measured dependent variable (i.e., acceleration, velocity or displacement) as a function of time. The length in time of the signature is the same as the segment length. The signatures for two extreme types of data are useful to know for reference purposes. If the record is white noise, the signature is zero except for the initial spike of amplitude y_s. If the response of a damped, single-degree-of-freedom system to white noise is analyzed, the signature is a damped cosine wave which is the free vibration decay curve of the oscillator subjected to an initial displacement y_s.

As was indicated on figure 2, the analysis was implemented on a general purpose digital computer and on an on-line Randomdec computer. Both methods have advantages and disadvantages. The software approach requires digitization of the data. Once this is done, the process is digital so accuracy and repeatability of calculations is assured. Also, the data is available for other types of analysis. The accuracy of the digitization process is limited, however, by practical limitations such as computer storage, amplitude quantization, and digitization rates. The sample rate available for this work was 1,000 points per second. The laboratory tests were recorded on a standard FM analog instrumentation tape recorder at 60 ips and could be played back at 1-7/8 ips so the maximum effective sample rate was 32,000 points per second. A frequency of 16 KHz, therefore, is the upper limit that could be distinguished, but time histories at or near this frequency are poorly represented digitally since only 2 points per cycle exist. Frequencies in the range of 10 to 15 KHz were of interest in the laboratory study so significant errors were possible. If signatures are desired for a wide range in frequency, one may have to digitize several times. Low frequencies require a long record length but can tolerate a low digitizing rate whereas high frequencies need only a short record but a high digitizing rate. The only compatible

combination is a long record digitized at a high rate which may be more costly than separate digitized records. In cases where the excitation is somewhat intermittant, say, light traffic on a bridge, it is usually convenient to digitize the entire record rather than separating out the low amplitude portions occurring when no traffic is present. This results in digitizing a large amount of data that is not analyzed since Randomdec analysis uses only that data which occurs above a certain amplitude (y_s).

The "ON-LINE RANDOMDEC COMPUTER" is a hybrid computer which performs the filtering and segment selection on the analog signal, then converts the analog signal to digital form for averaging. The input is the analog tape containing the time history. This process avoids digitizing errors but is susceptible to variations in analog equipment. When monitoring a structure over a long period of time, equipment calibrations should be checked periodically to ensure repeatability. A comprehensive way of checking the calibration of the system is to have a standard tape and the corresponding signatures for different filter settings. Periodically, this tape can be re-analyzed and the signatures compared. The advantage of the on-line system is the ease of operation. With no input to prepare, no turnaround time and visual display, many runs and comparisons can be made quickly. In the Ames system, two signatures could be displayed and superposed for convenient comparisons.

Regardless of which computer system is used, several parameter choices have to be made. The time history is usually filtered is isolate certain frequency ranges. For instance, as may be seen on figure 52 which shows the signature of an unfiltered signal from field tests, the large amplitude low frequency components are superposed on the high frequency components which contain the flaw information. Thus, if a small flaw is to be detected, a high-pass filter should be used to filter out the large amplitude low frequencies which can mask the effects of small flaws and a low-pass filter should be used to eliminate high frequency noise. The filter bandwidth should encompass one or more peaks of the response spectrum. If the response spectrum is flat in the filtered range, the signature resembles that of white noise for wide bandwidths but appears more meaningful as the bandwidth narrows. However, this damped sinusoidal appearance is due only to the filter characteristics. An example of this is shown in figure 53 where white noise is band-pass filtered with the given bandwidth. As the bandwidth narrows, as a percent of center frequency, the distortion

becomes more severe. When the filter bandwidth is twice the center frequency (1 to 4 KHz), the filter induces a half cycle of significant distortion. However, when the bandwidth is about 25 percent of the center frequency, the filter induces three cycles of distortion. Even if the response is peaked within a narrow filter bandwidth, the signature will be distorted by the filter. Choosing proper filter bandwidth to minimize distortion but maximize certain signature characteristics is a problem that deserves more study.

Another parameter to be chosen is the initial amplitude, y_s, (bias level) of the signature. There are practical reasons for not choosing either very low or very high values. The signal-to-noise ratio decreases as the amplitude of vibration decreases so a low bias level can produce distorted signatures. On the other hand, very high values require much more data since few large amplitude peaks occur. Unless amplitude-dependent properties are specifically being studied, a bias level near the rms of the time history is preferable. The variation of signatures with bias level was investigated and examples from Beam No. 2 are given. Figure 54 shows signatures for bias levels of 0.1, 0.3, and 0.4 volts with the rms of the time history about 0.2 volts. The shape of the signatures remains the same with small variations in amplitudes when they are scaled to the same level. This shows that the structure is relatively free from amplitude-dependent nonlinearities and significant variations in bias level can be tolerated.

The length of the signature is optional also. Changes in a signature due to a flaw may first occur after several cycles in the signature. Also, noise distortion of signatures is often confined to the beginning of a signature so the length should be several cycles. As shown later, signature length was usually about 10 cycles of the predominant frequency in the bandwidth being considered.

The length of record is also chosen. For the work on the special-purpose computer, 4,096 samples were used to ensure that repeatable signatures would be obtained. Figure 55 shows a superposition of four signatures. Each of the four signatures in the upper one has 512 samples and each in the lower has 4,096. A considerable difference in repeatability is seen.

APPENDIX B

INSTRUMENTATION

The data acquisition systems were designed to be usable over a frequency range of 0 to 20 KHz. This does not mean that the frequency response of the measurements was flat over this range, but that frequency content could be examined over this range realizing that there would be some rise in response of the accelerometers as they approached their resonant peaks. In both the field test and the laboratory test the excitation near the resonant frequencies of the accelerometers was low enough so that ringing of the accelerometers was avoided. The upper frequency range of 20 KHz was selected as the upper range which might be expected for ambient excitation in the field. Of course, the technique could be extended to higher frequencies if artificial excitation were provided, but this was outside the scope of the present study.

Field Equipment and Procedure

The field equipment was designed to be portable and to provide six hours of operation without recharging batteries. Since the vibration levels on the bridge were unknown, a measurement system was selected with a wide range of sensitivity. As shown on figure 56, the sensitivity ranged from 0.06 to 6 volts per g. Also, an amplifier with two outputs which differed by a gain of 10 was selected to increase the dynamic range of the measurements. This proved to be quite practical because it eliminated the need to make gain changes in the field. Low vibration level stations such as upper and lower flanges needed the full gain of the high gain channel to obtain acceptable recording levels whereas the high vibration level stations such as webs needed the low gain channel to prevent saturation of the tape.

Resonant frequency of the mounted accelerometers was approximately 29 KHz. The flat frequency range for $\pm$ 5 percent deviation in frequency response is 2 Hz to 5 KHz. Most of the data were taken with tape recorder FM amplifiers at unity gain and a speed of 30 ips which gave a recording bandwidth of 0 to 10 KHz. However, some recordings were made using direct record amplifiers which had a bandwidth of 100 Hz to 75 KHz so that a check could be made of frequency content in the range 10 to 20 KHz.

APPENDIX B

Field operation was quite simple. Voltage to the tape recorder was monitored by a voltmeter and was kept close to 28 V by adjusting a variable resistor. Before recording, outputs of the amplifiers were checked with an A.C. voltmeter and with a portable oscilloscope (when available). For some tapes a time code was prerecorded on the tape. In addition, in order to distinguish an end of record, a space was recorded with amplifiers off after each run.

Fairbank Laboratory Equipment

The laboratory equipment shown in figure 57 was designed to provide random excitation to the beam as well as to measure the response with accelerometers. Strain gage measurements, although not shown on the figure, were also taken but were not completely analyzed because of signal-to-noise ratio problems. Since a strain gage measures a strain, its signal drops off with increase in frequency whereas the signal of an accelerometer increases (for white noise input). A limited test was made using a low noise amplifier with the strain gages which indicated that this might be a feasible technique, but not with the equipment available for this test.

Resonant frequency of the mounted accelerometers was 35 KHz. The flat frequency range for $\pm$ 5 percent deviation was 2 Hz to 5 KHz. Although the accelerometers were used above this frequency range, repeatability of signatures by changing accelerometers of the same make and model was checked and was found to be good. All of the laboratory data were recorded on FM at 60 ips to provide a full 0 to 20 KHz bandwidth.

In the laboratory operation, the power amplifier to the shaker was turned up until levels suitable for recording were reached. Since recording level requirements are the same in either field or laboratory, the sensitivity of the accelerometers may be used to judge the relative levels of excitation. As may be seen on figures 56 and 57, the laboratory level of 7 mv/g was considerably lower than the 600 mv/g used in the field tests. Thus, the excitation level in the field was much lower than those used in the laboratory, a difference which could not be avoided since the laboratory tests preceeded the field tests.

An Irig-B time code signal was put on the tape to identify the various runs.

APPENDIX C

AUXILIARY OBSERVATIONS

A number of observations were made during the tests which do not have a direct bearing on the original purpose, but which are important foundation material for future work. The purpose of this appendix is to point out some results in these auxiliary areas.

Signatures of Similar Structures

From the main body of the report, it appears that once a standard is established, changes in the structure (i.e., crack growth) can be detected. The question arises, what do we do if we have an old structure for which we have no standards and would like to determine its soundness at once? One possibility for doing this is that, if a number of elements in a structure are the same (i.e., similar eyebars), we may be able to isolate a defective member by looking at the ensemble of signatures for like structures. A comparison of interest in this regard is shown on figure 58, which compares signatures taken at locations of symmetry on the beam Stations 1-4 and on figure 59, Stations 5-8. If the beam including welds were perfectly symmetrical, then these signatures should be exactly the same for the shaker excitation at the centerline. Comparison of signatures at Stations 1 to 4 is interesting in that standard signatures for Stations 1 and 3 are very similar whereas the signatures for Stations 2 and 4 are quite different. This is quite remarkable when one considers that the crack histories of Stations 1 and 3 turned out to be very similar in both crack initiation and growth whereas the crack histories of Stations 2 and 4 were quite different. This would indicate that there was something quite different in the welds at Stations 2 and 4 and opens up the possibility of judging welds with standard signatures. Of course, this is based on one observation and much more experimentation would be needed to establish interpretations of the signatures. It is interesting to note that the signatures more distant from the welds Stations 5-8 are quite similar and only show minor variations.

APPENDIX C

Effects of Added Masses

The sensitivity of signatures due to changes such as cracks has been shown in the laboratory tests and the question of sensitivity to changes in a real bridge under natural excitation is of interest. Although it was not feasible to start a crack in the field bridge, some simple experiments were conducted to test the sensitivity of signatures. Since it was noted on Beam No. 1 that addition of the clip gages caused changes in signatures, it was thought that the effect of adding a small C clamp on the bridge structure would be of interest. A 7-1/2 cm C clamp was clamped about 30 cm distance from Station 5 and the results are shown on figure 60. The change in the signature is apparent. Of course, effects of actual cracks on signatures in the field is needed but is beyond scope of the present work.

Hand Held Accelerometers

The difficulty of attaching accelerometers at the stations on the mounting studs and then connecting the electrical lead is a procedure which should be simplified. One possibility would be to attach the accelerometer by some sort of clamp or magnet or by a manually depressed spring. Some preliminary tests of this concept were made by holding accelerometers firmly on the stations by hand pressure. Reasonably comparable signatures were obtained so some similar technique appears to be feasible to speed up testing.

REFERENCES

1. Tung, C. C.: Random Response of Highway Bridges to Vehicle Loads. Jour. Eng. Mech. Div. Proc. ASCE, Oct. 1967.

2. Dodds, C. V. and Robson, J. D.: The Description of Road Surface Roughness. Jour. Sound & Vibration, vol. 31, no. 2, Nov. 22, 1973.

3. Lewis, P. T.: The Noise Generated by Single Vehicles in Freely Flowing Traffic. Jour. Sound & Vibration, 1973.

4. Lee, Y. W.: Statistical Theory of Communication. John Wiley and Sons, Inc., 1963.

5. Bendat, J. S. and Piersol, A. G.: Measurement and Analysis of Random Data. John Wiley and Sons, Inc., 1966.

6. McLamore, V. R., Hart, G. C. and Stubbs, I. R.: Ambient Vibration of Two Suspension Bridges. Jour. Structural Div. Proc. ASCE, 1971.

7. Cole, H. A., Jr.: On-Line Failure Detection and Damping Measurement of Aerospace Structures by Random Decrement Signatures. NASA CR-2205, 1973.

8. Frank, K. H. and Galambos, C. F.: Influence of Yielding on the Fatigue Strength of Steel Beams. FHWA Office of Research (to be published).

9. Crandall, S. H. and Wittig, L. E.: Chladni's Patterns for Random Vibration of a Plate. Proceedings of Dynamic Response of Structures Symposium held at Stanford University, 1971. Pergamon Press, Inc.

STATION NO.	COORDINATES x Meters y		LOCATION AND DESCRIPTION
	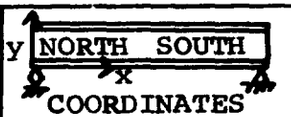		
1	0.96	0.79	Middle of web, east side, $\ddot{z}$
2	3.45	2.28	Upper flange, east side, $\ddot{y}$ halfway between web and outer edge
3	3.53	0.69	Middle of web, west side, $\ddot{z}$
4	13.58	0.76	On web near cross brace, west side, $\ddot{z}$ 11.4 cm, north of vertical [illegible]er
5	13.70	0.36	Gross bracing gusset, west s[illegible], $\ddot{x}$ 4.45 cm from outside edge, 21.6 cm above bottom
6	13.82	0.74	On web near cross brace, west side, $\ddot{z}$
7	14.22	0.74	On web near cross brace, west side, $\ddot{z}$
8	14.30	0	Lower flange, west side, $\ddot{y}$ halfway between web and outer edge

Table I.- Field test transducer locations.

TEST NO.	TEST DATE	TIME	TRAFFIC	WIND	TEMP. °F	WEATHER	COMMENTS
1	8-30-73	8:00-10:00 a.m.	Heavy 50 mph	Nil	65-75	High Fog to Clear	
2	9-26-73	10:00-11:00 a.m.	Light 50 mph	Nil	72-76	Clear	
3	10-25-73	9:00-10:30 a.m.	Medium 50 mph	Light	60	Cloudy	Rain previous day Pavement damp
4	11-21-73	1:30-2:30 p.m.	Light 50 mph	Light	58	Clear	
5	12-21-73	9:00-10:00 a.m.	Medium 50 mph	Southerly 20 mph	50	Rainy	Pavement wet
6	1-25-74	7:30-8:30 a.m.	Heavy Stop&Go	Light	42	Cloudy	Sta. 2 accel. pad came off Hand held for this run
7	3-5-74	10:30-11:40 a.m.	Medium 50 mph	Nil	50	Cloudy	
8	3-18-74	3:50-5:40 p.m.	Medium 50 mph	Light	68	Clear	
9	4-30-74	4:15-5:10 p.m.	Medium 50 mph	Northerly 10-15 mph	60	Clear	
10	5-1-74	7:30-8:15 a.m.	Heavy 40 mph	Light	52	High Fog to Clear	
11	5-1-74	8:15-9:00 a.m.	Medium 50 mph	Light	55	Clear	Standard test not run Several variations run

Table II.- Field test log.

SHAKER AT A								
TEST 1000 CYCLES	STATIONS							
	1	2	3	4	5	6	7	8
Std.-300	1.5	2.1	1.4	2.6	1.7	1.6	2.2	1.3
300-400	0.4	1.4	1.3	0.8	1.2	1.5	0.6	0.7
400-433	1.1	1.8	1.2	2.9	1.3	2.1	1.2	2.0
433-442	1.5	1.4	1.3	2.4	1.5	1.5	1.3	2.1
442-Std.	1.5	1.7	1.1	2.6	1.2	0.9	1.7	1.6

SHAKER AT B								
TEST 1000 CYCLES	STATIONS							
	1	2	3	4	5	6	7	8
Std.-300	1.8	1.9	1.4	1.1	1.5	0.7	1.0	1.4
300-400	0.9	1.3	1.2	1.3	1.1	0.7	1.1	1.5
400-433	0.9	1.8	2.4	2.5	2.2	1.2	1.8	2.7
433-442	1.1	1.5	1.5	1.7	1.4	0.7	1.2	0.7
442-Std.	1.1	1.1	0.9	1.4	1.0	1.4	1.7	1.3

SHAKER AT C								
TEST 1000 CYCLES	STATIONS							
	1	2	3	4	5	6	7	8
Std.-300	1.6	1.8	2.1	1.7	1.9	1.7	2.1	1.2
300-400	1.8	1.4	1.1	1.1	1.8	1.2	1.7	0.9
400-433	1.5	1.2	0.8	1.6	1.3	0.5	1.1	0.6
433-442	0.6	1.4	1.5	2.0	1.6	1.3	1.9	1.0
442-Std.	2.1	0.5	1.0	1.5	2.3	1.1	1.4	1.2

Comparisons of signatures.

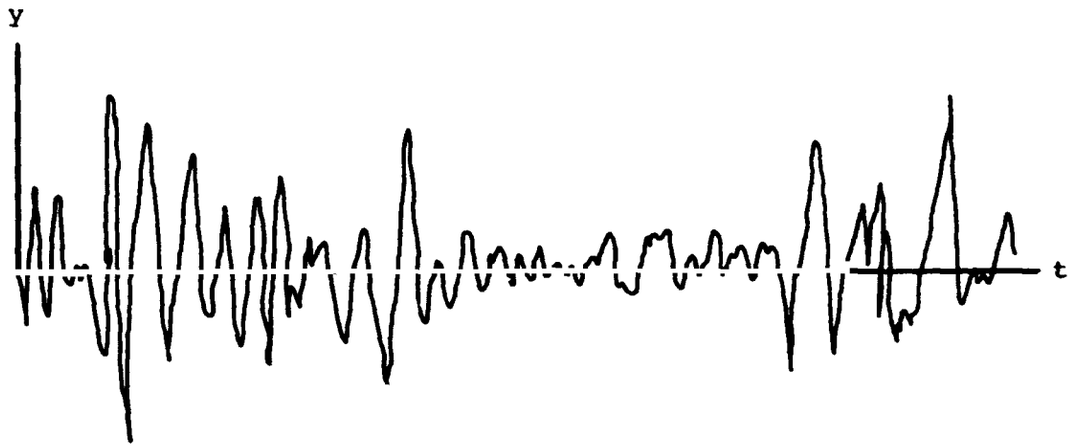

(a) Typical measured time history.

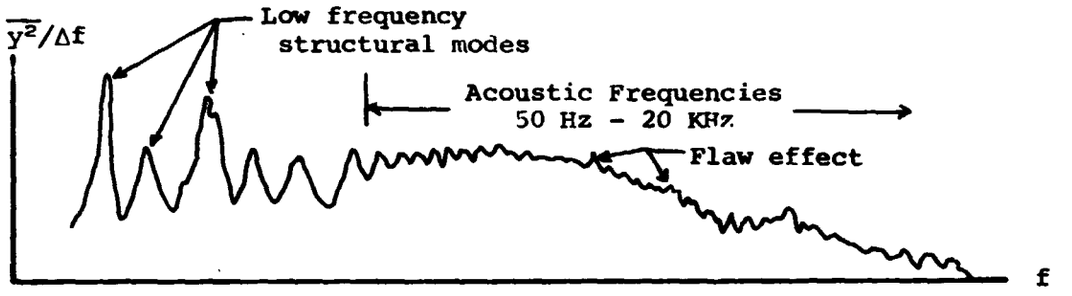

(b) Power spectral density.

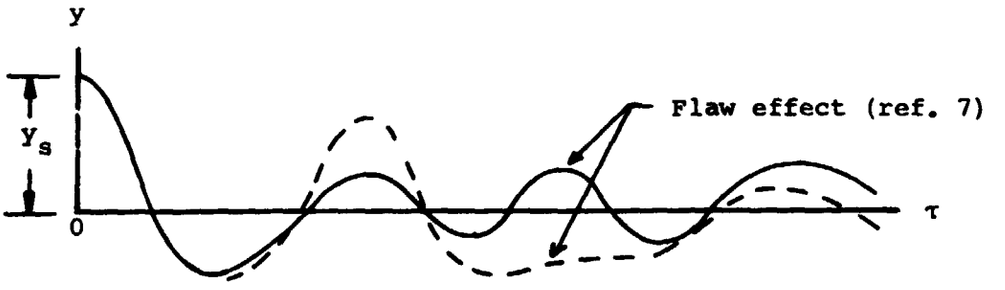

(c) Random decrement average (Randomdec).

Figure 1.- Signature concepts.

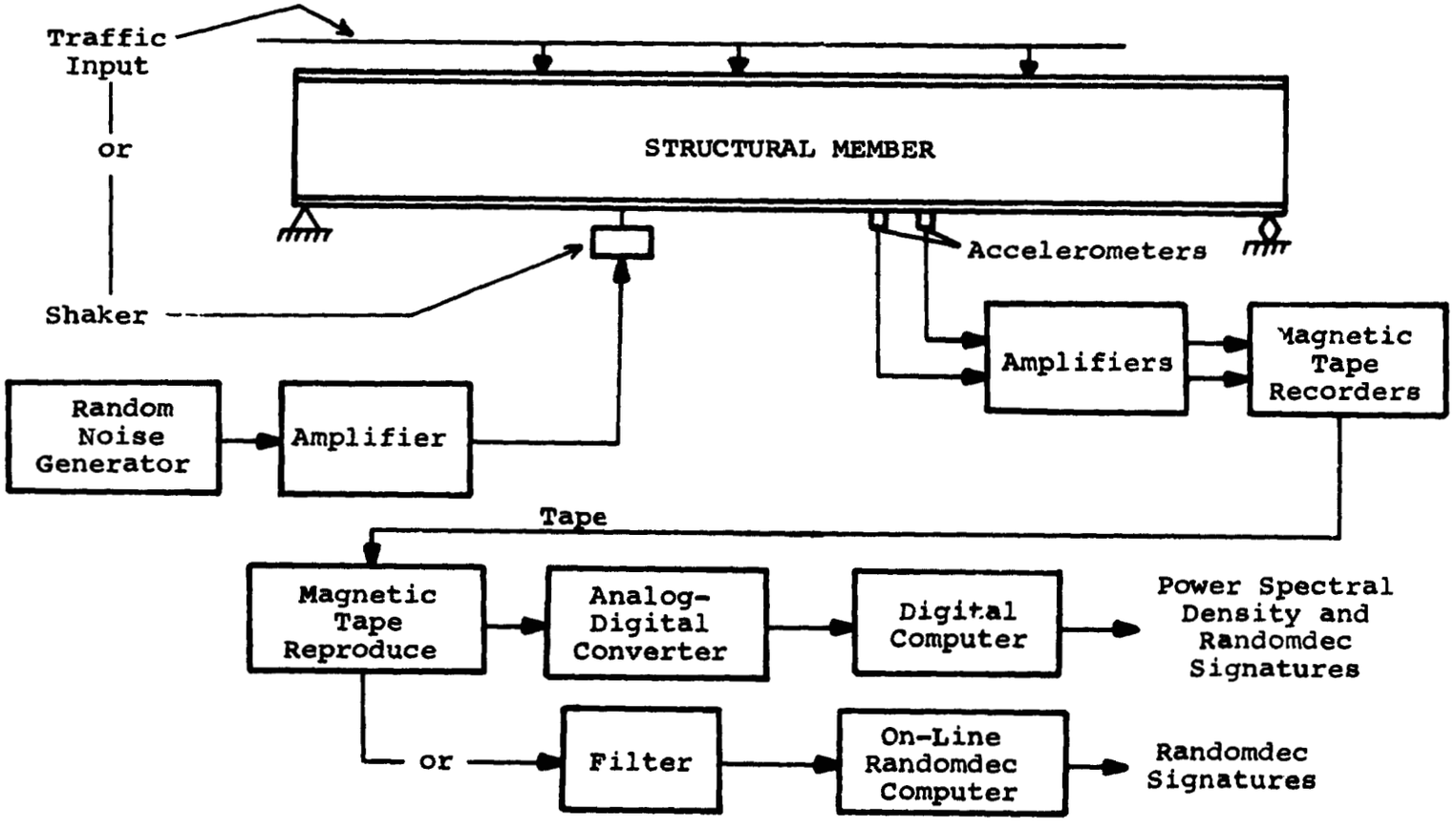

Figure 2.- System components and data flow.

Figure 3.- 101-85 Separation, looking north on Highway 101.

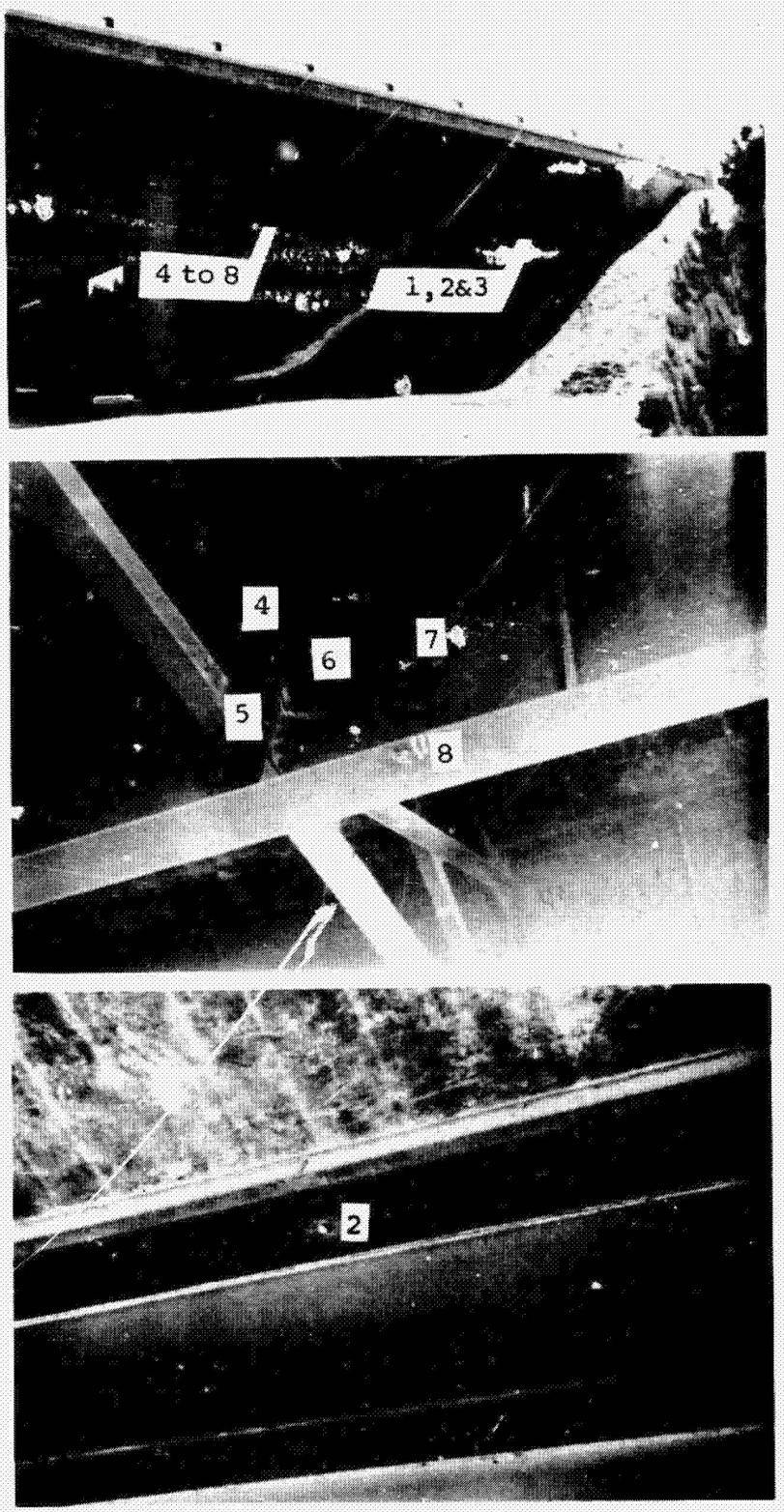

Figure 4.- Accelerometer stations.

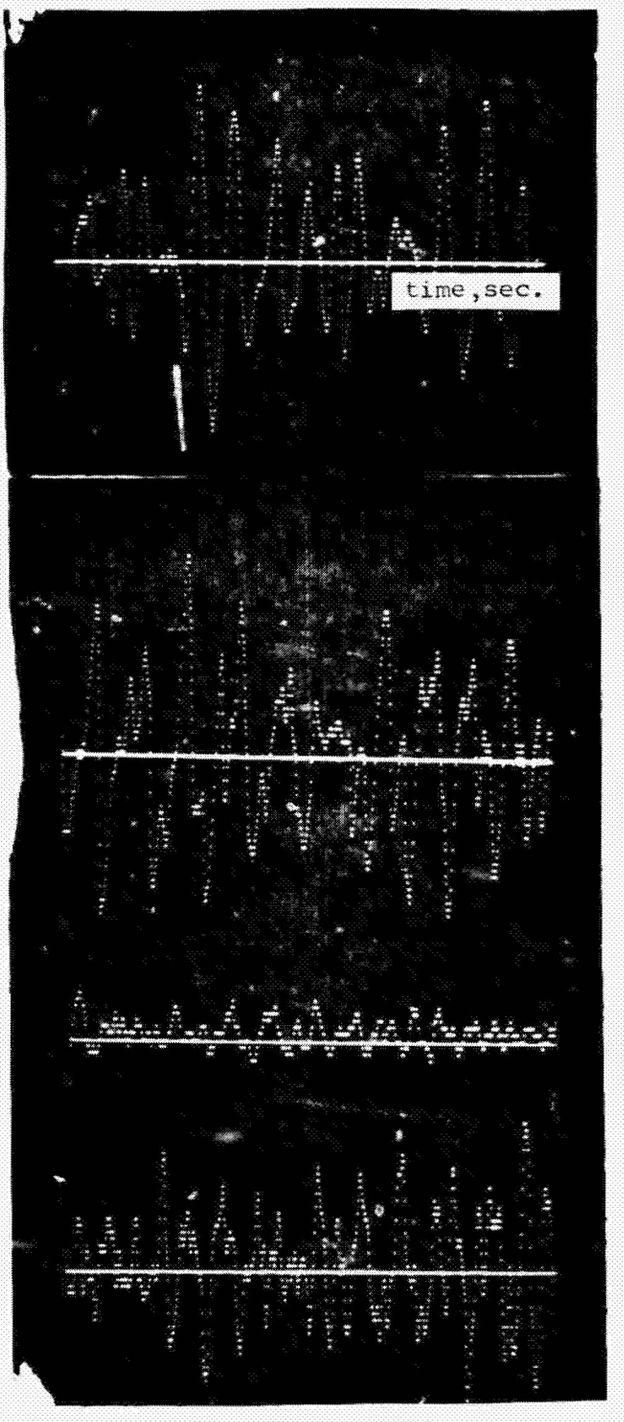

Figure 5.- Typical samples of data from accelerometer outputs at Station 7; Filter 1-10 KHz.

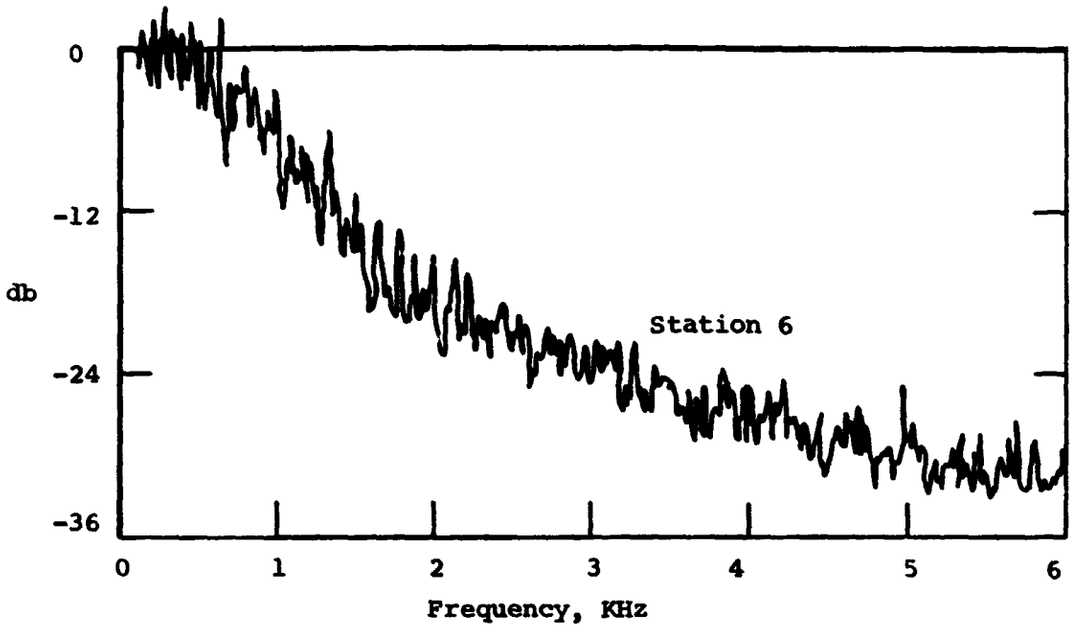

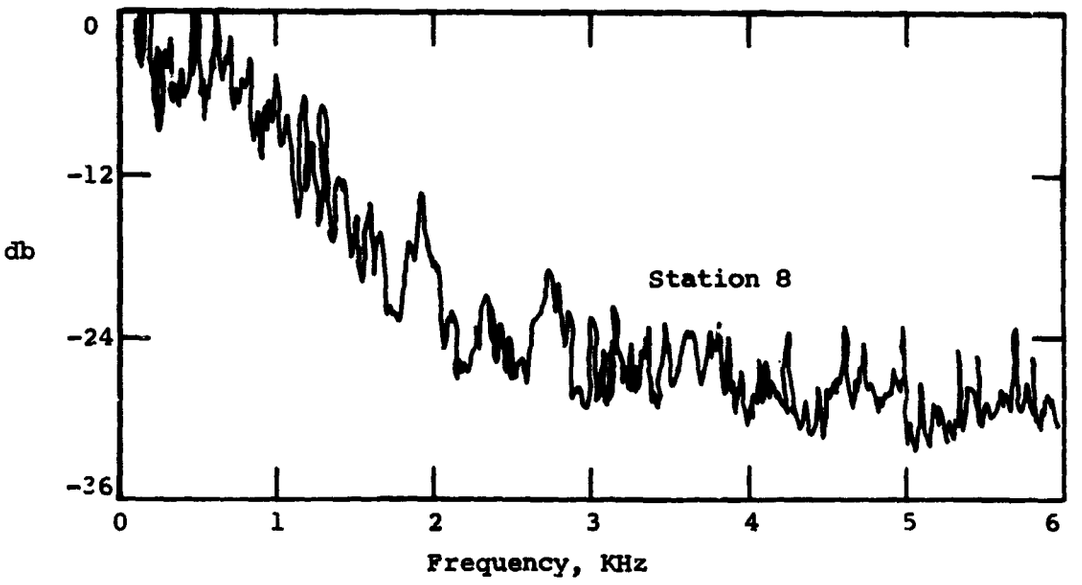

Figure 6.- Typical power spectral densities of field stations.

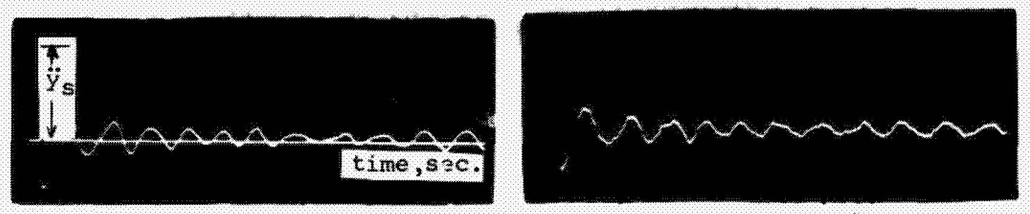

Test No. 1

Test No. 6*

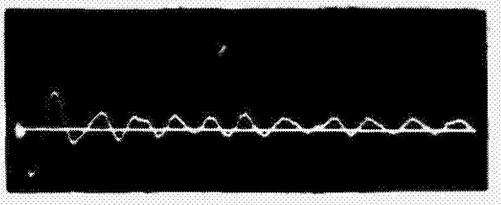

Test No. 2

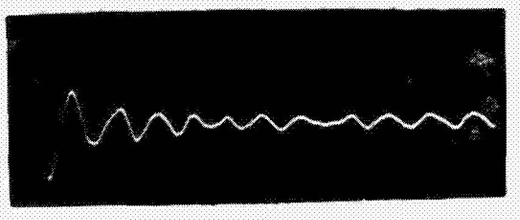

Test No. 7

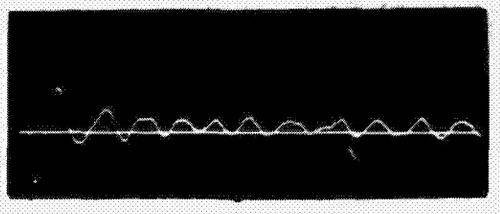

Test No. 3

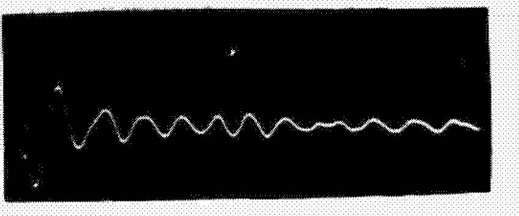

Test No. 8

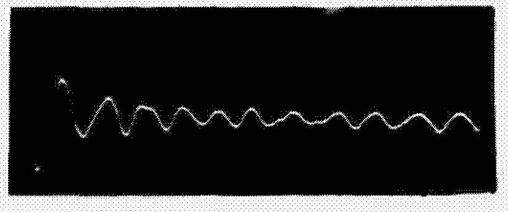

Test No. 4

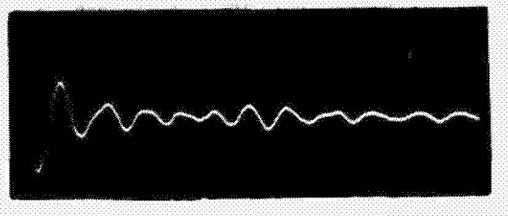

Test No. 9

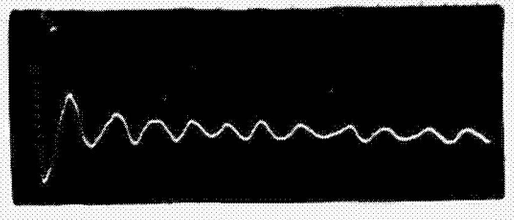

Test No. 5

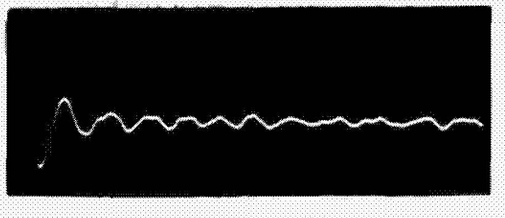

Test No. 10

(a) Signatures at Station 1.

Figure 7.- Field tests.

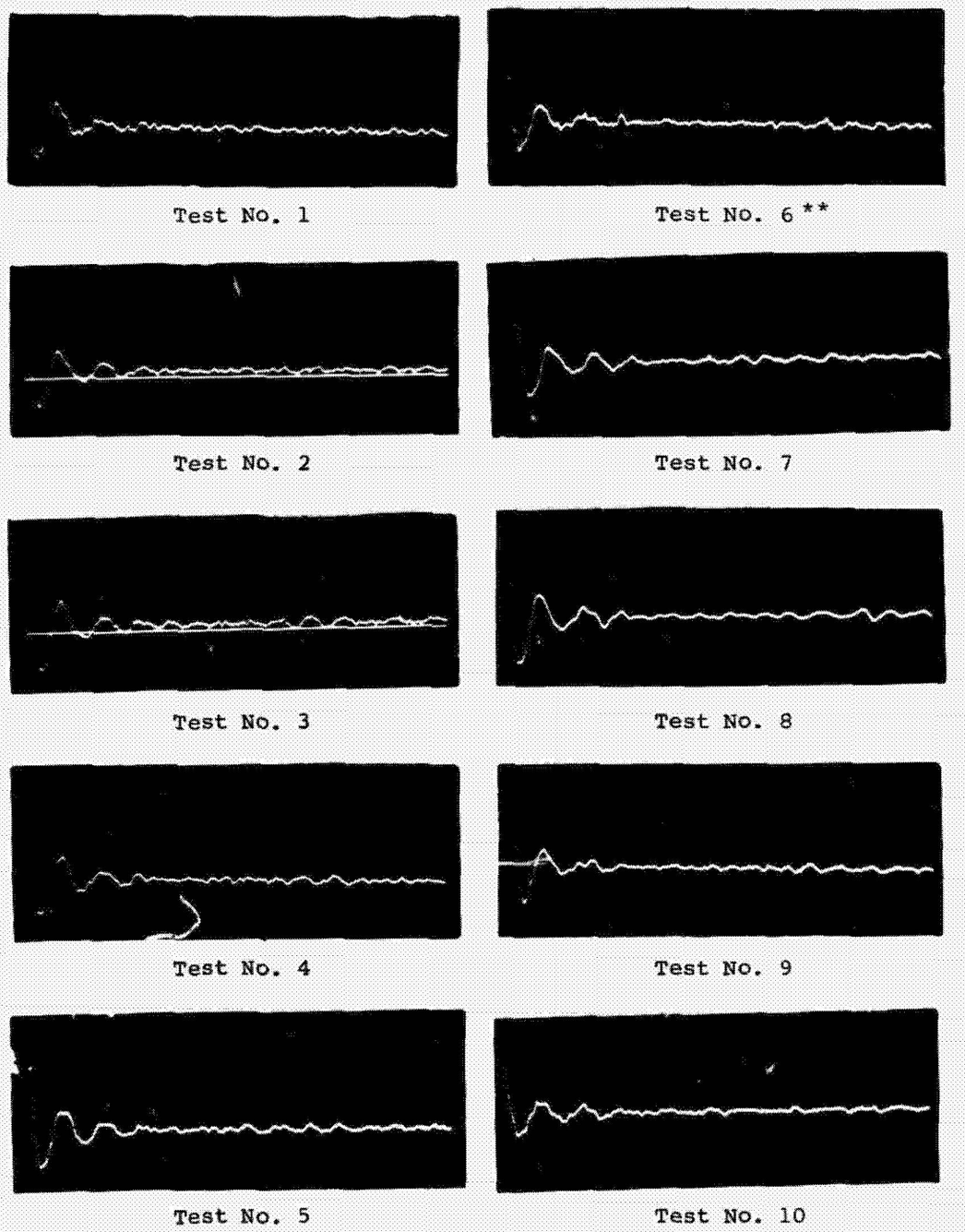

Test No. 1

Test No. 6 **

Test No. 2

Test No. 7

Test No. 3

Test No. 8

Test No. 4

Test No. 9

Test No. 5

Test No. 10

(b) Signatures at Station 2.

Figure 7.- Continued.

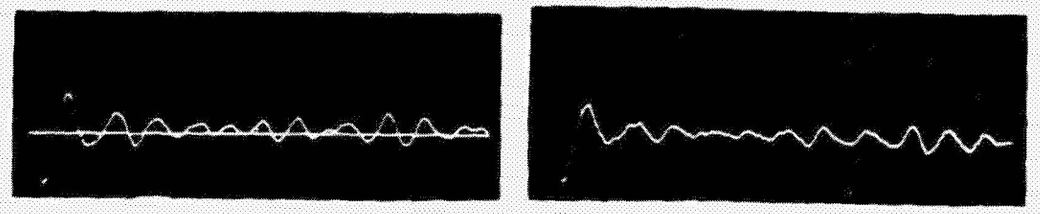

Test No. 1

Test No. 6*

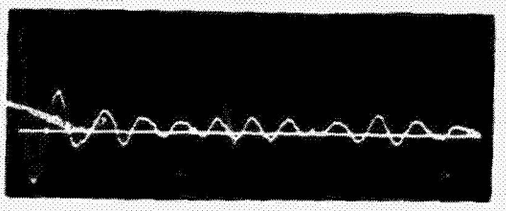

Test No. 2

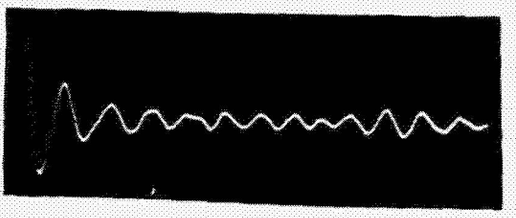

Test No. 7

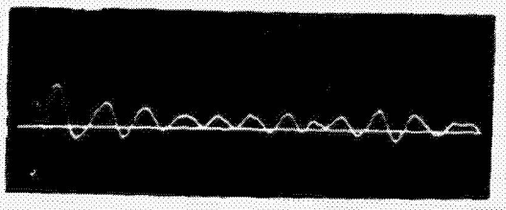

Test No. 3

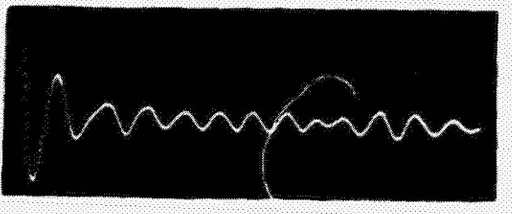

Test No. 8

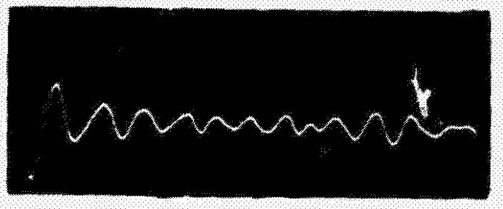

Test No. 4

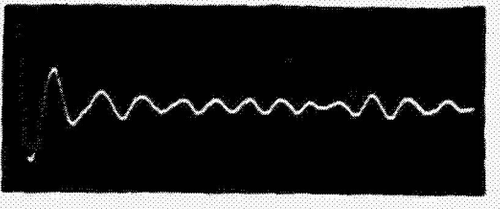

Test No. 9

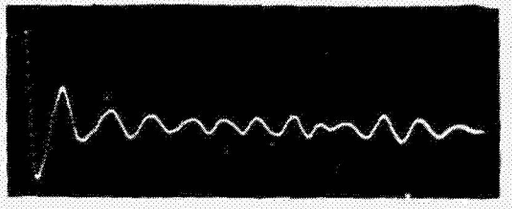

Test No. 5

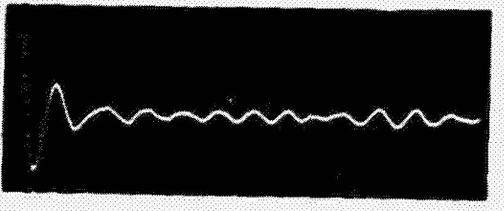

Test No. 10

(c) Signatures at Station 3.

Figure 7.- Continued.

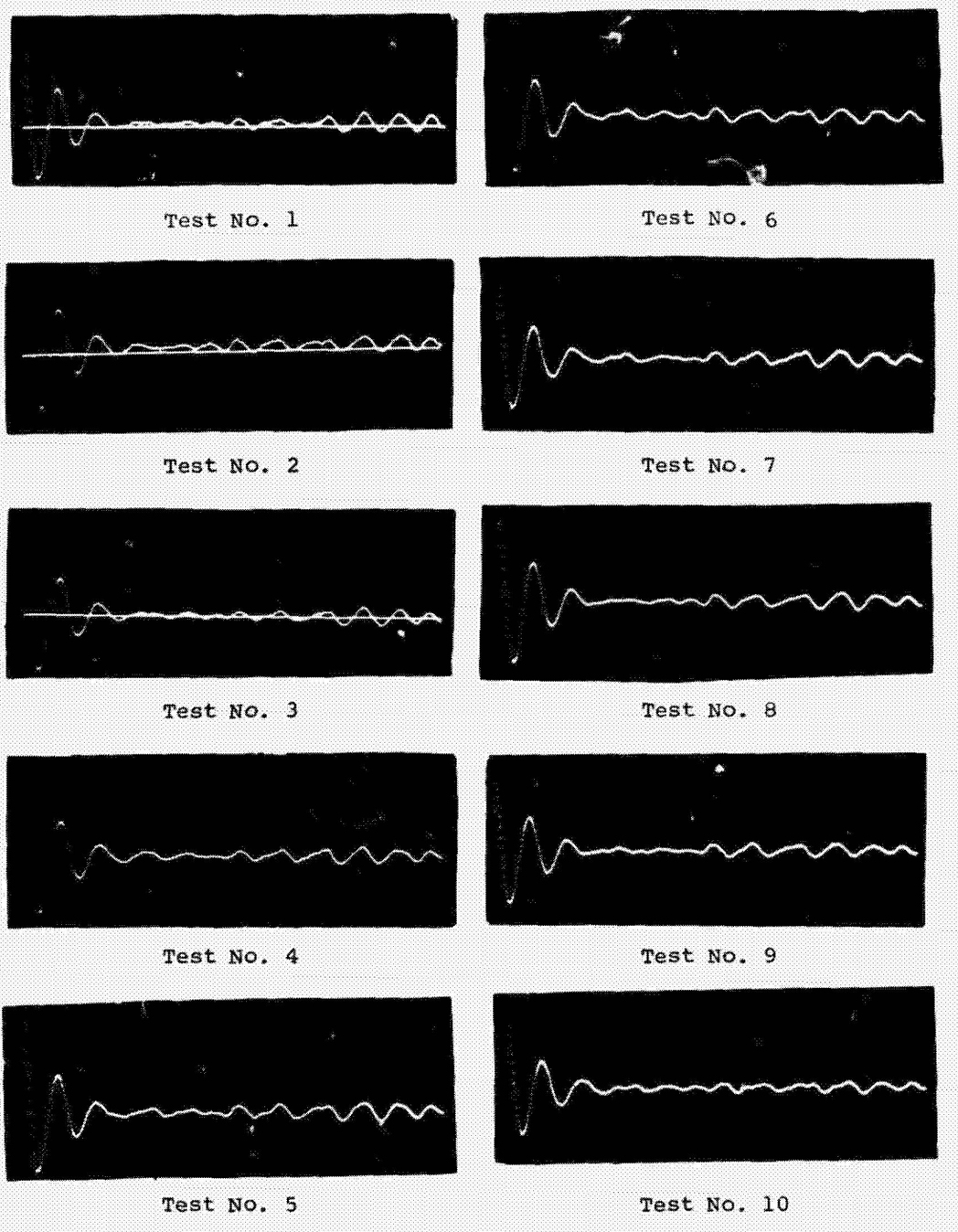

(d) Signatures at Station 4.

Figure 7.- Continued.

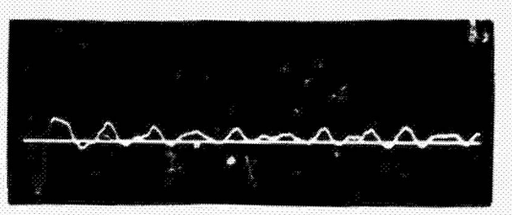

Test No. 1

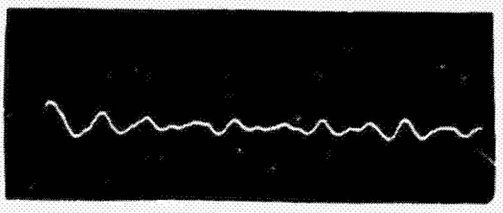

Test No. 6

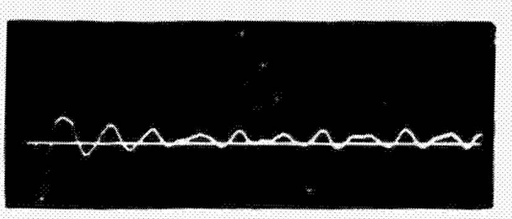

Test No. 2

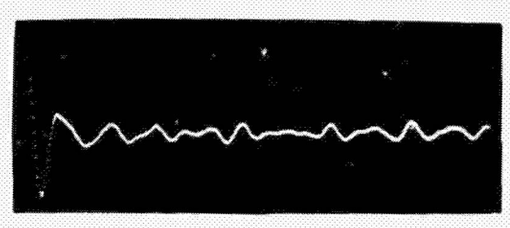

Test No. 7

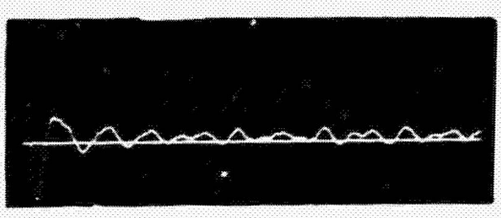

Test No. 3

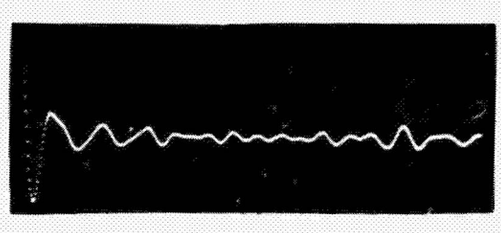

Test No. 8

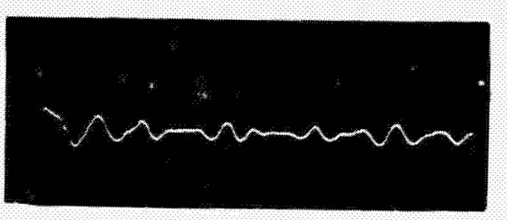

Test No. 4

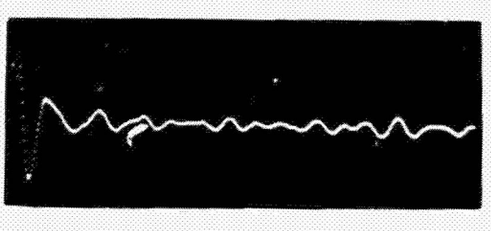

Test No. 9

Test No. 5

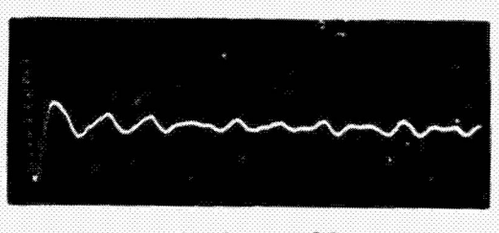

Test No. 10

(e) Signatures at Station 5.

Figure 7.- Continued.

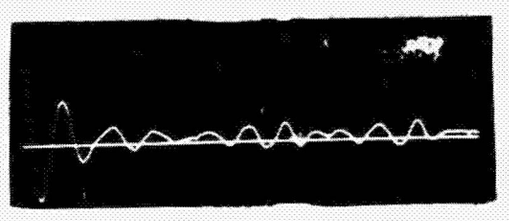

Test No. 1

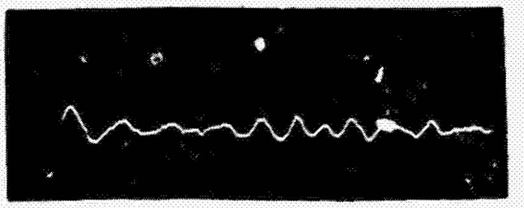

Test No. 6*

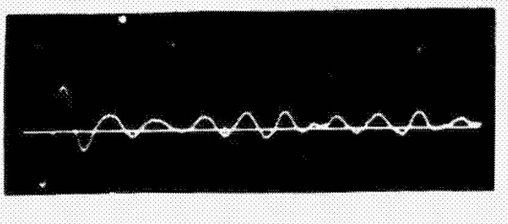

Test No. 2

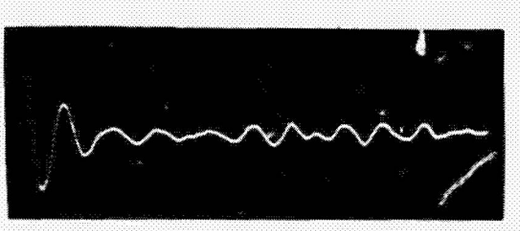

Test No. 7

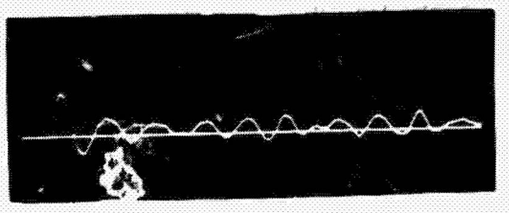

Test No. 3

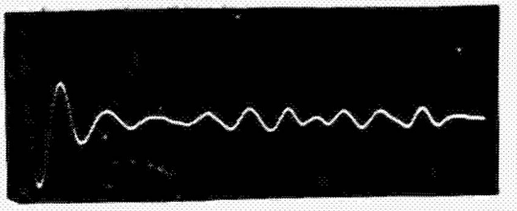

Test No. 8

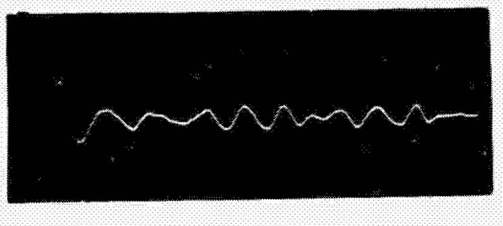

Test No. 4

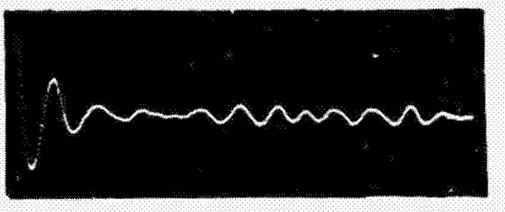

Test No. 9

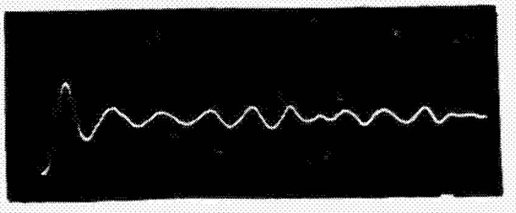

Test No. 5

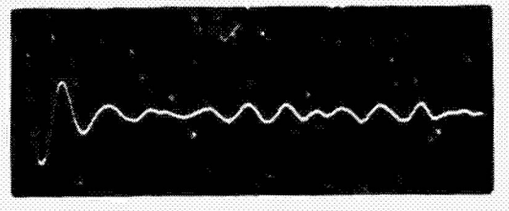

Test No. 10

(f) Signatures at Station 6.

Figure 7.- Continued.

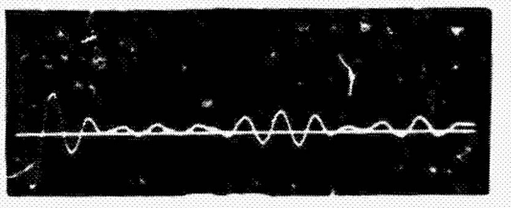

Test No. 1

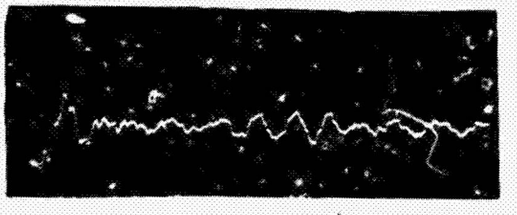

Test No. 6*

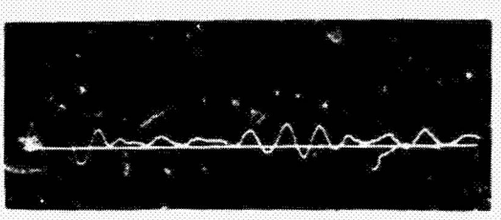

Test No. 2

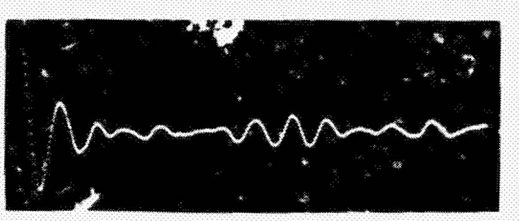

Test No. 7

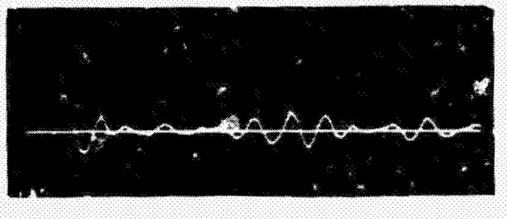

Test No. 3

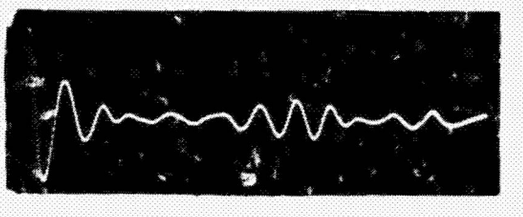

Test No. 8

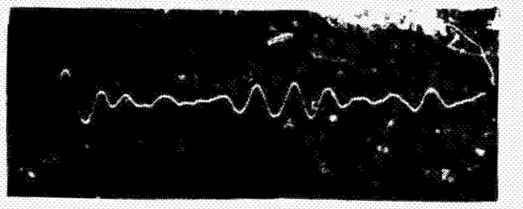

Test No. 4

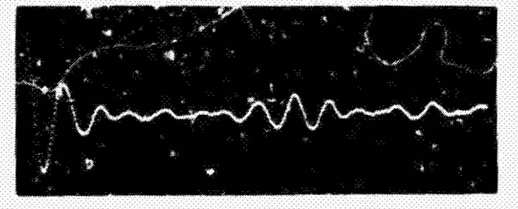

Test No. 9

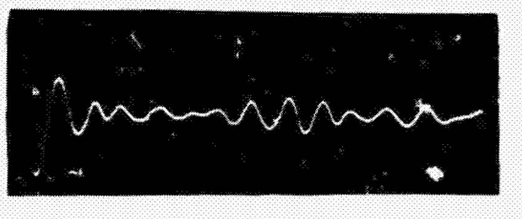

Test No. 5

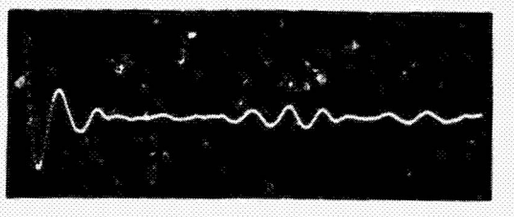

Test No. 10

(g) Signatures at Station 7.

Figure 7.- Continued.

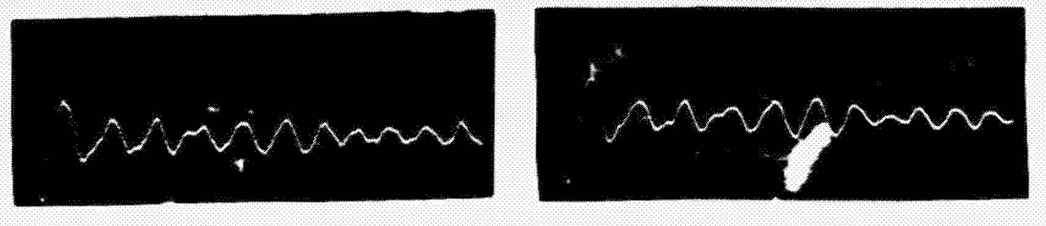

Test No. 1

Test No. 6

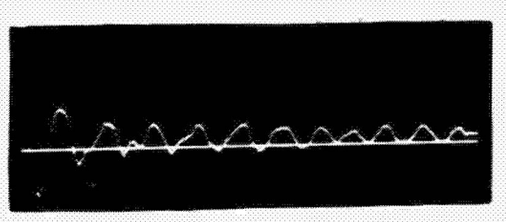

Test No. 2

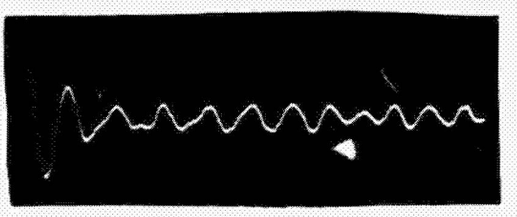

Test No. 7

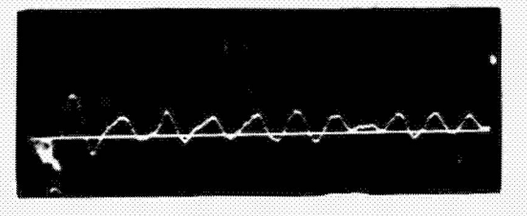

Test No. 3

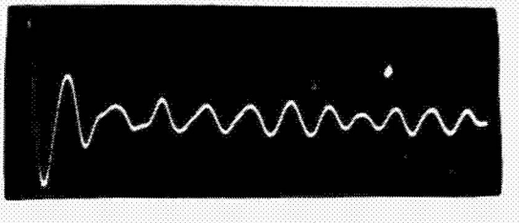

Test No. 8

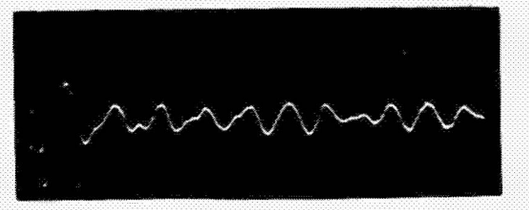

Test No. 4

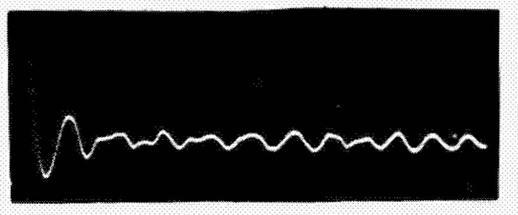

Test No. 9

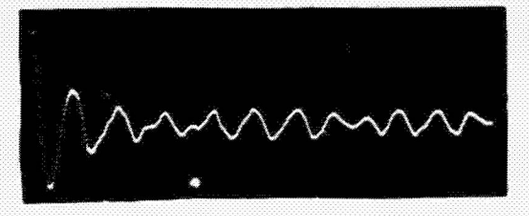

Test No. 5

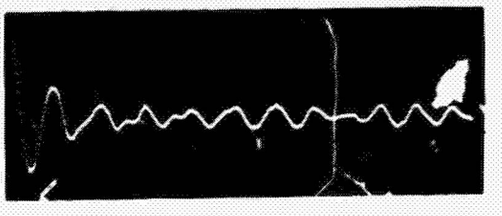

Test No. 10

(h) Signatures at Station 8.

Figure 7.- Concluded.

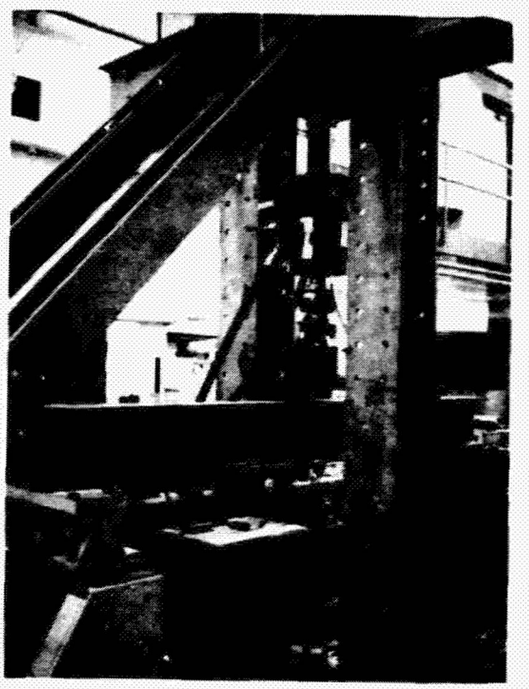

Figure 8.- Laboratory test configuration.

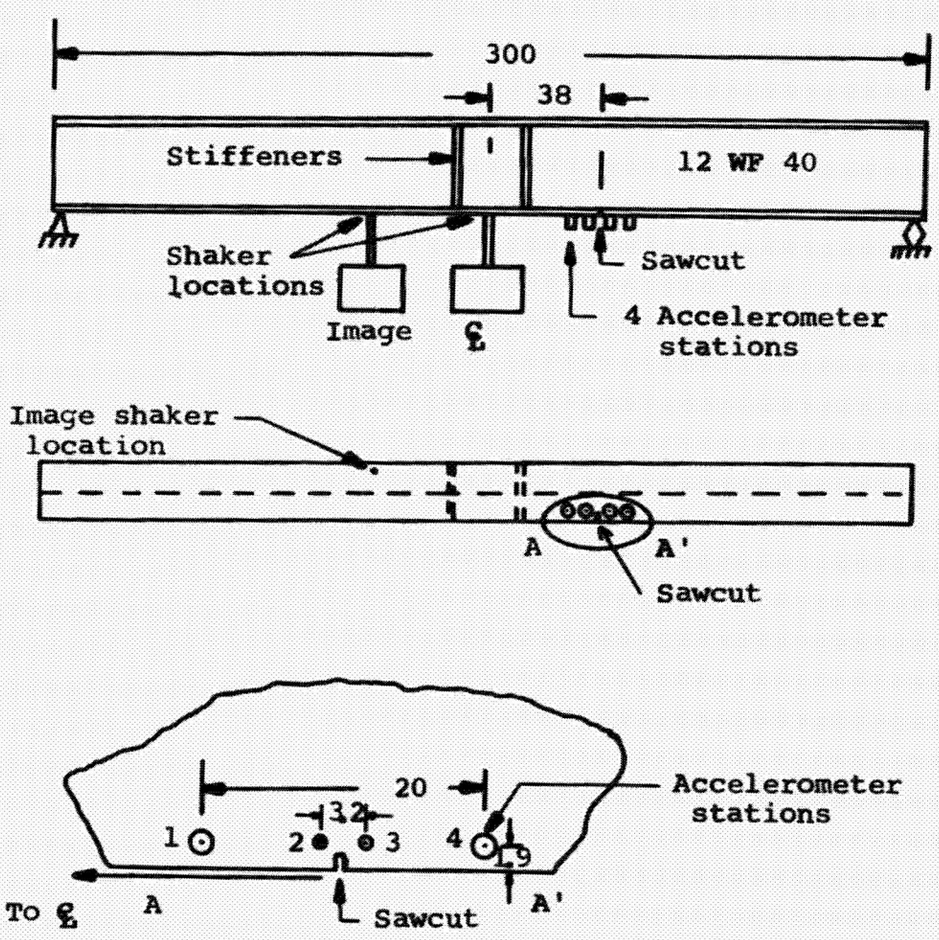

Figure 9.- Beam No. 1 configuration.

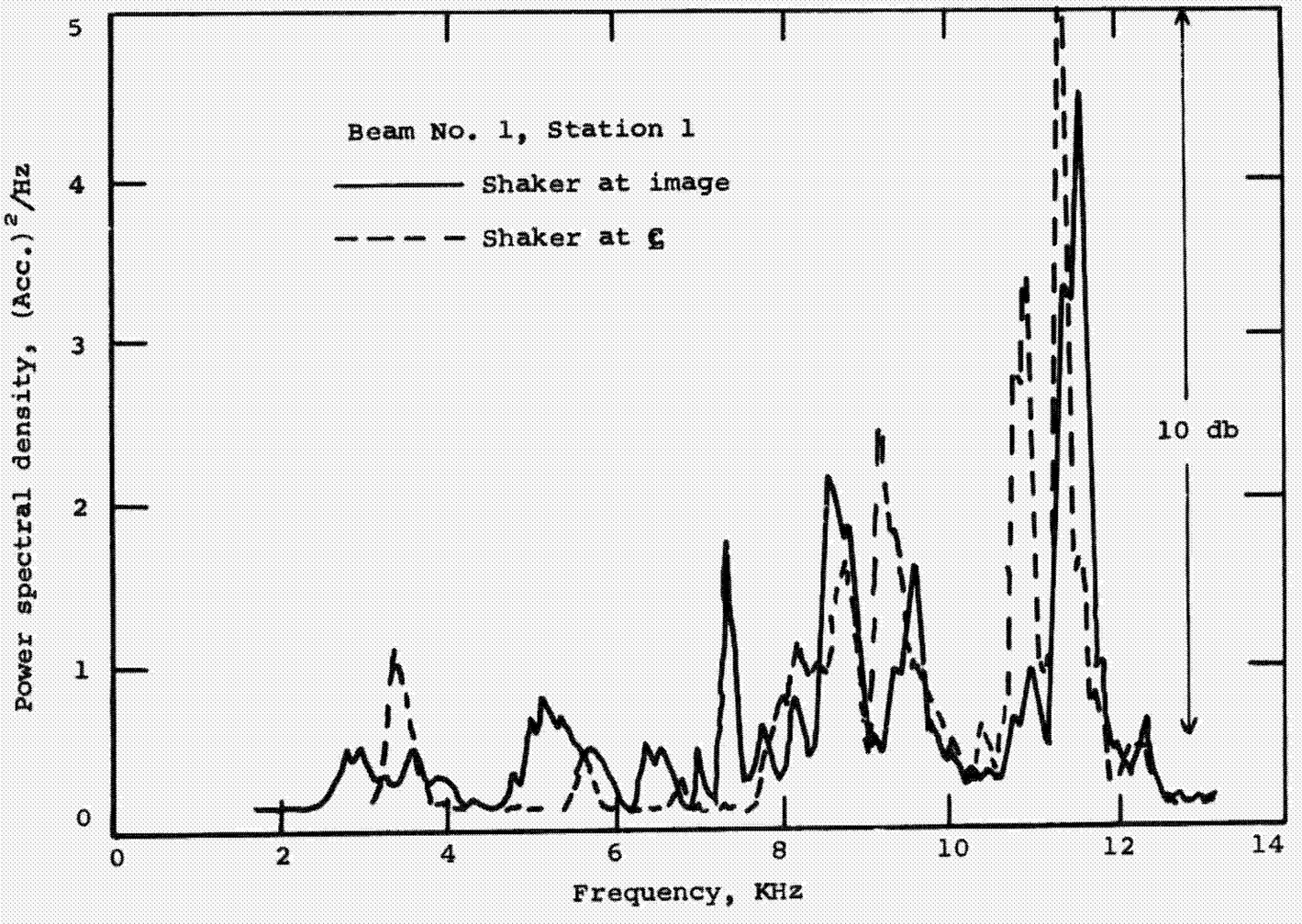

Figure 10.- Effect of shaker location on power spectral density at Station 1.

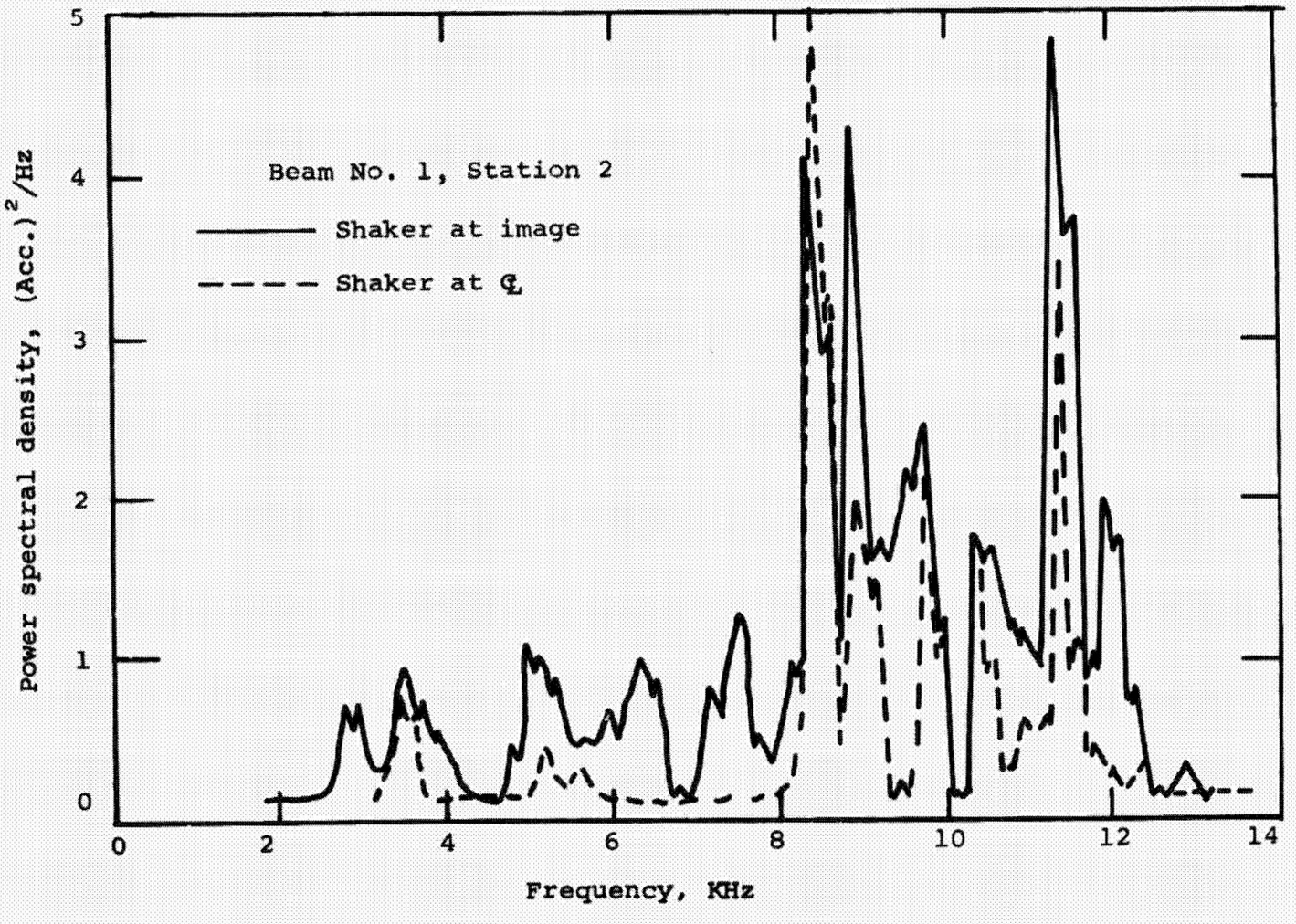

Figure 11.- Effect of shaker location on power spectral density at Station 2.

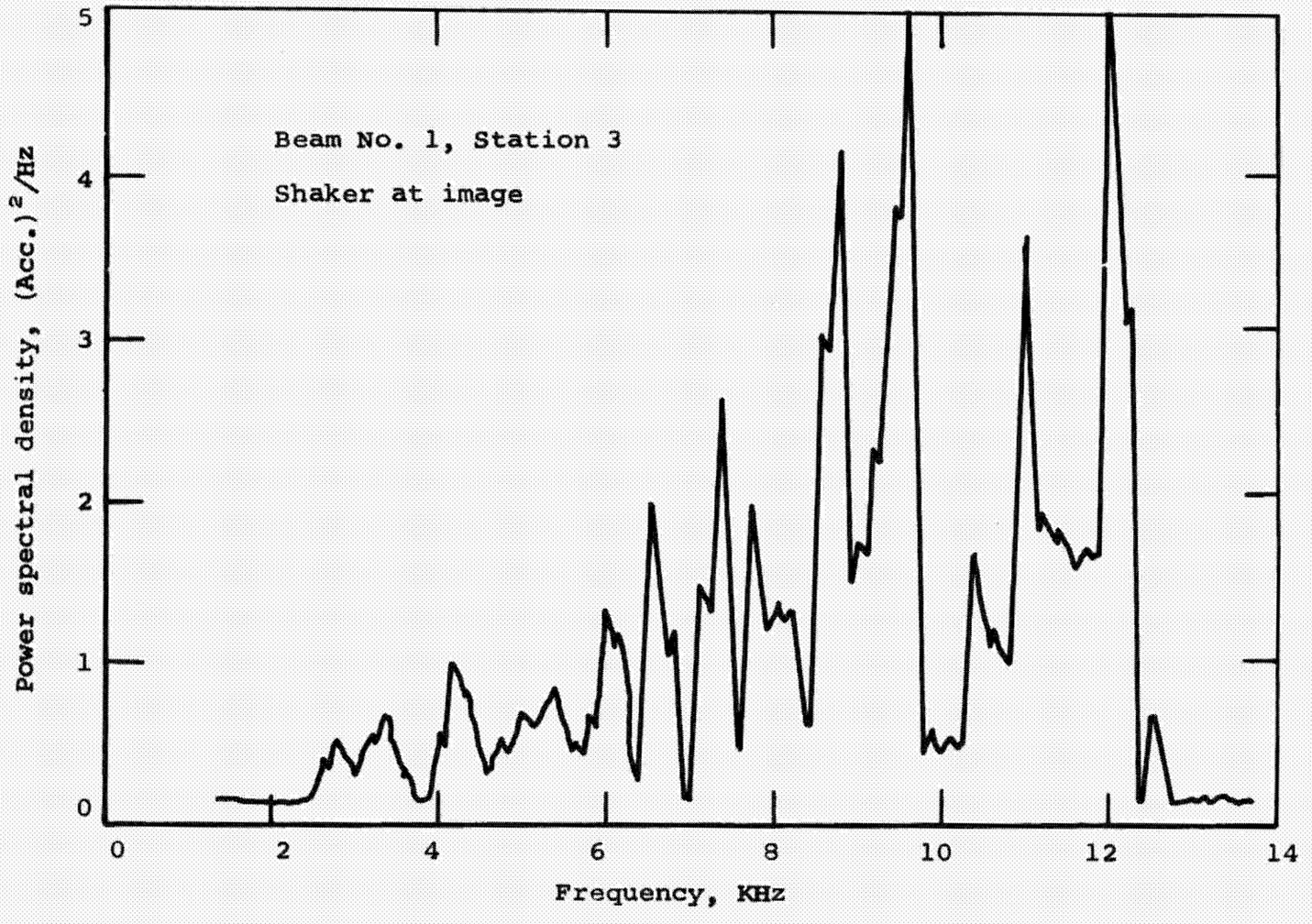

Figure 12.- Power spectral density of Station 3.

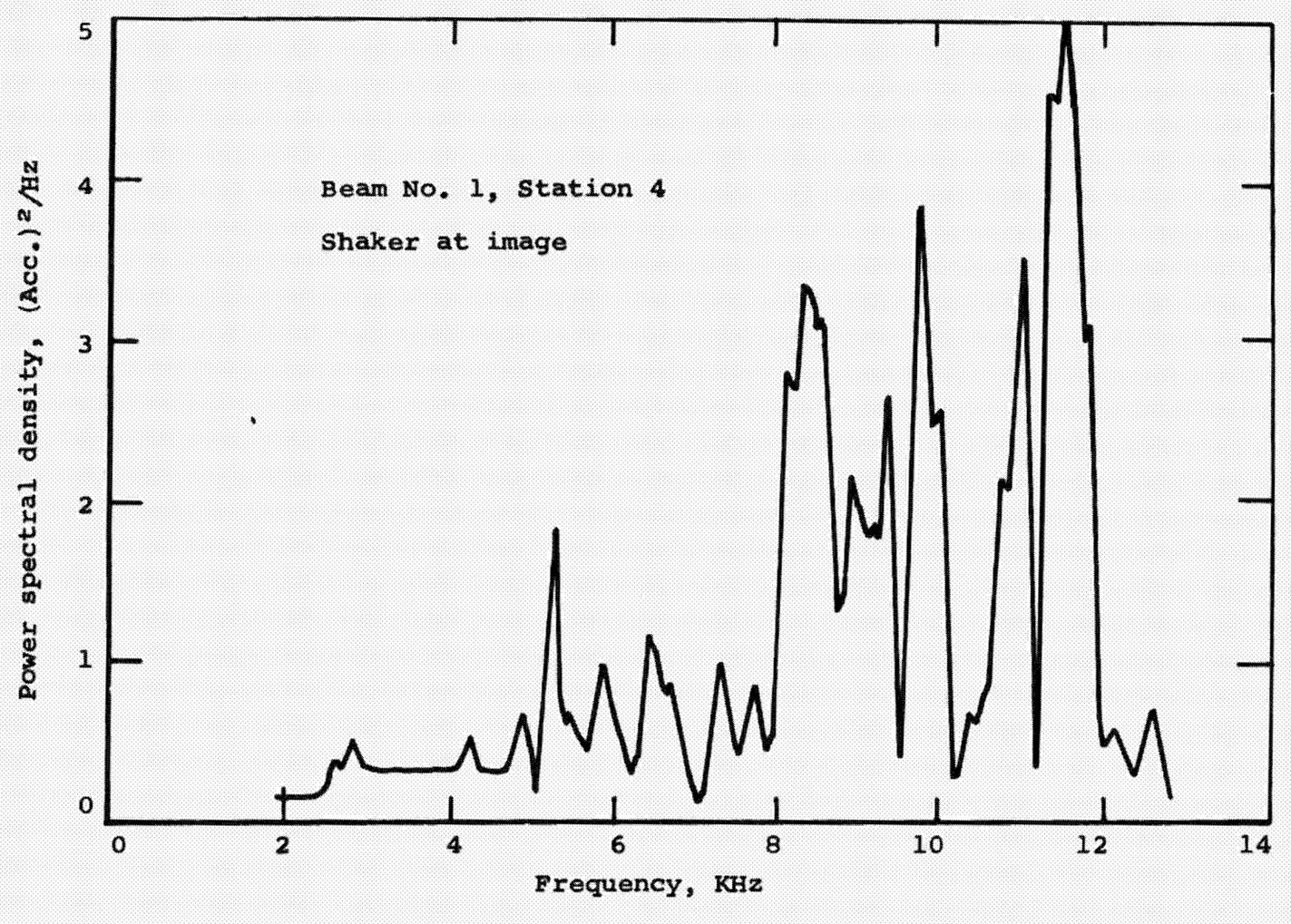

Figure 13.- Power spectral density of Station 4.

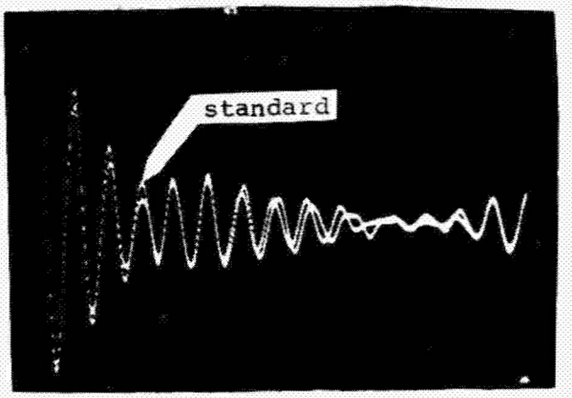

Sawcut and 1.35 cm Crack

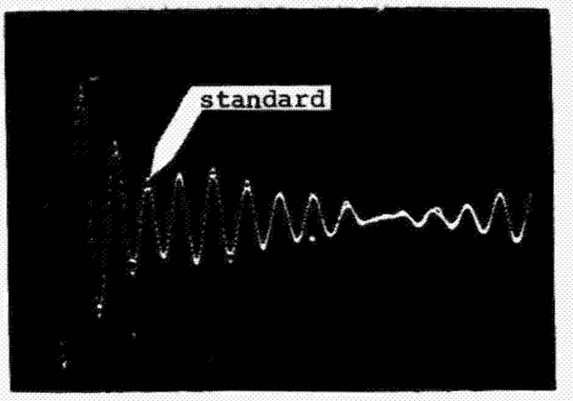

Sawcut and 2.41 cm Crack

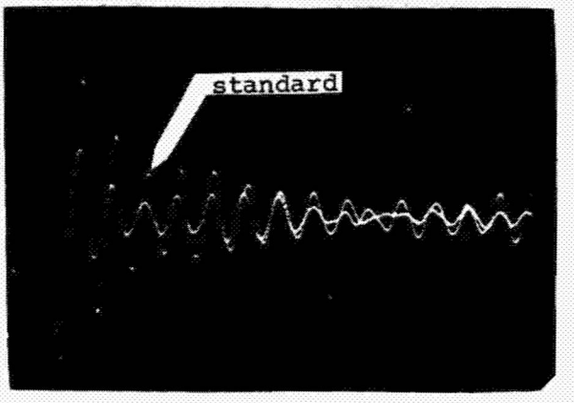

Sawcut and 10.0 cm Crack

Figure 14.- Comparison of signatures of several cracks with standard at Station 3; Filter 10,250-15,000 Hz.

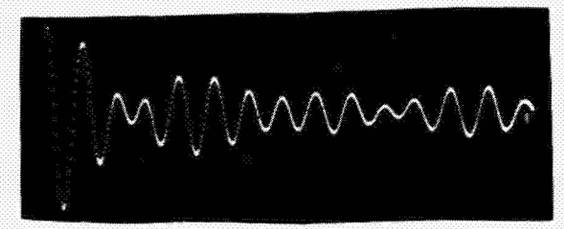

Beam Intact

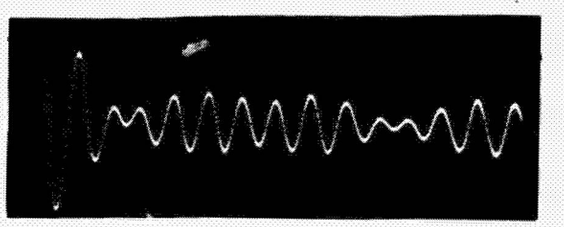

0.54 cm Sawcut

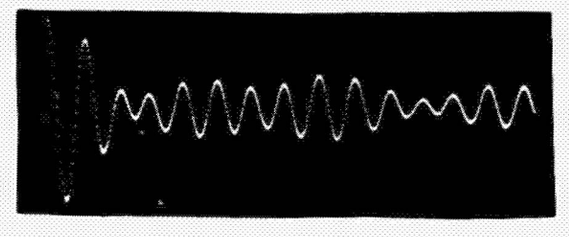

Sawcut and Clip Gage

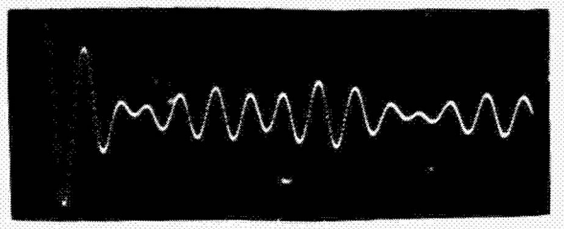

1.35 cm Crack

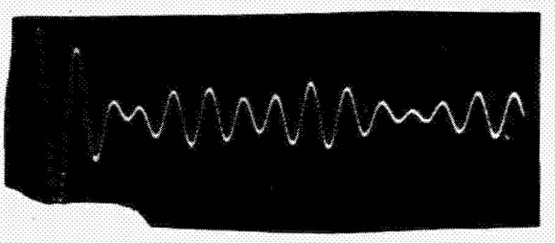

2.41 cm Crac

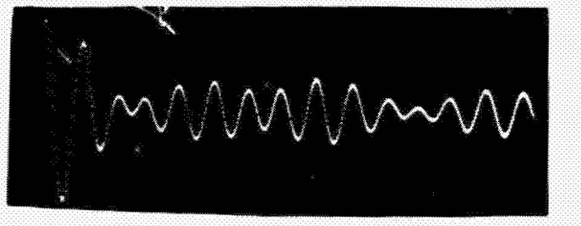

3.91 cm Crack

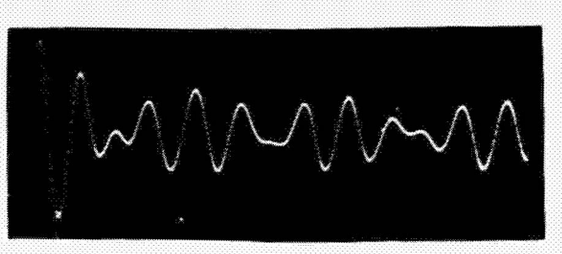

10.0 cm Crack

Figure 15.- Beam No. 1 at Station 1; Filter 8-15 KHz.

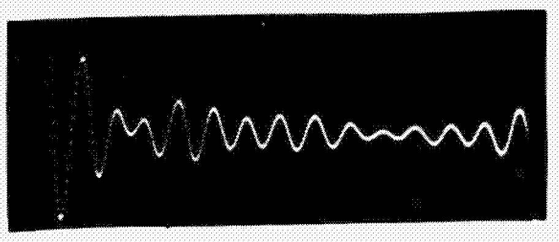

Beam Intact

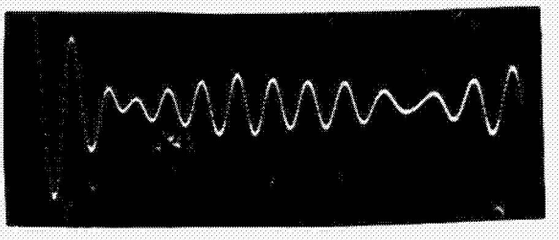

0.54 cm Sawcut

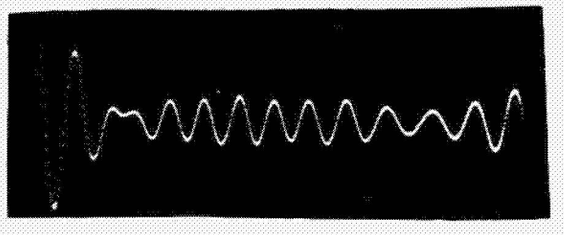

Sawcut and Clip Gage

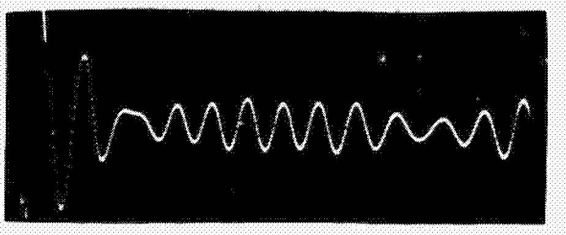

1.35 cm Crack

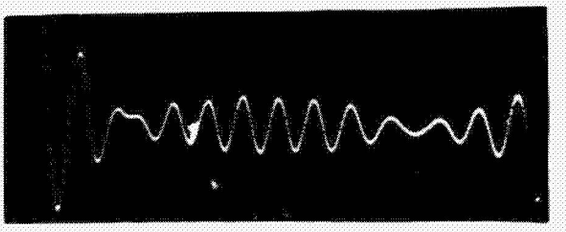

2.41 cm Crack

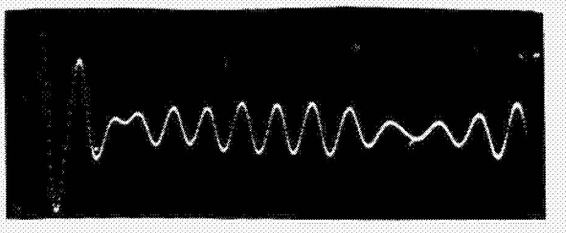

3.91 cm Crack

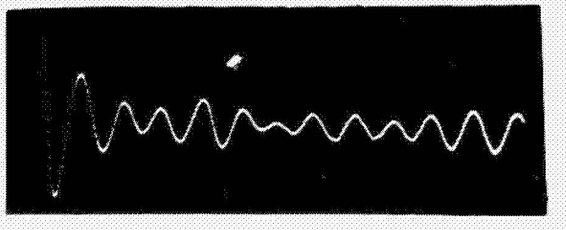

10.0 cm Crack

Figure 16.- Beam No. 1 at Station 2; Filter 8-15 KHz.

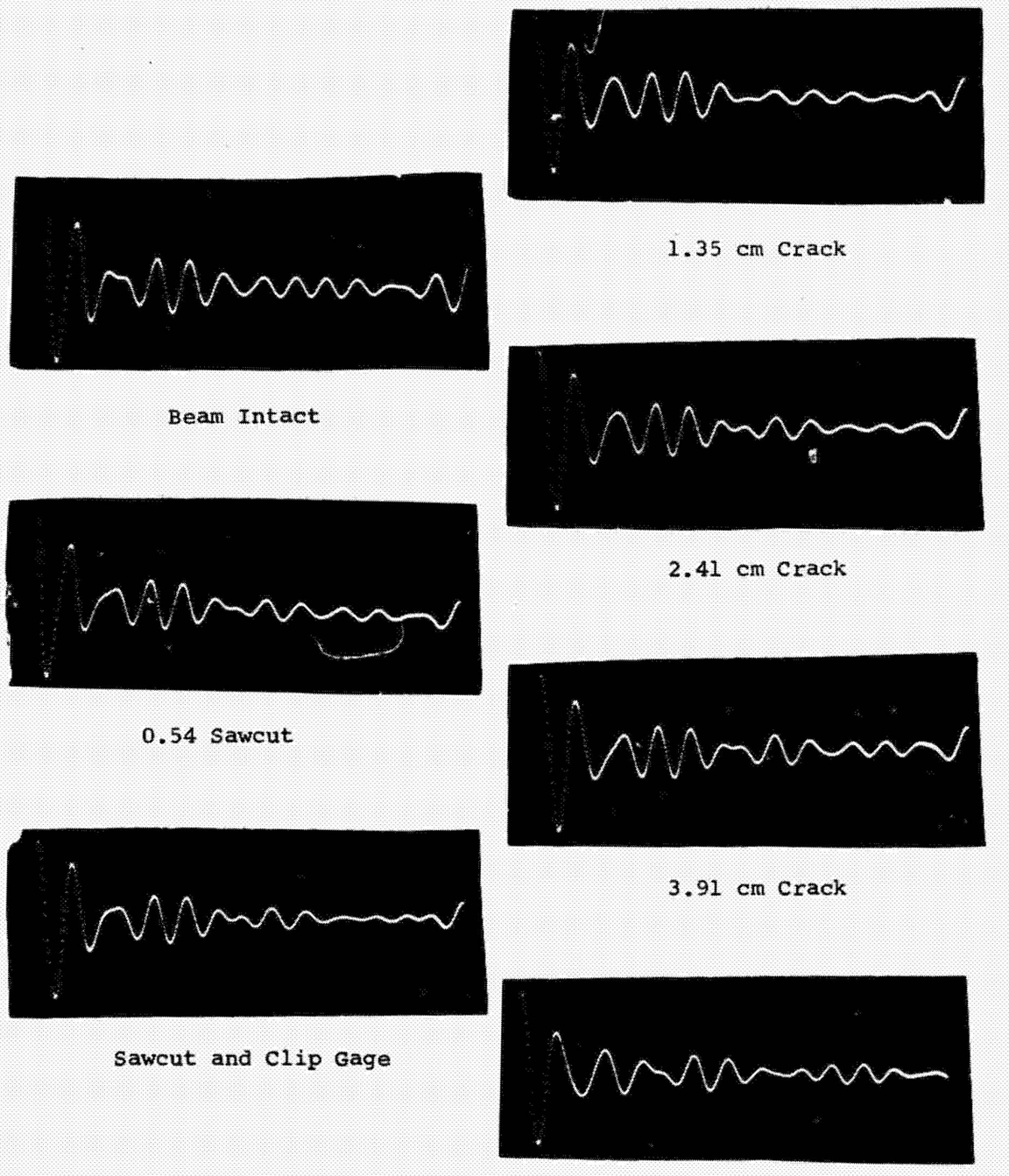

Figure 17.- Beam No. 1 at Station 3; Filter 8-15 KHz.

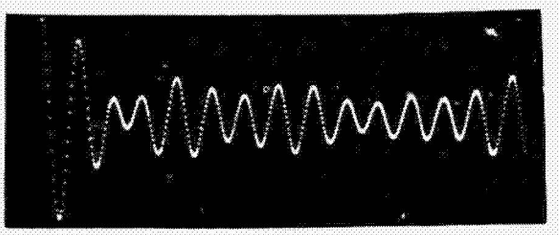

Beam Intact

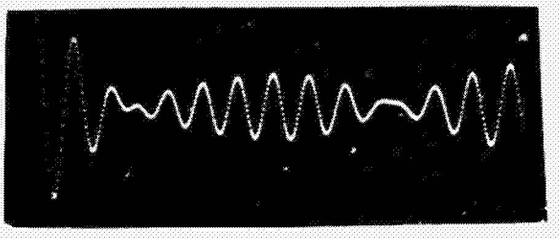

0.54 cm Sawcut

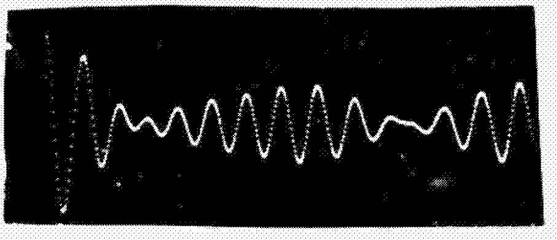

Sawcut and Clip Gage

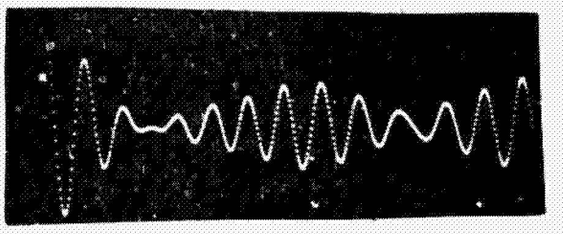

1.35 cm Crack

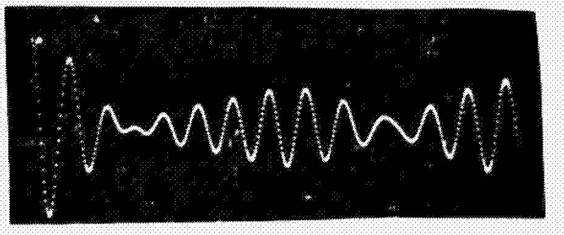

2.41 cm Crack

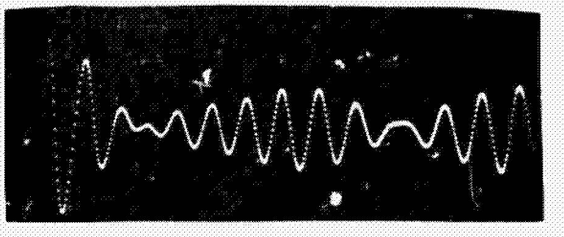

3.91 cm Crack

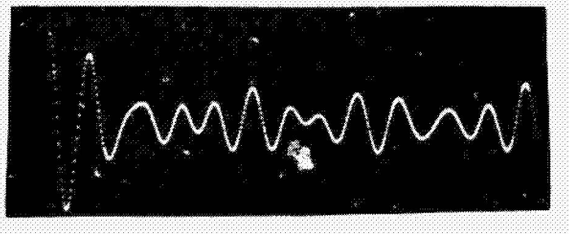

10.0 cm Crack

Figure 18.- Beam No. 1 at Station 4; Filter 8-15 KHz.

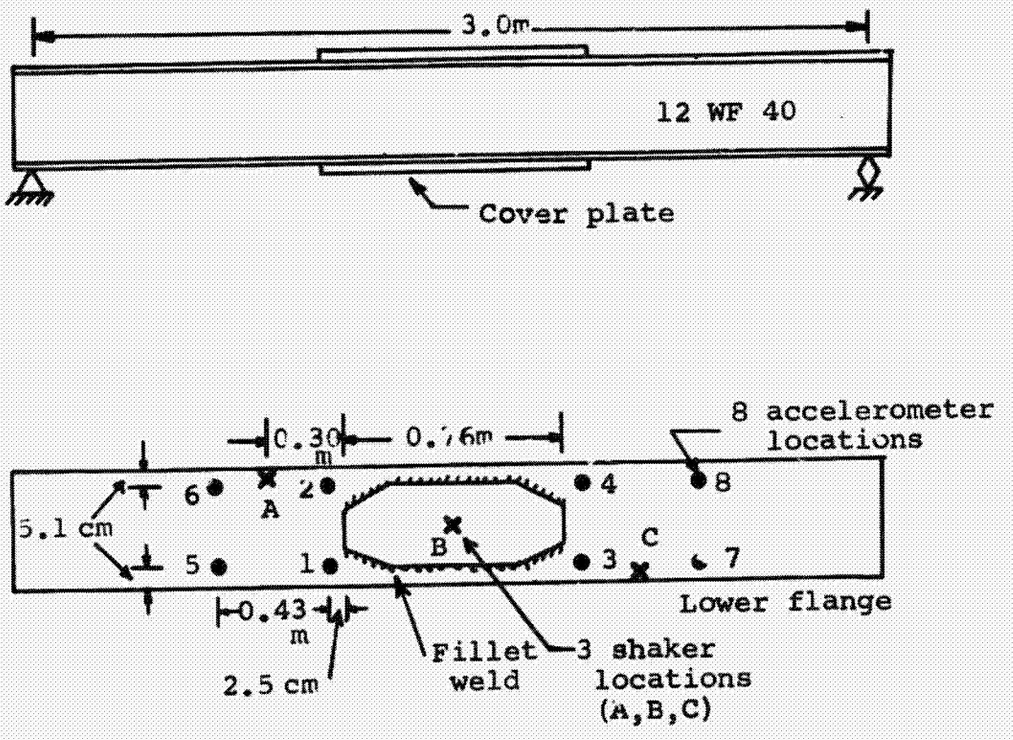

Figure 19.- Beam No. 2 configuration.

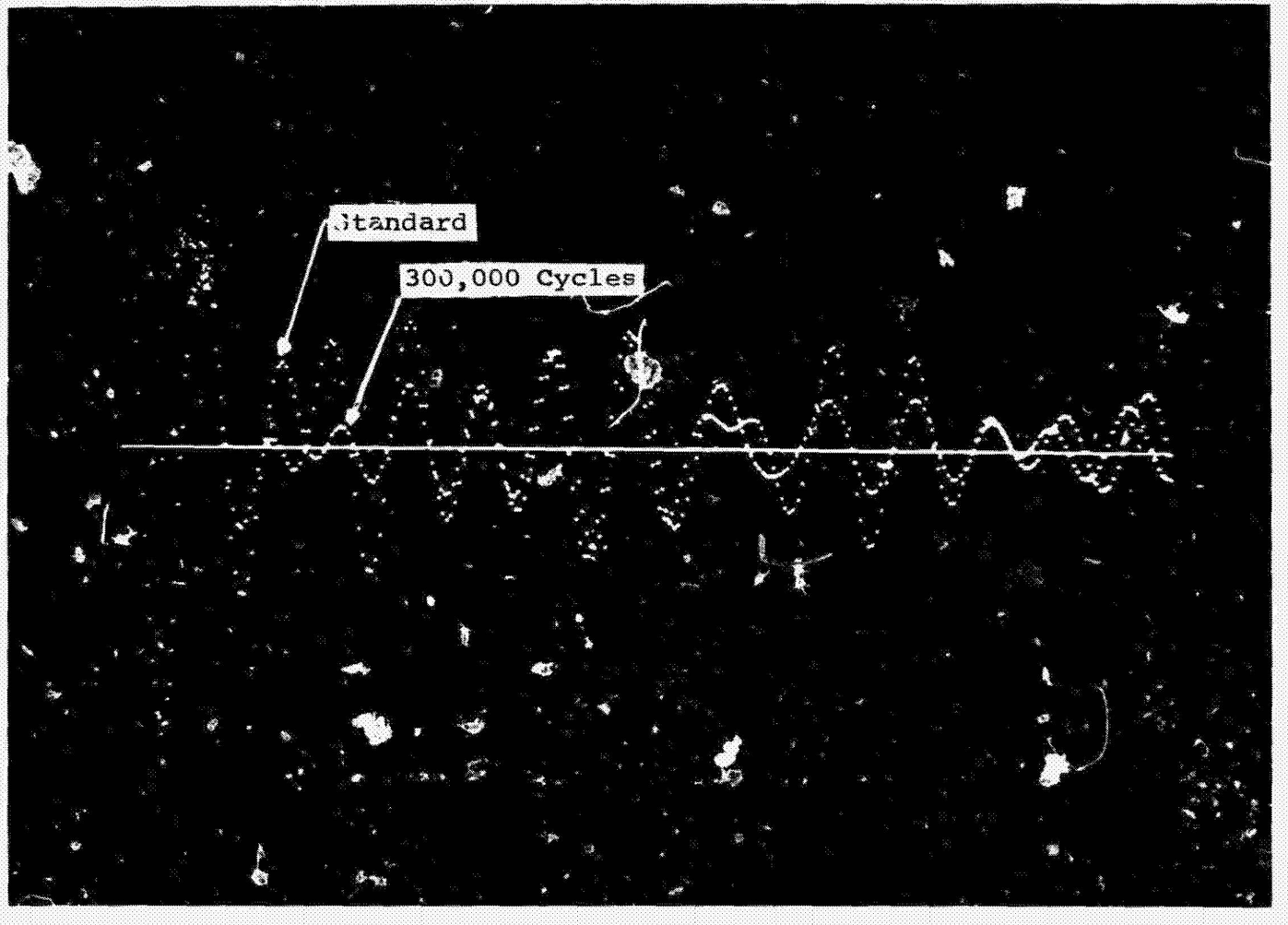

Figure 20.- Comparison of signatures at Station 2, Shaker at A; Filter 8 K-15 kHz.

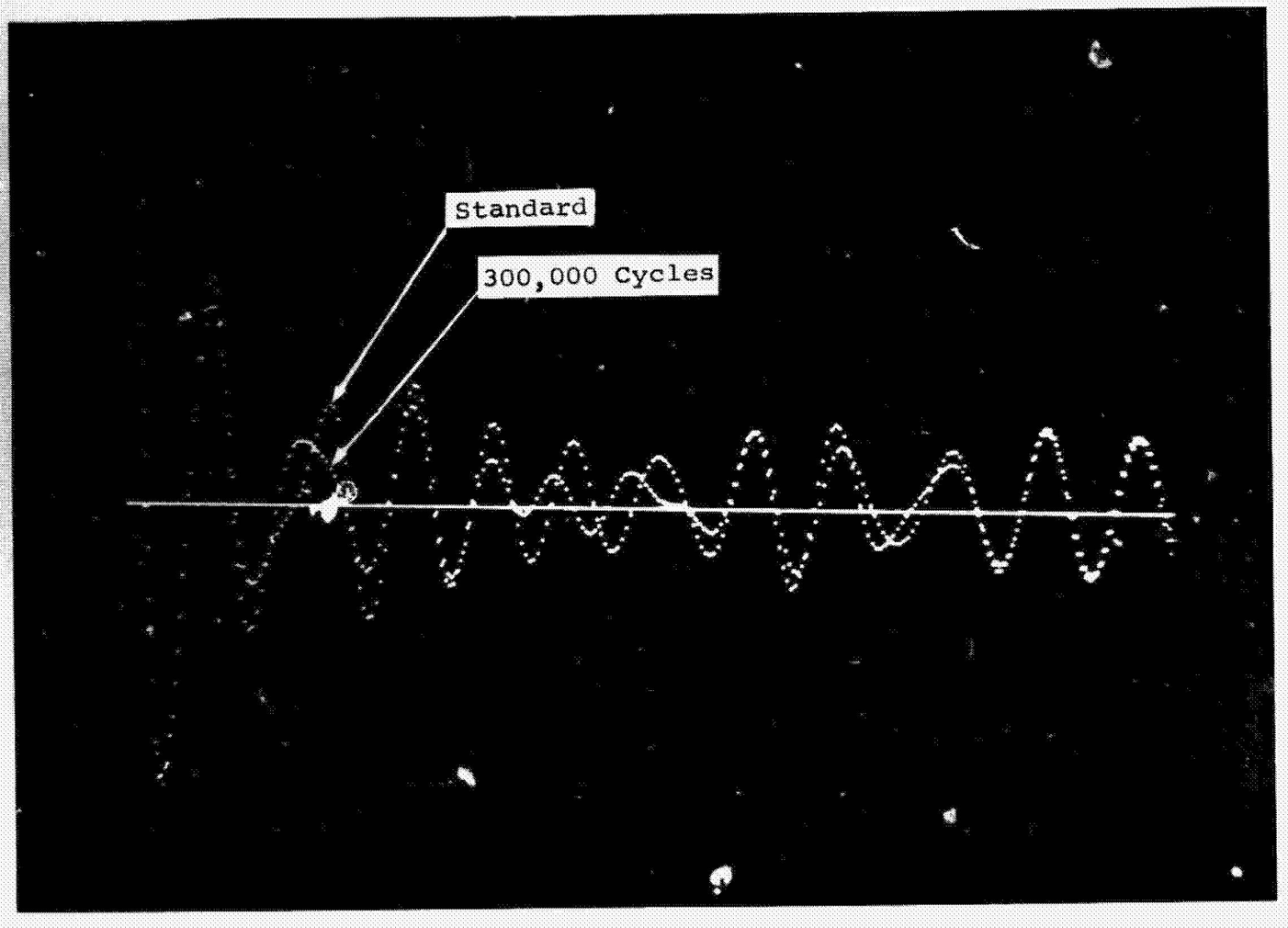

Figure 21.- Comparison of signatures at Station 6, Shaker at A; Filter 8 K-15 KHz.

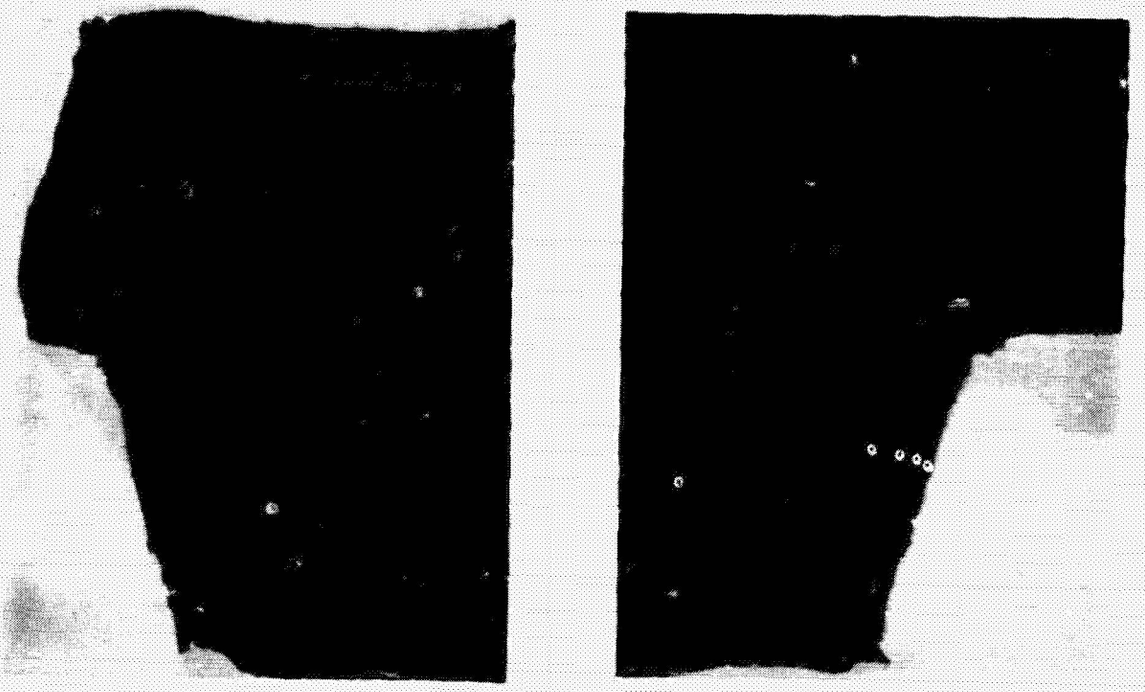

Station 1 Station 2

Station 3

Figure 22.- Impressions of final cracks.

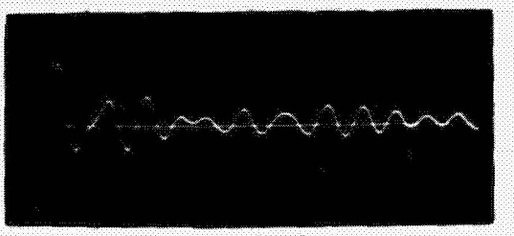

Standard

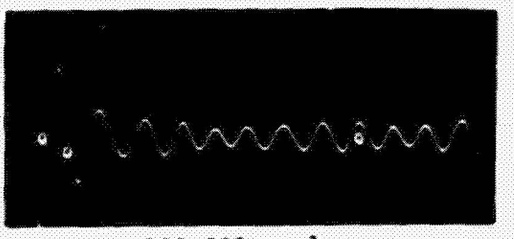

300,000 cycles

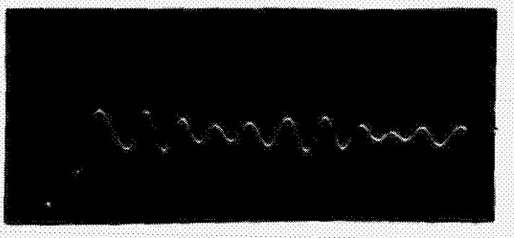

400,000 cycles

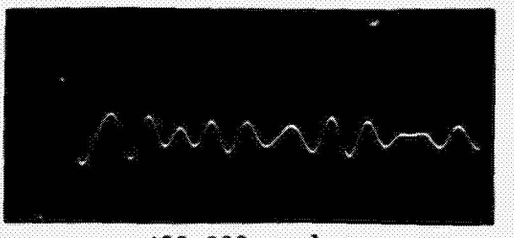

433,000 cycles

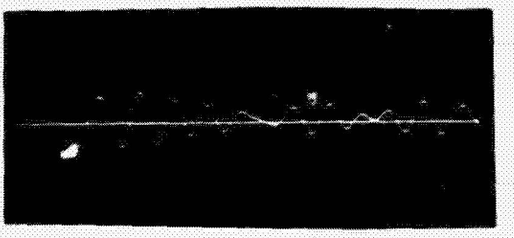

442,000 cycles

Figure 23.- Signature of Beam No. 2 at Station 1, Shaker at A.

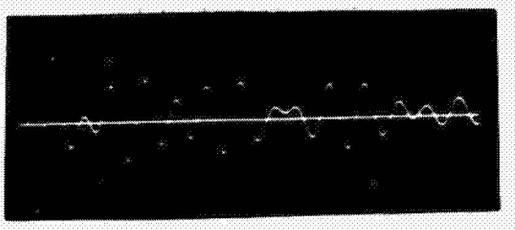

Standard

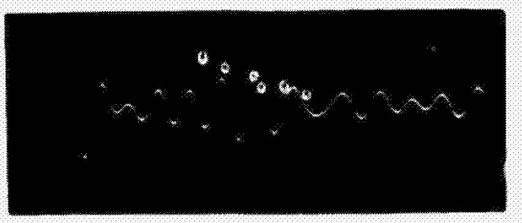

300,000 cycles

400,000 cycles

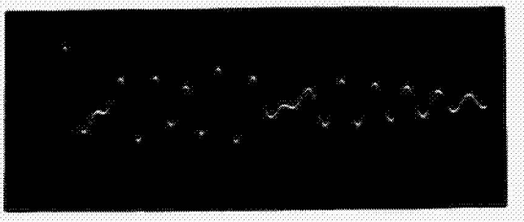

433,000 cycles

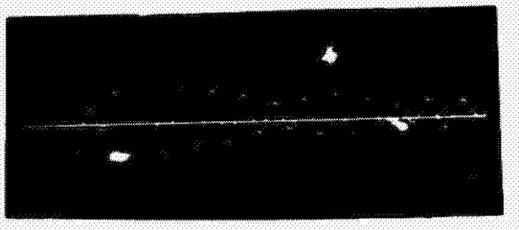

442,000 cycles

Figure 24.- Signature of Beam No. 2 at Station 2, Shaker at A.

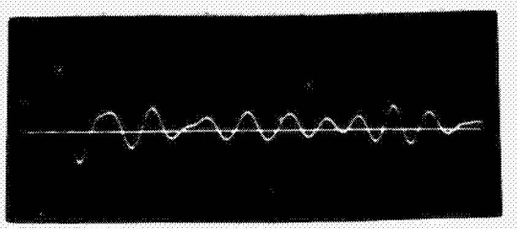

Standard

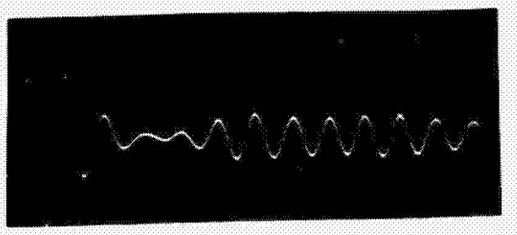

300,000 cycles

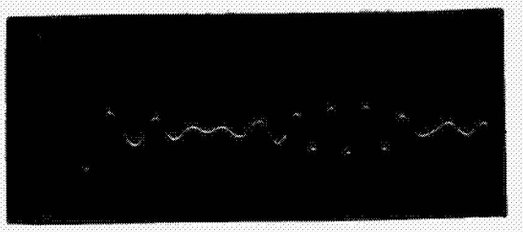

400,000 cycles

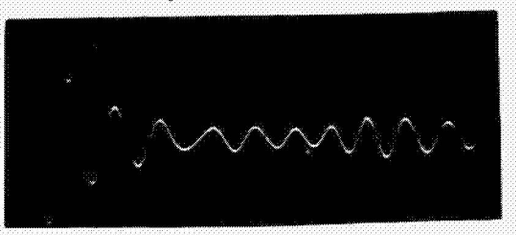

433,000 cycles

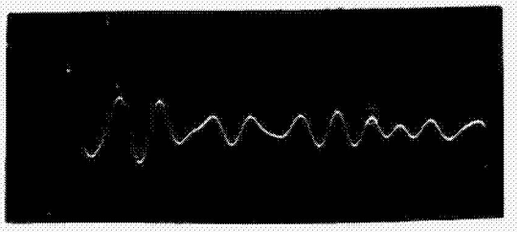

442,000 cycles

Figure 25.- Signature of Beam No. 2 at Station 3, Shaker at A.

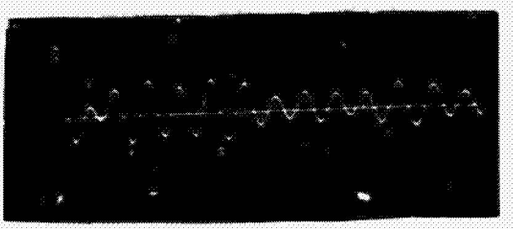

Standard

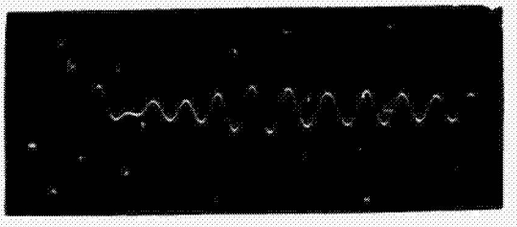

300,000 cycles

400,000 cycles

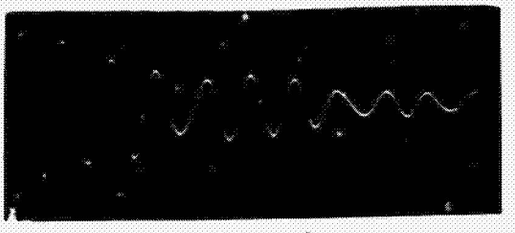

433,000 cycles

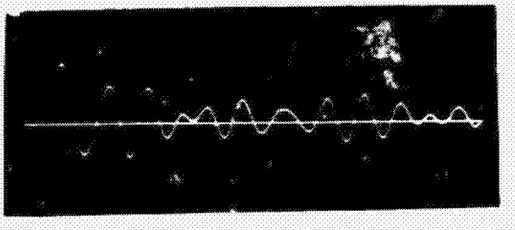

442,000 cycles

Figure 26.- Signature of Beam No. 2 at Station 4, Shaker at A.

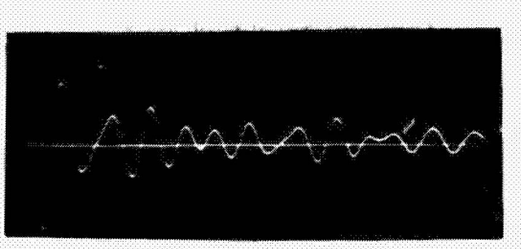

Standard

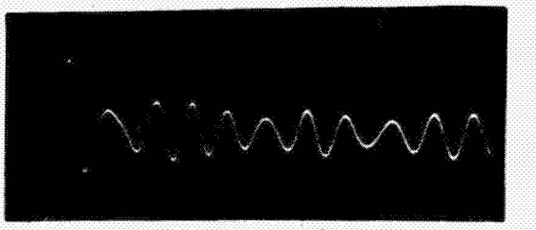

300,000 cycles

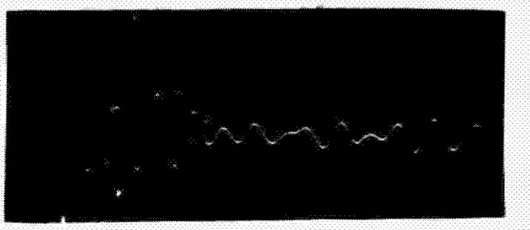

400,000 cycles

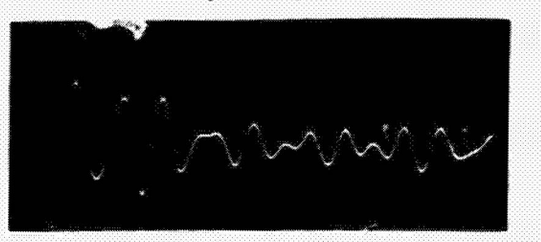

433,000 cycles

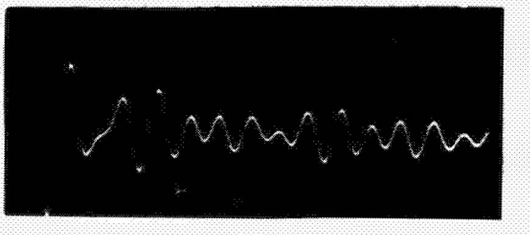

442,000 cycles

Figure 27.- Signature of Beam No. 2 at Station 5, Shaker at A.

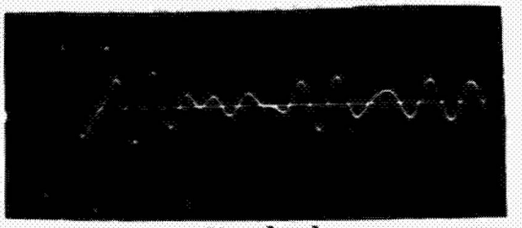

Standard

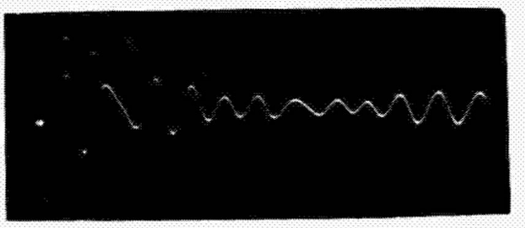

300,000 cycles

400,000 cycles

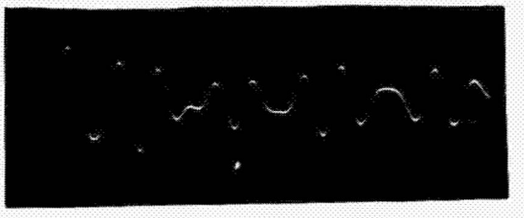

433,000 cycles

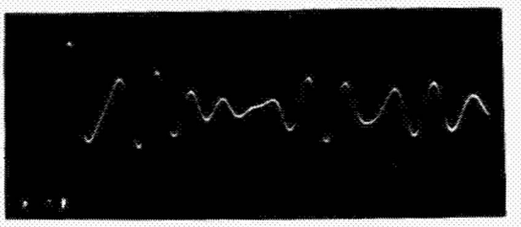

442,000 cycles

Figure 28.- Signature of Beam No. 2 at Station 6, Shaker at A.

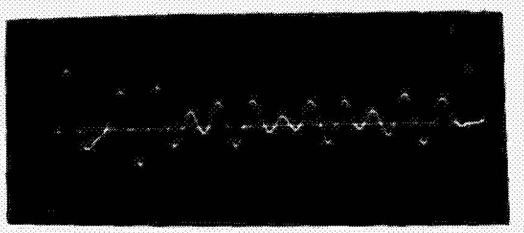

Standard

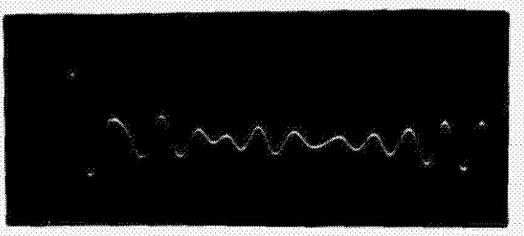

300,000 cycles

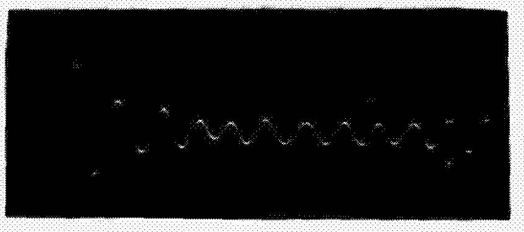

400,000 cycles

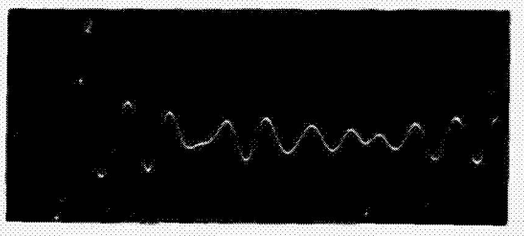

433,000 cycles

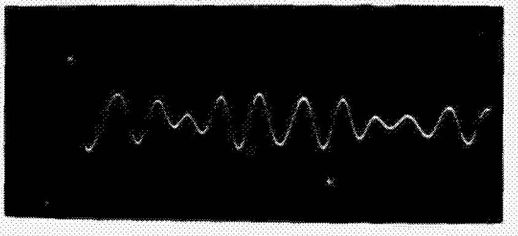

442,000 cycles

Figure 29.- Signature of Beam No. 2 at Station 7, Shaker at A.

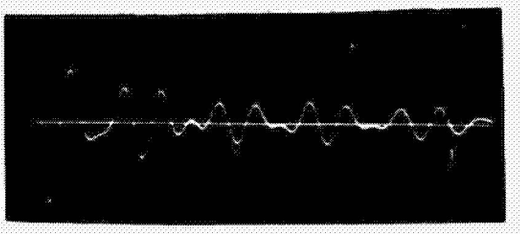

Standard

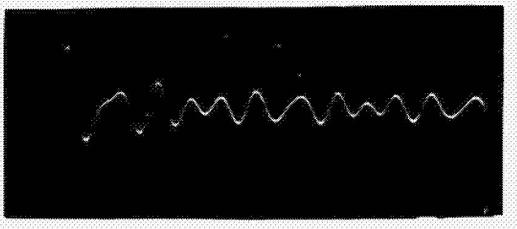

300,000 cycles

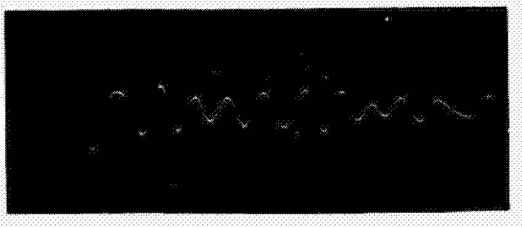

400,000 cycles

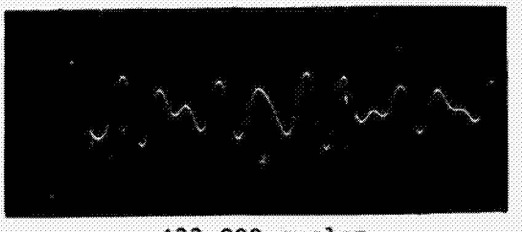

433,000 cycles

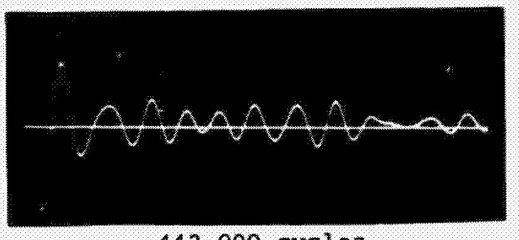

442,000 cycles

Figure 30.- Signature of Beam No. 2 at Station 8, Shaker at A.

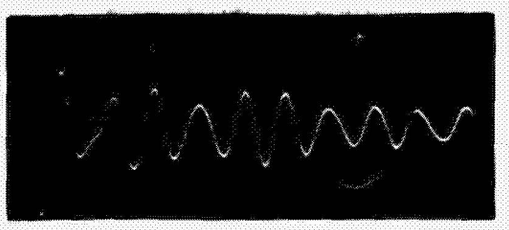

Standard

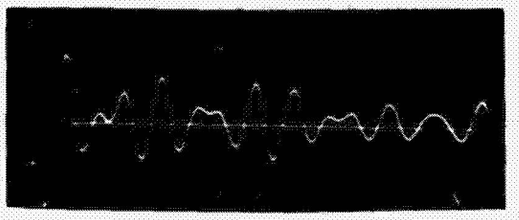

300,000 cycles

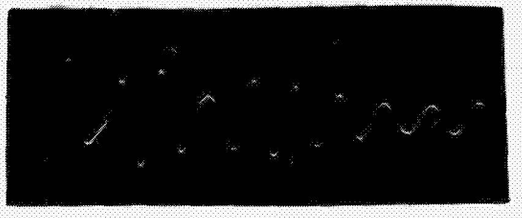

400,000 cycles

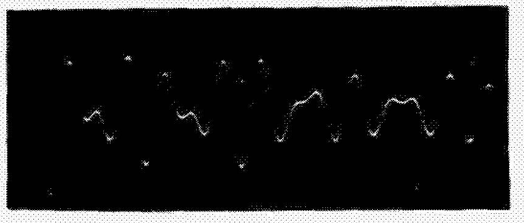

433,000 cycles

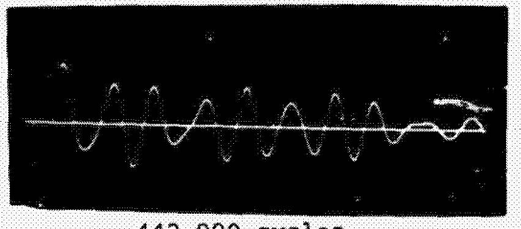

442,000 cycles

Figure 31.- Signature of Beam No. 2 at Station 1, Shaker at B.

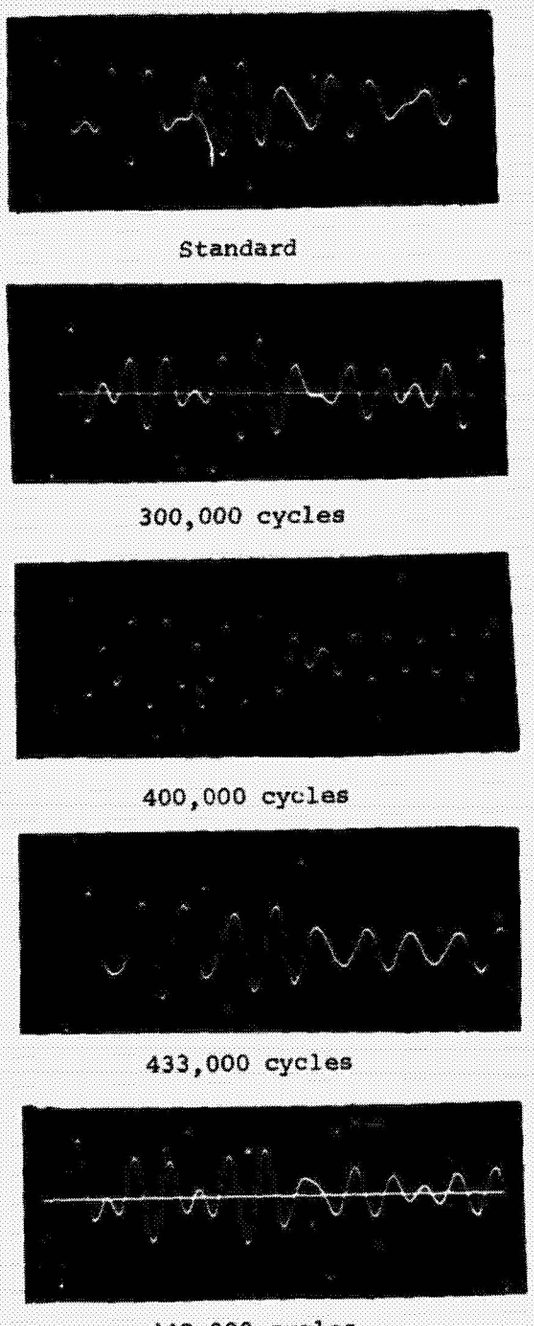

Figure 32.- Signature of Beam No. 2 at Station 2, Shaker at B.

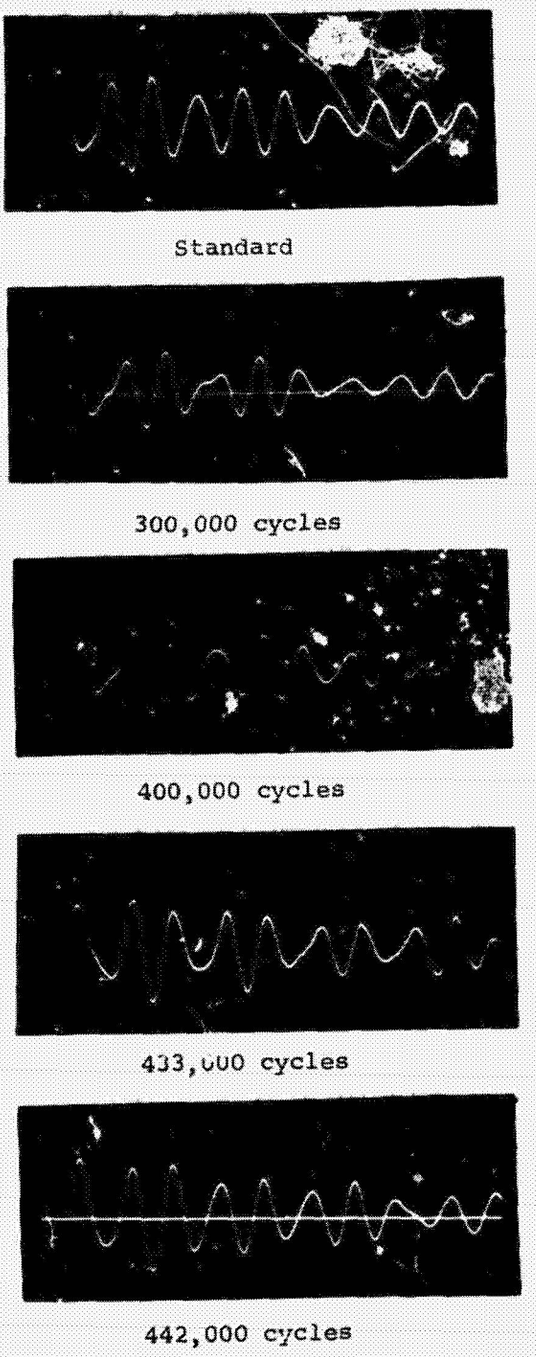

Figure 33.- Signature of Beam No. 2 at Station 3, Shaker at B.

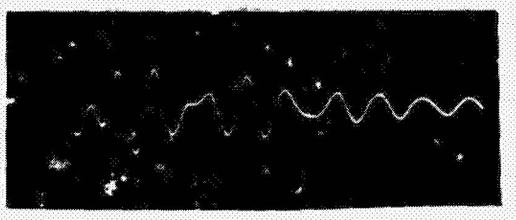

Standard

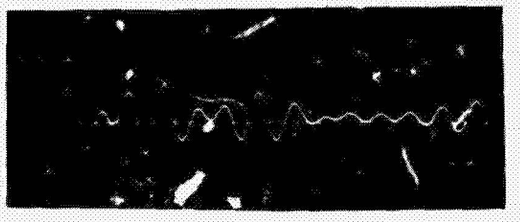

300,000 cycles

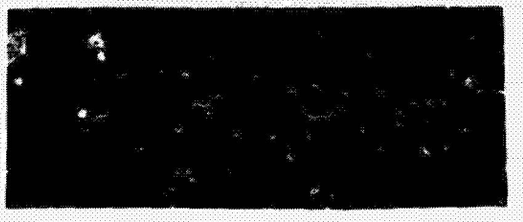

400,000 cycles

433,000 cycles

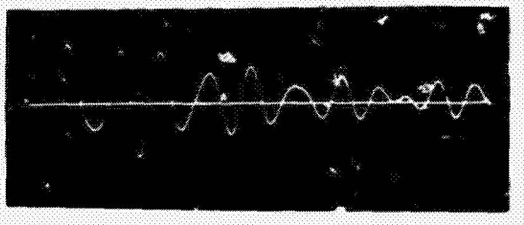

442,000 cycles

Figure 34.- Signature of Beam No. 2 at Station 4, Shaker at B.

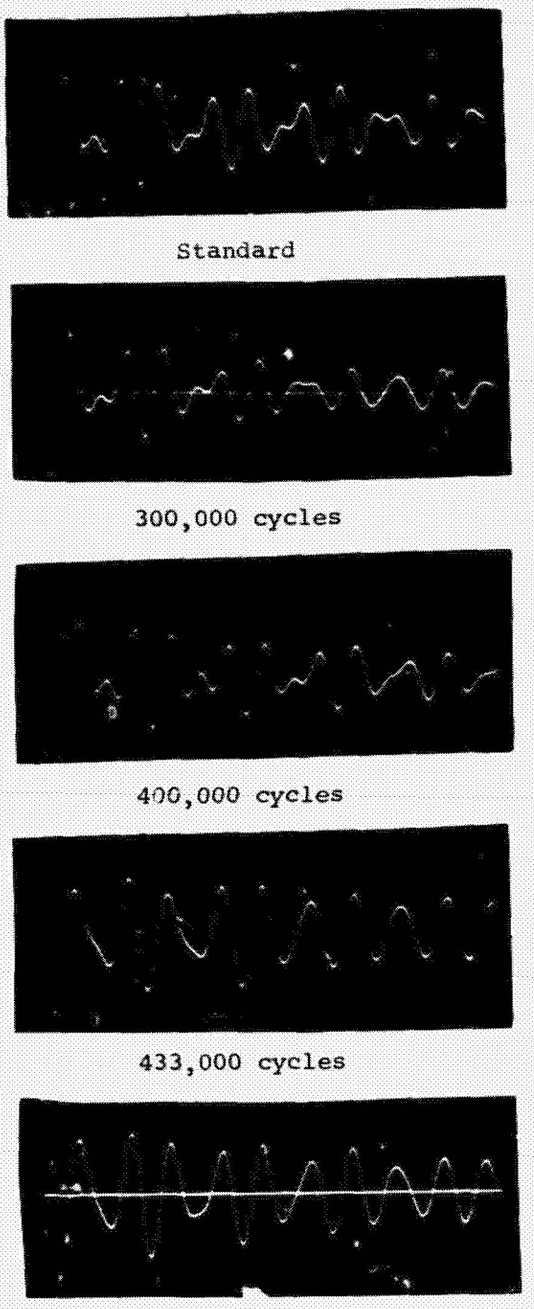

Figure 35.- Signature of Beam No. 2 at Station 5, Shaker at B.

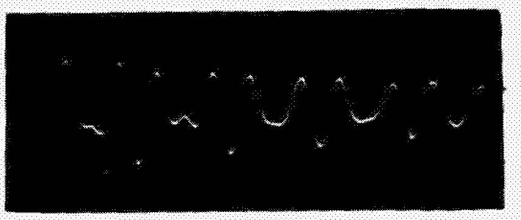

Standard

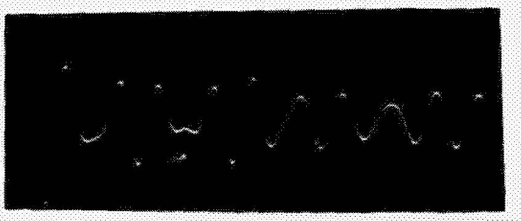

300,000 cycles

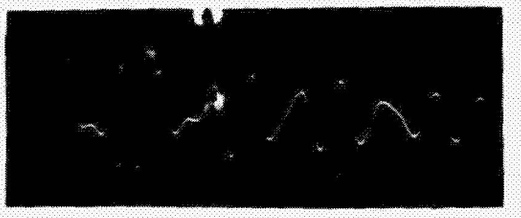

400,000 cycles

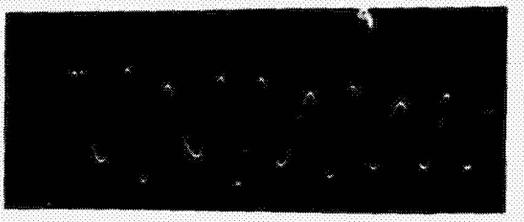

433,000 cycles

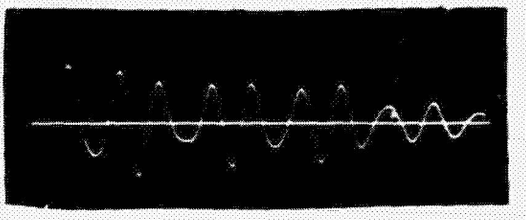

442,000 cycles

Figure 36.- Signature of Beam No. 2 at Station 6, Shaker at B.

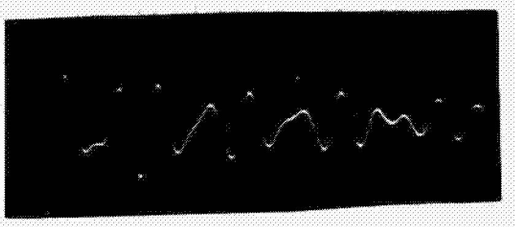

Standard

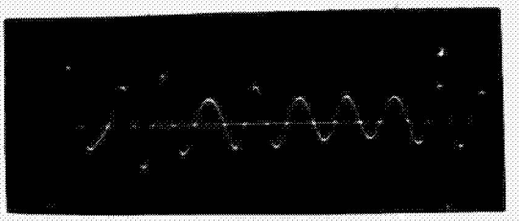

300,000 cycles

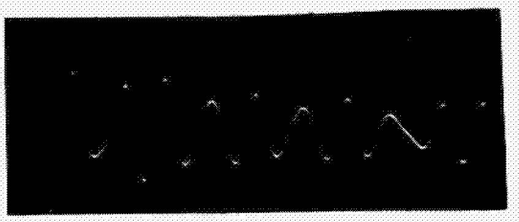

400,000 cycles

433,000 cycles

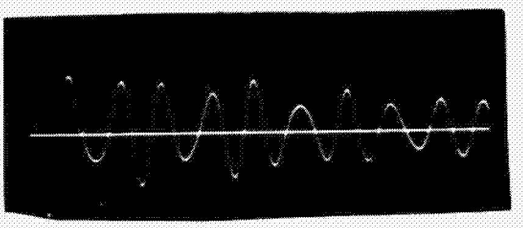

442,000 cycles

Figure 37.- Signature of Beam No. 2 at Station 7, Shaker at B.

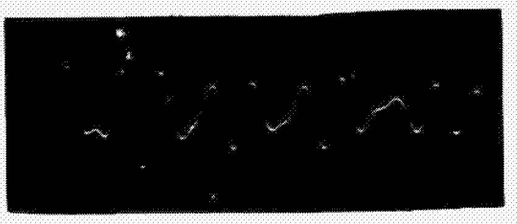

Standard

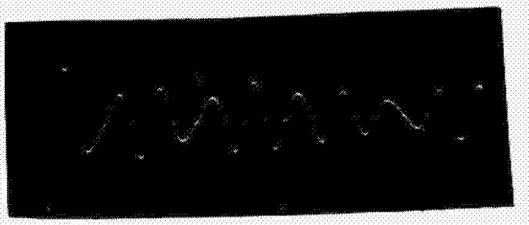

300,000 cycles

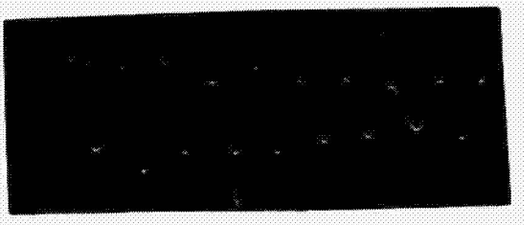

400,000 cycles

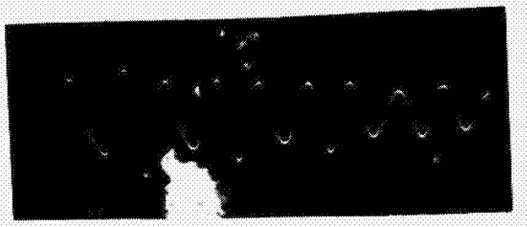

433,000 cycles

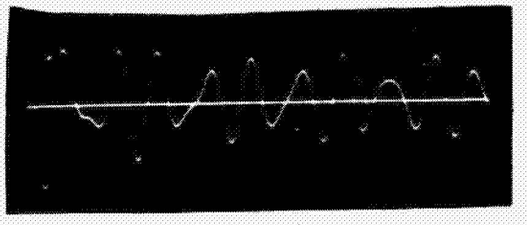

442,000 cycles

Figure 38.- Signature of Beam No. 2 at Station 8, Shaker at B.

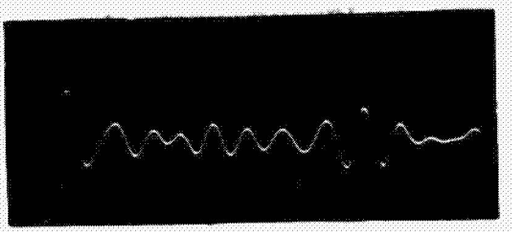

Standard

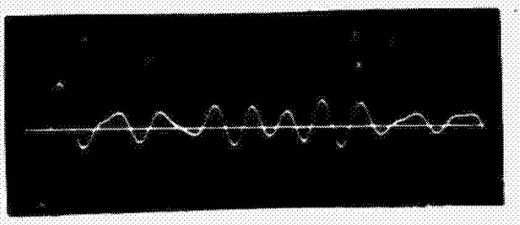

300,000 cycles

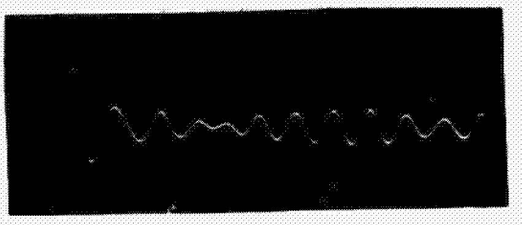

400,000 cycles

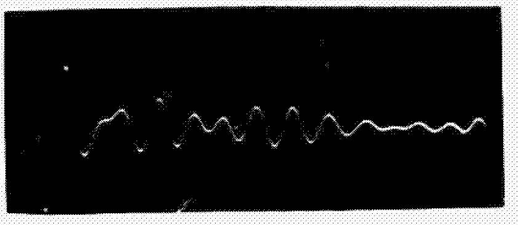

433,000 cycles

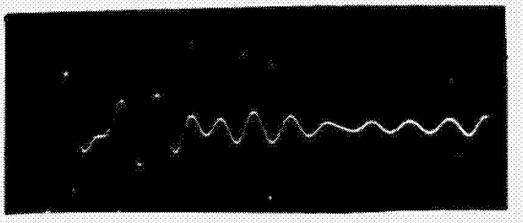

442,000 cycles

Figure 39.- Signature of Beam No. 2 at Station 1, Shaker at C.

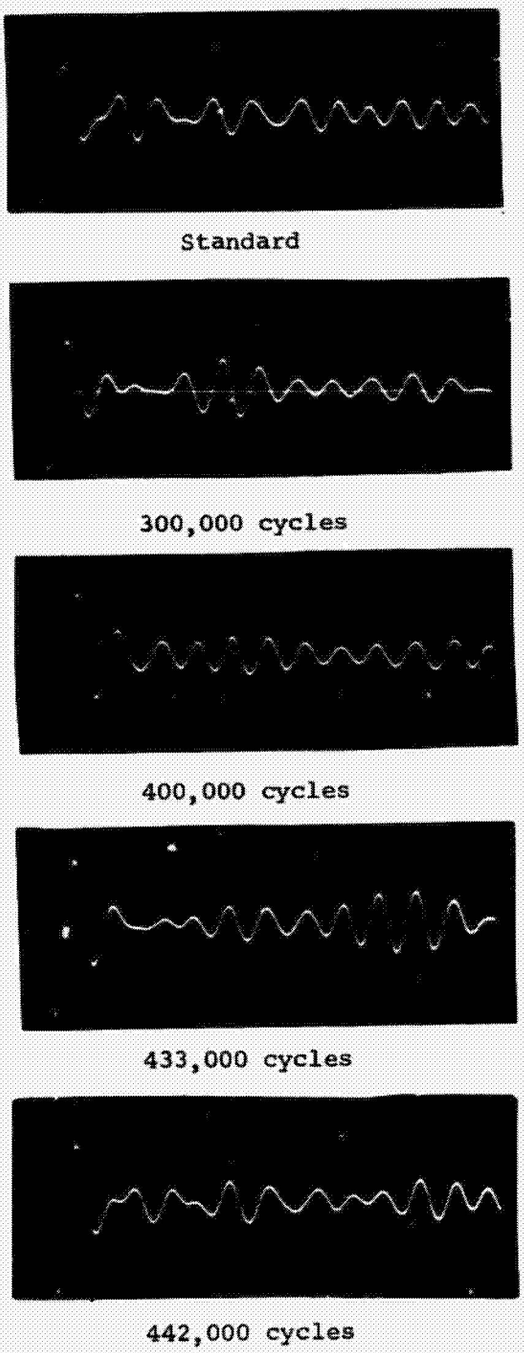

Figure 40.- Signature of Beam No. 2 at Station 2, Shaker at C.

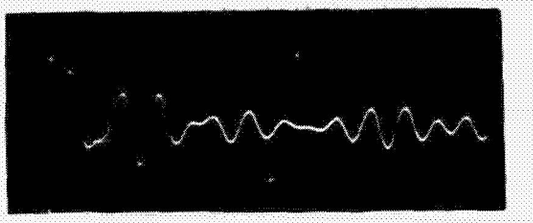

Standard

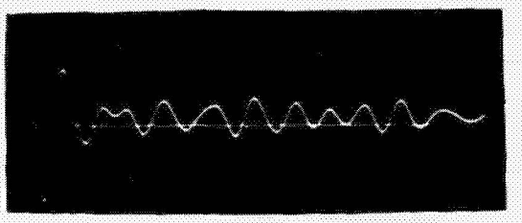

300,000 cycles

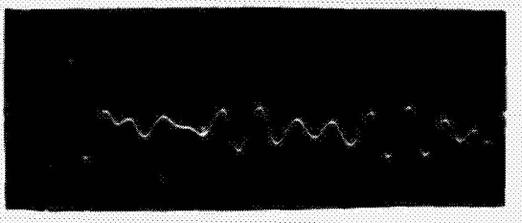

400,000 cycles

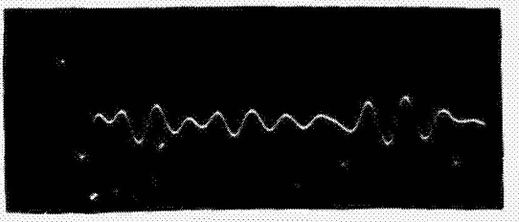

433,000 cycles

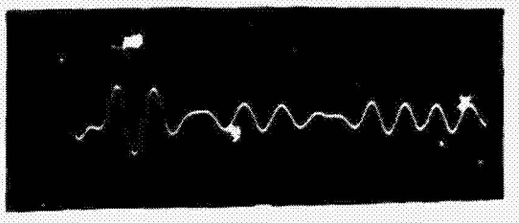

442,000 cycles

Figure 41.- Signature of Beam No. 2 at Station 3, Shaker at C.

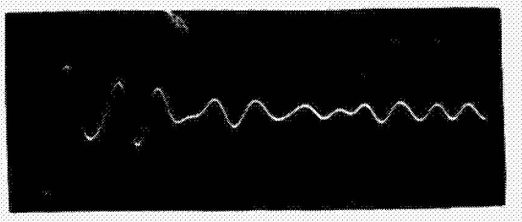

Standard

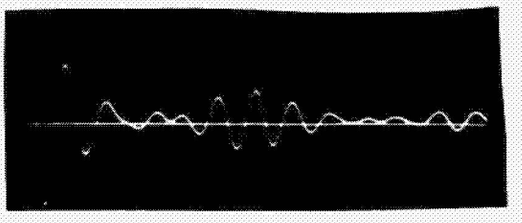

300,000 cycles

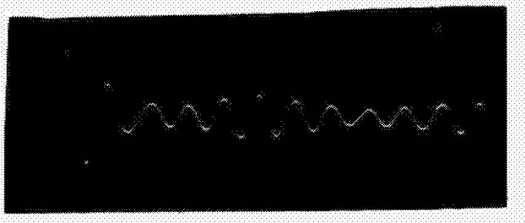

400,000 cycles

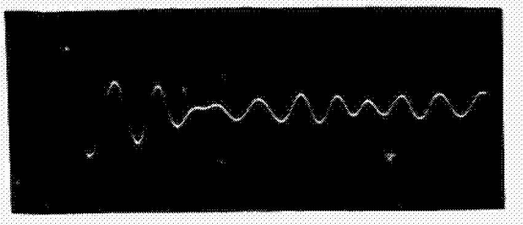

433,000 cycles

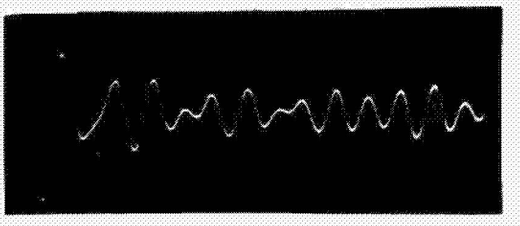

442,000 cycles

Figure 42.- Signature of Beam No. 2 at Station 4, Shaker at C.

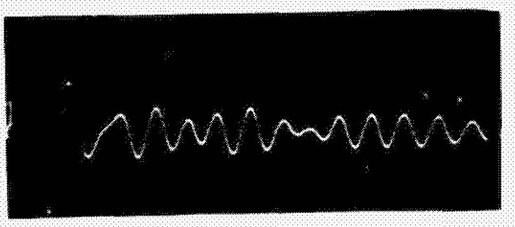

Standard

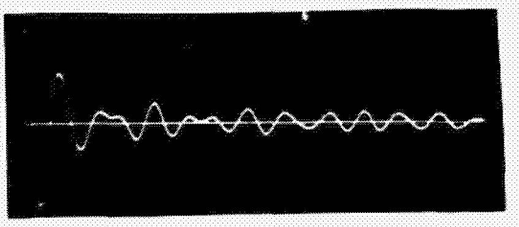

300,000 cycles

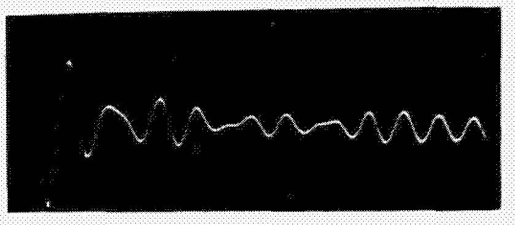

400,000 cycles

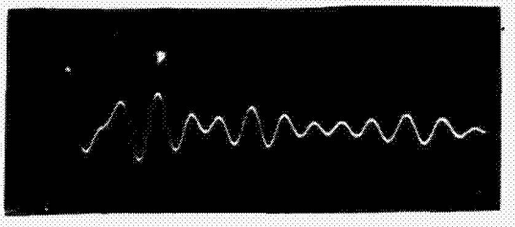

433,000 cycles

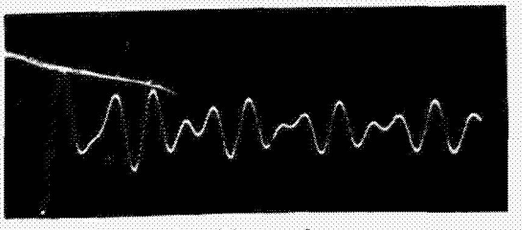

442,000 cycles

Figure 43.- Signature of Beam No. 2 at Station 5, Shaker at C.

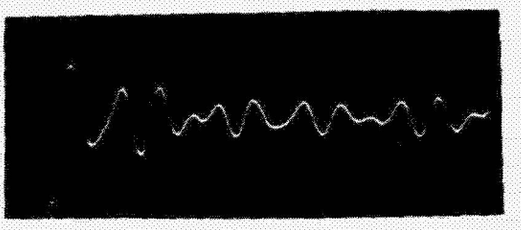

Standard

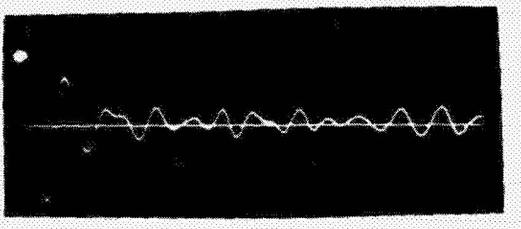

300,000 cycles

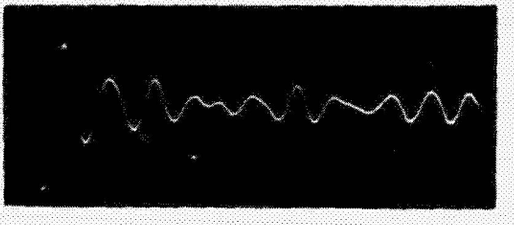

400,000 cycles

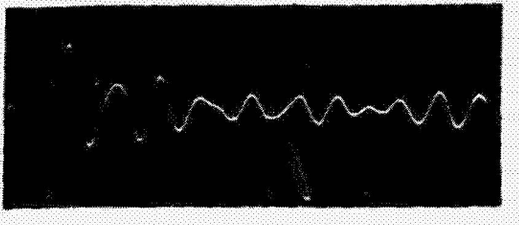

433,000 cycles

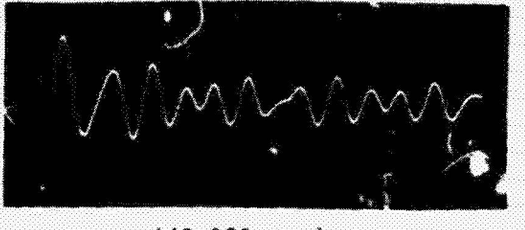

442,000 cycles

Figure 44.- Signature of Beam No. 2 at Station 6, Shaker at C.

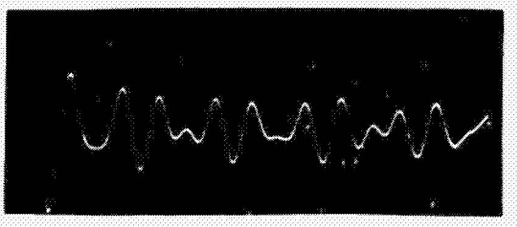

Standard

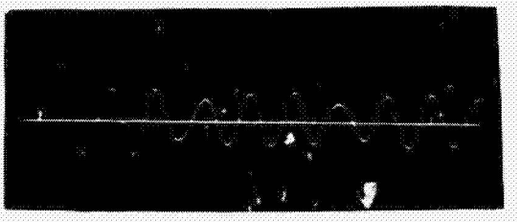

300,000 cycles

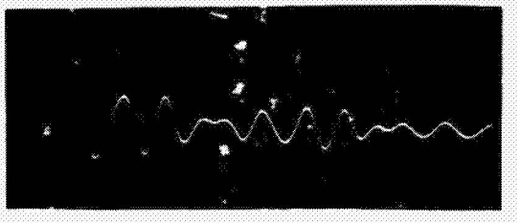

400,000 cycles

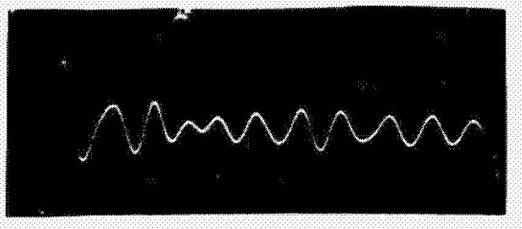

433,000 cycles

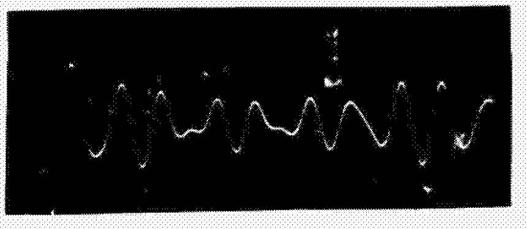

442,000 cycles

Figure 45.- Signature of Beam No. 2 at Station 7, Shaker at C.

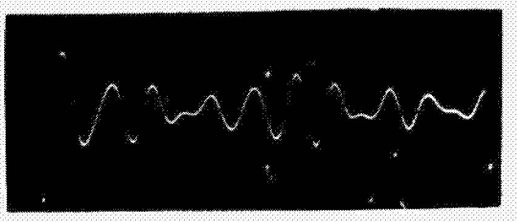

Standard

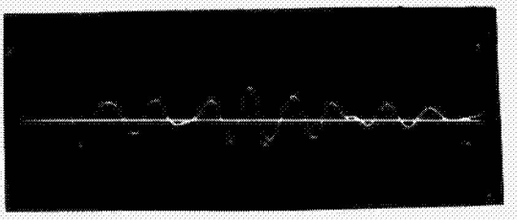

300,000 cycles

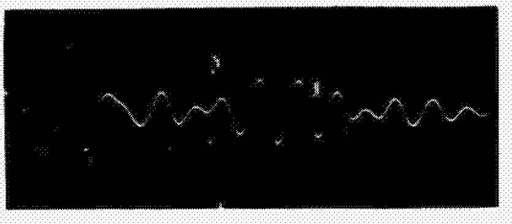

400,000 cycles

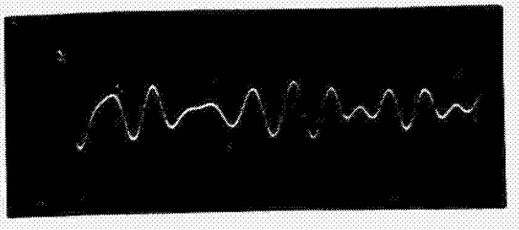

433,000 cycles

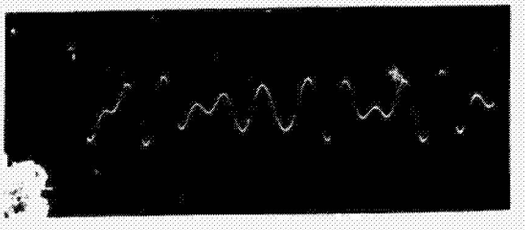

442,000 cycles

Figure 46.- Signature of Beam No. 2 at Station 8, Shaker at C.

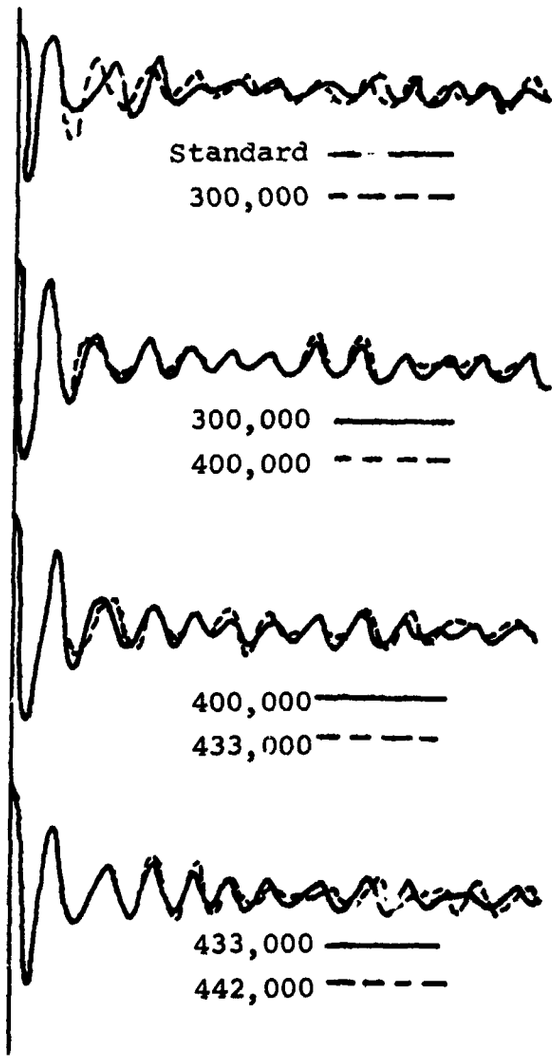

Figure 47.- Signatures of Beam No. 2, Station 1 superposed.

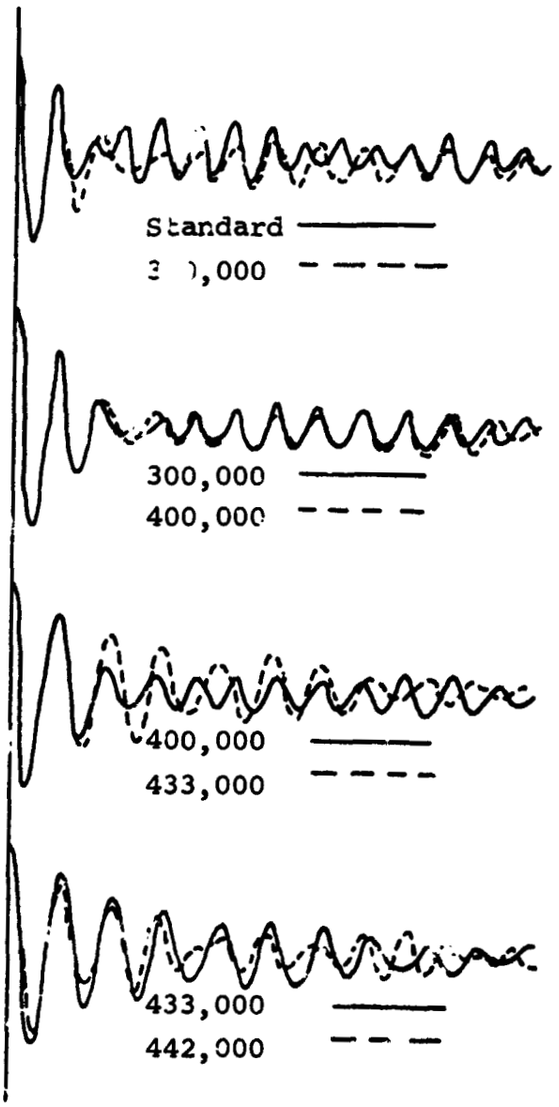

F re 48.- Signatures of Beam No. 2, Station 4 superpo ed.

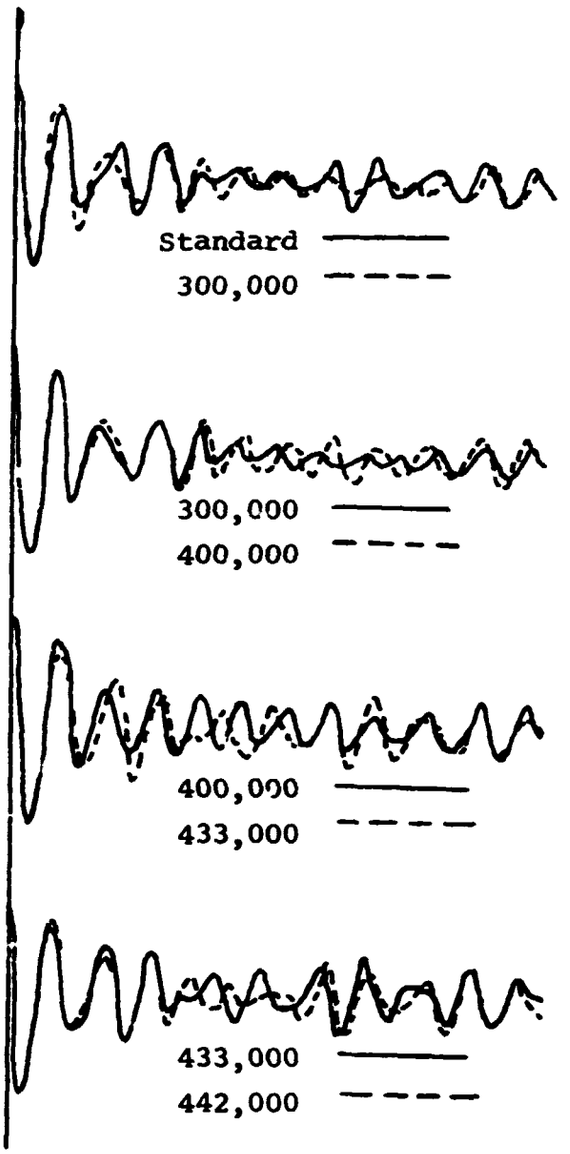

Figure 49.- Signatures of Beam No. 2, Station 6 superposed.

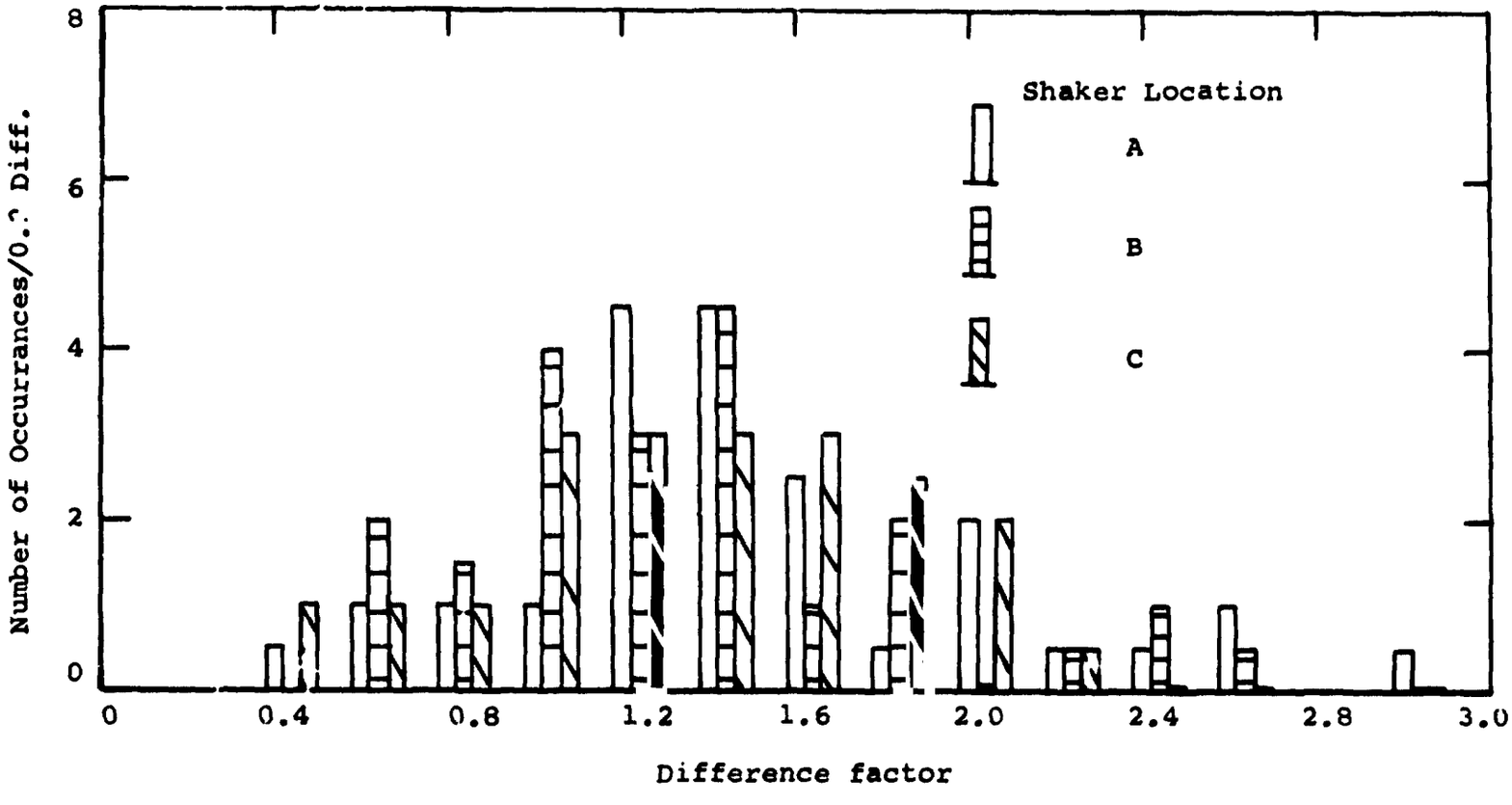

Figure 50.- Distribution of difference factors for three shaker locations.

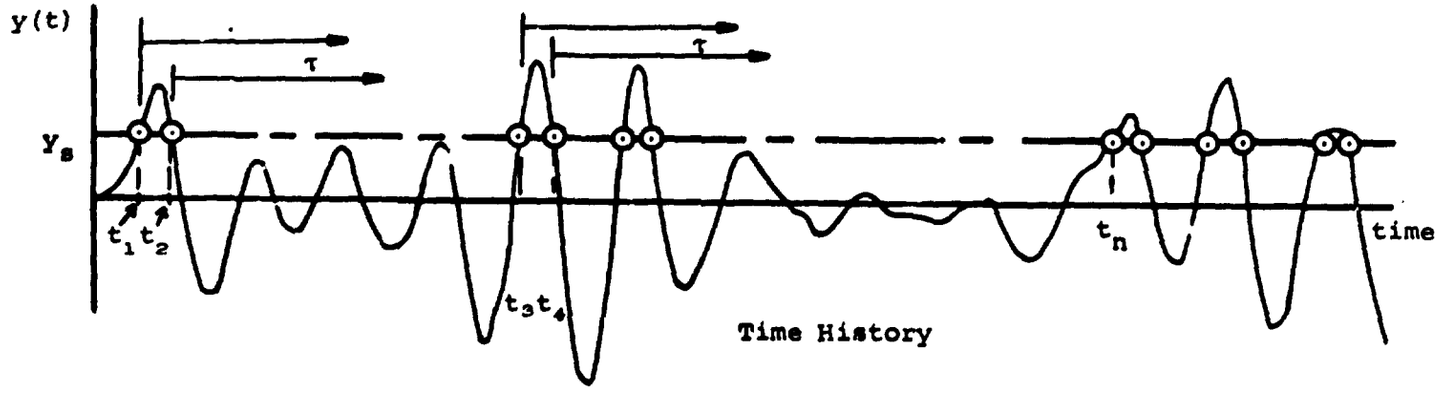

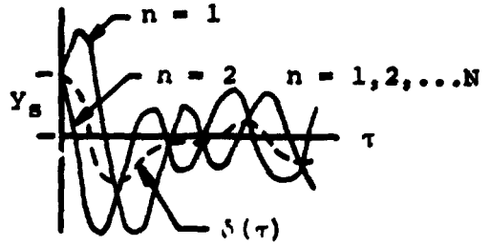

Ensemble Average

$$\delta(\tau) = \frac{1}{N}\sum_{n=1}^{N} y(t_n + \tau)$$

where t_n = t's when $y = y_s$

Randomdec Signature

Figure 51.- Evolution of Randomdec signature.

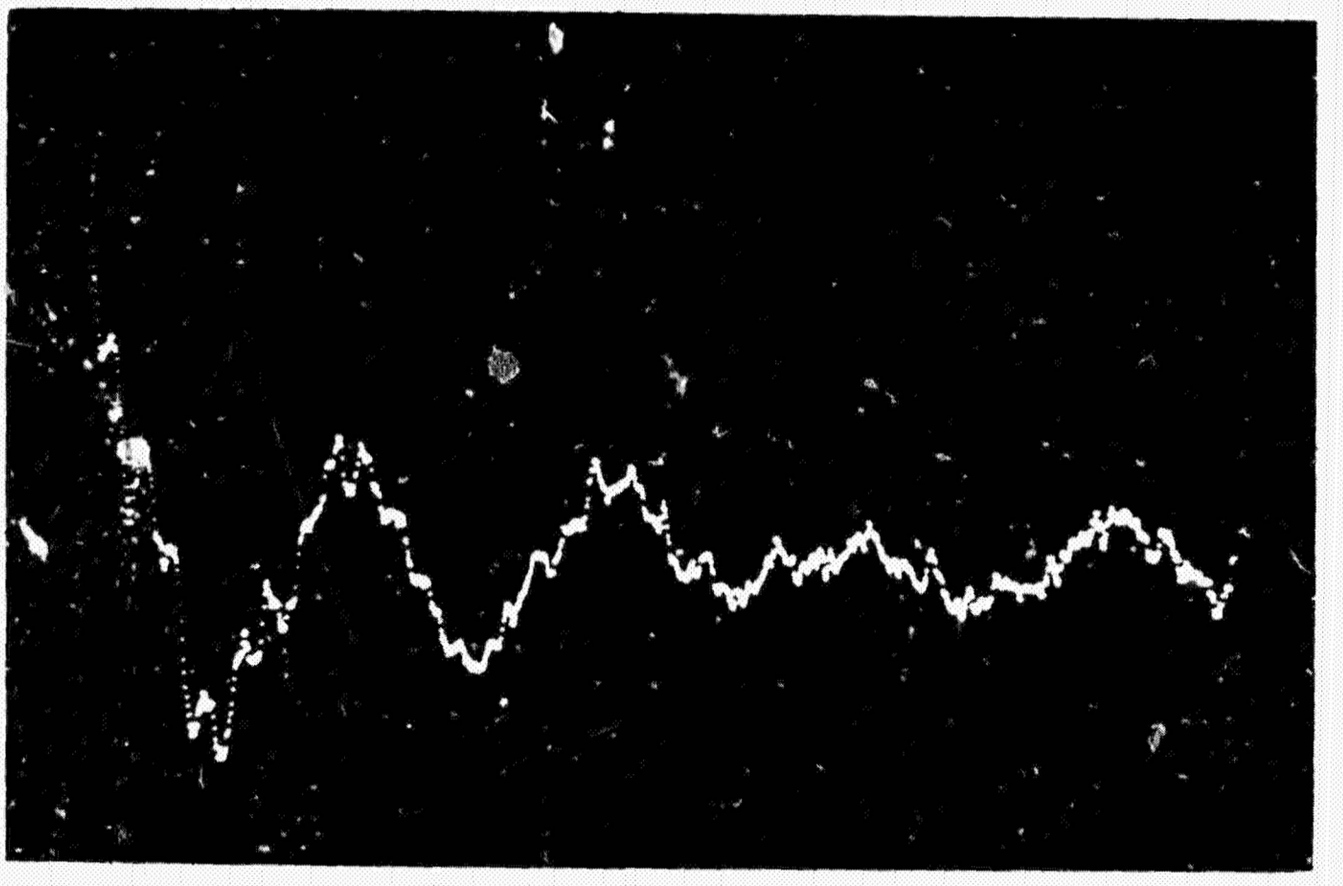

Figure 52.- Unfiltered signature.

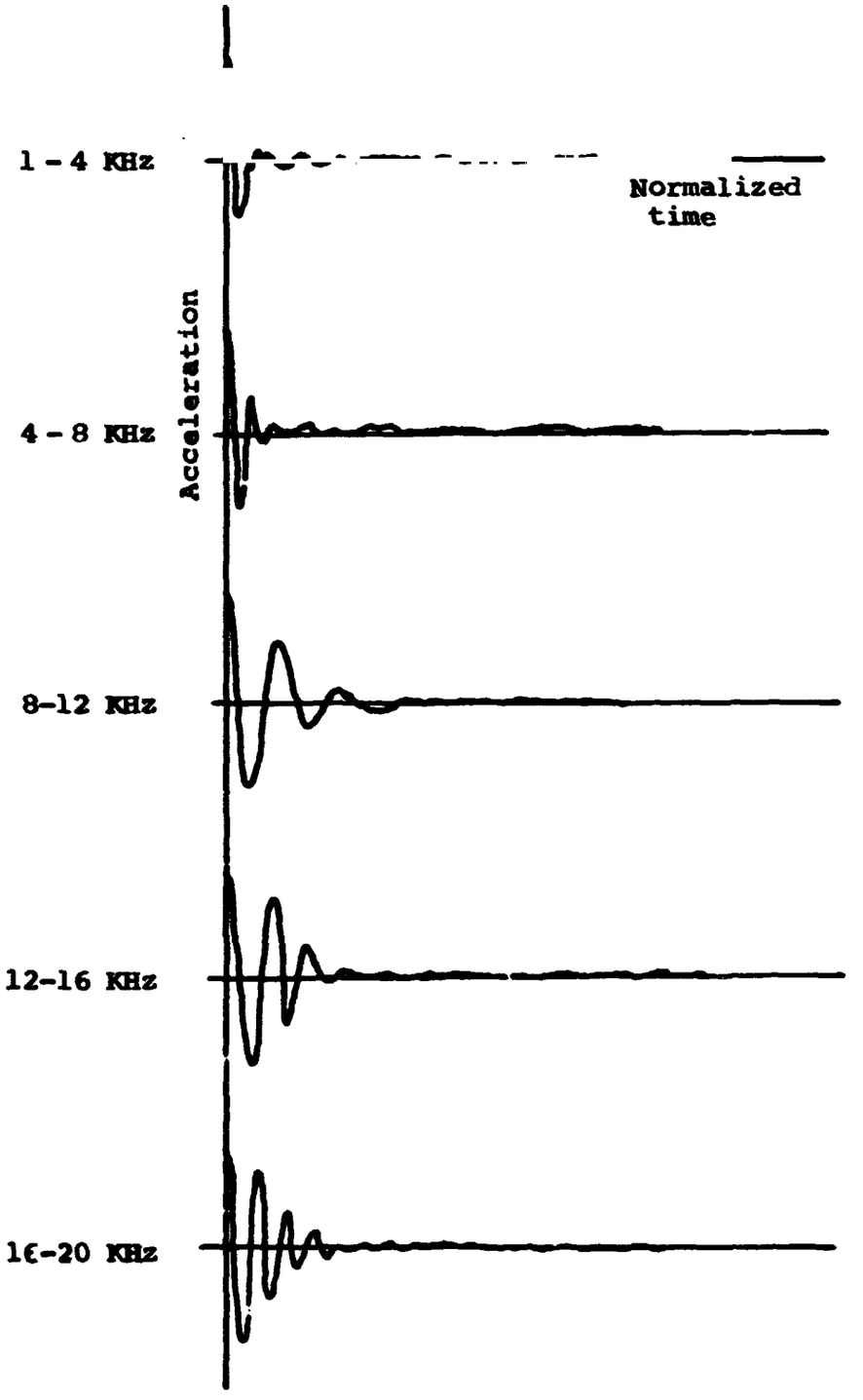

Figure 53.- Signatures . filtered broadband noise.

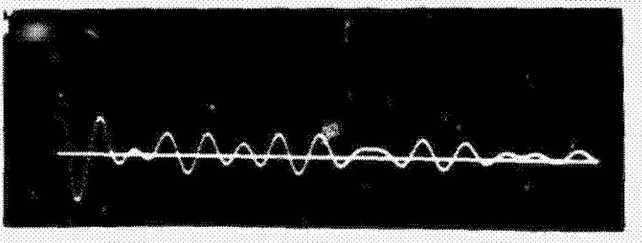

Bias Level = 0.1

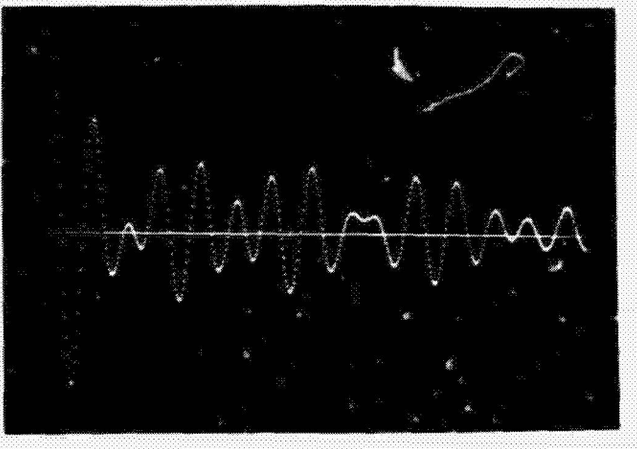

Bias Level = 0.3

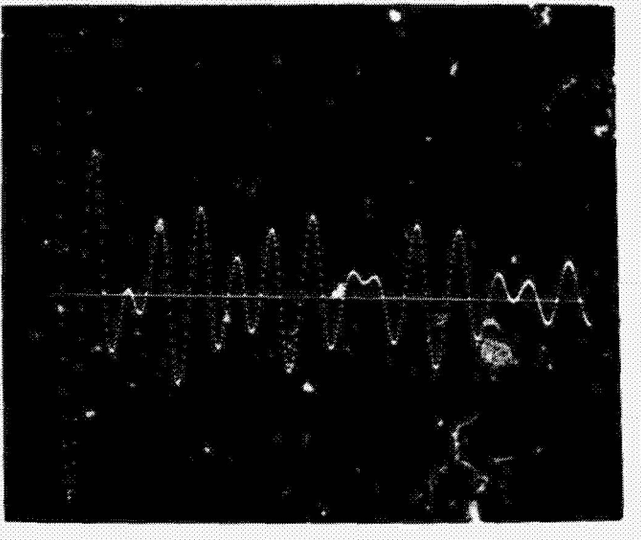

Bias Level = 0.4

Figure 54.- Signatures at Station 1 for different bias levels.

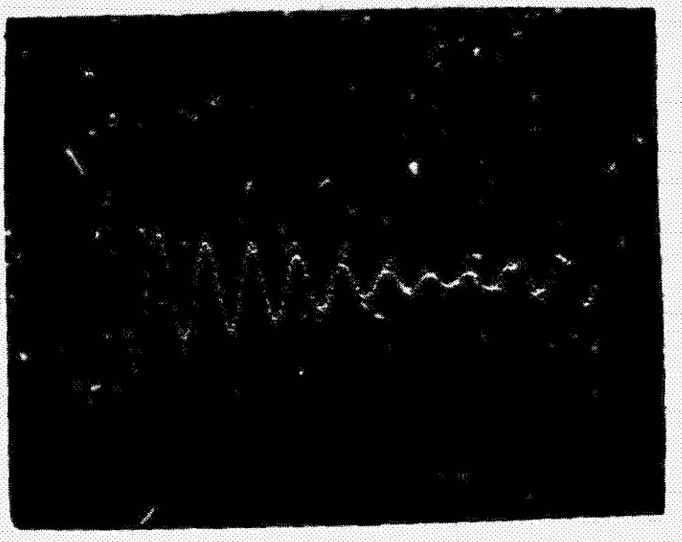

4 Signatures, 512 Samples Each

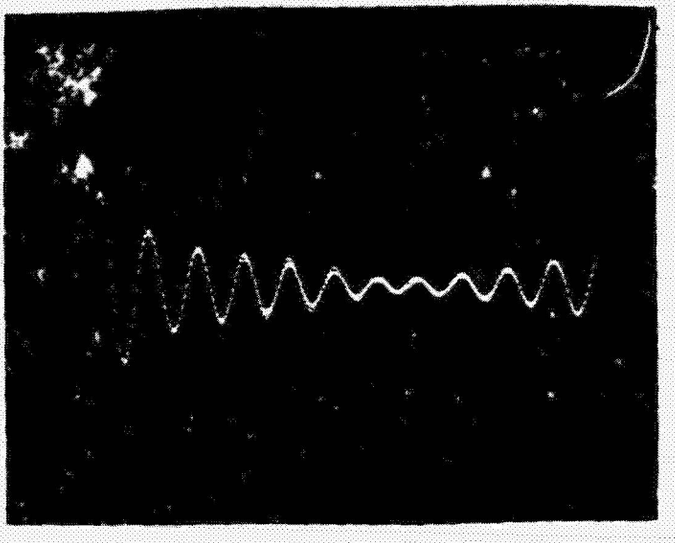

4 Signatures, 4096 Samples Each

Figure 55.- Variation of repeatability with record length.

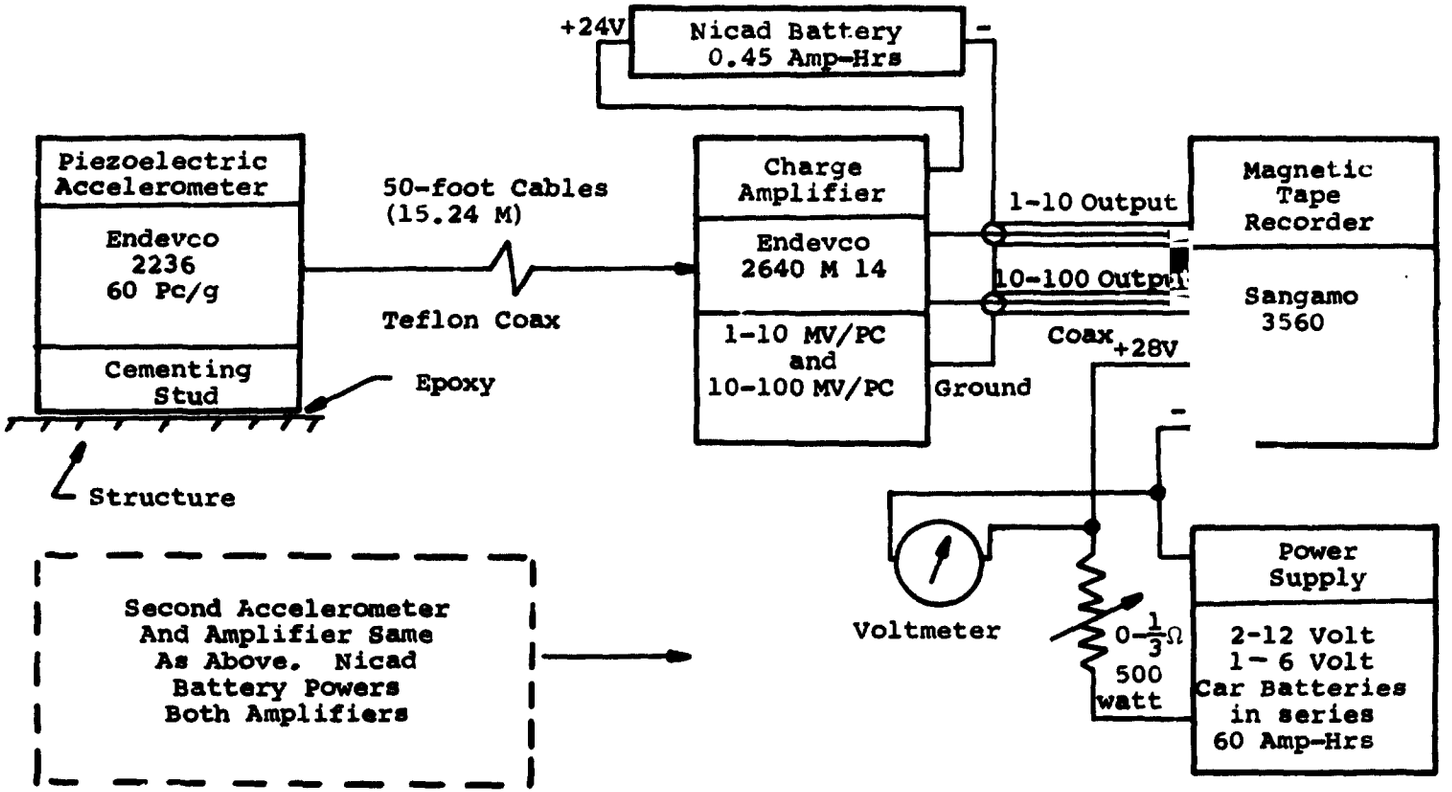

Figure 56.- Field equipment.

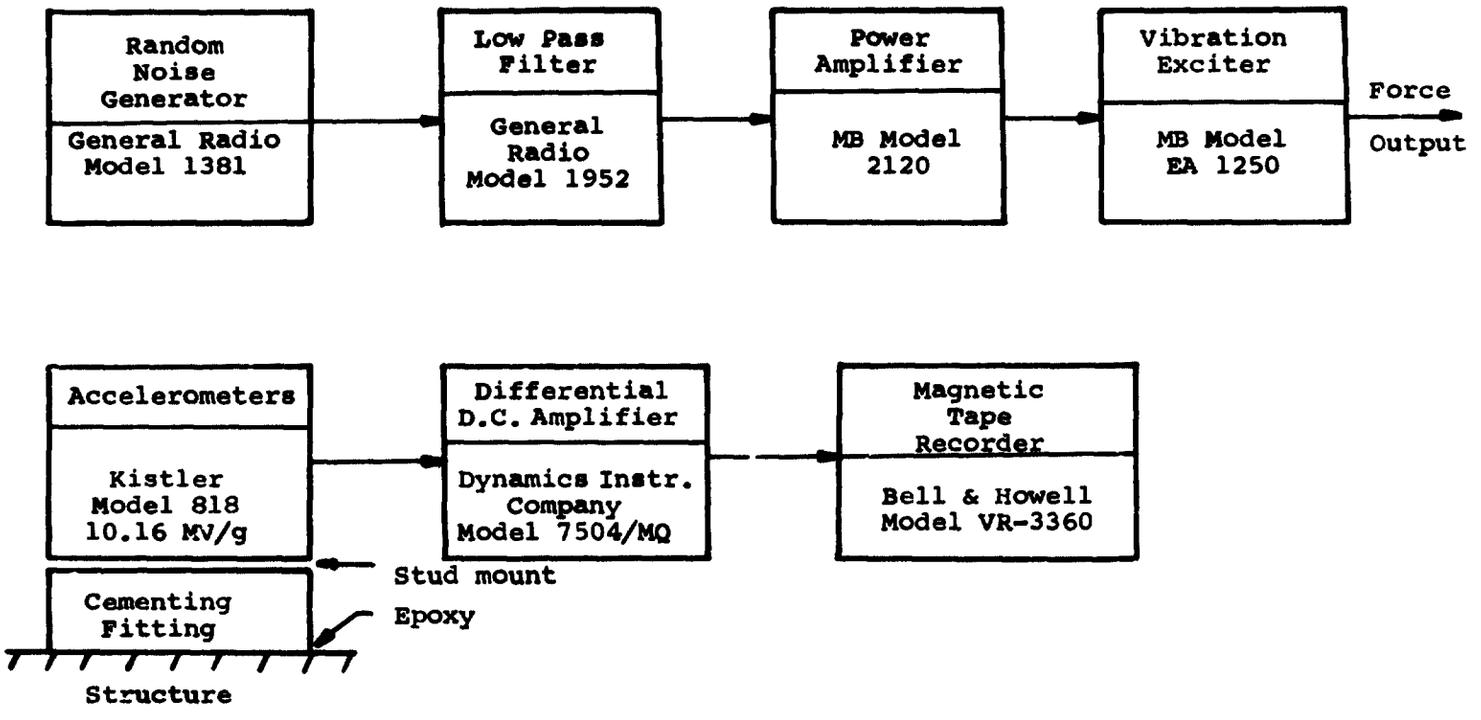

Figure 57.- Laboratory equipment.

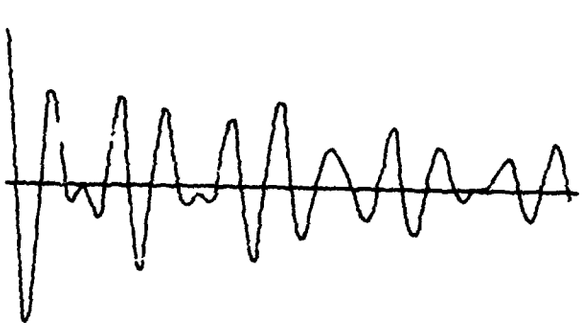

Station 2

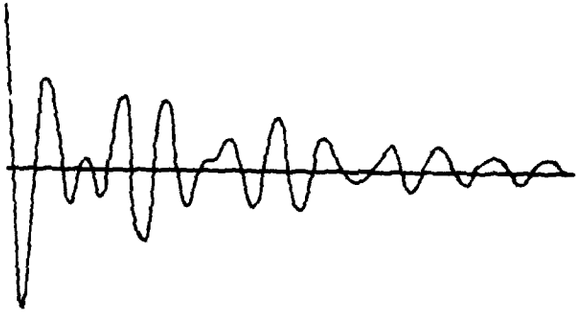

Station 4

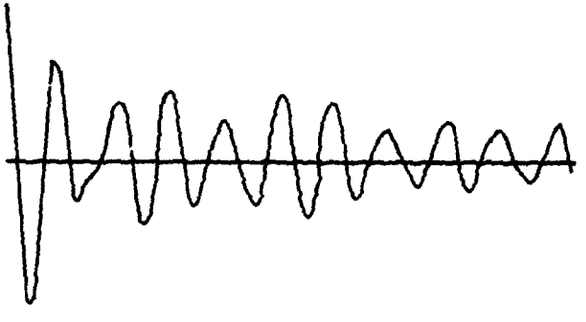

Station 1

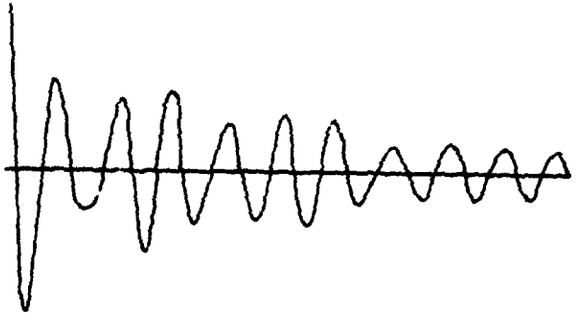

Station 3

Figure 58.- Standard signatures taken at symmetrical locations on Beam No. ., Shaker at B.

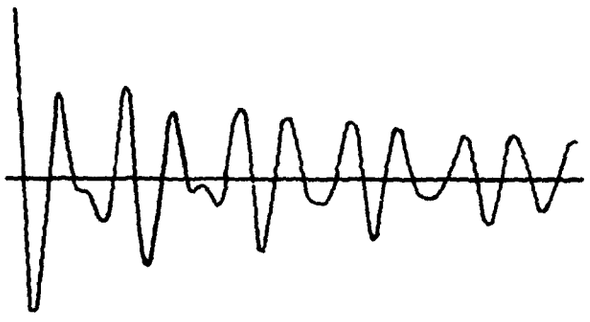

Station 6

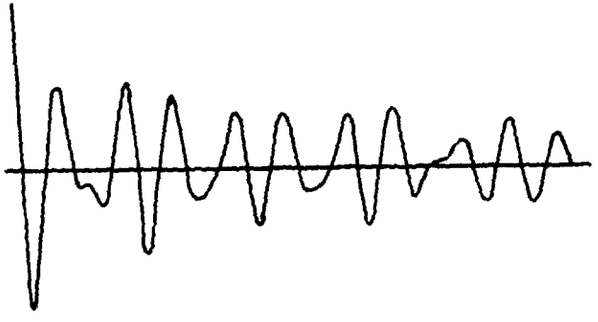

Station 8

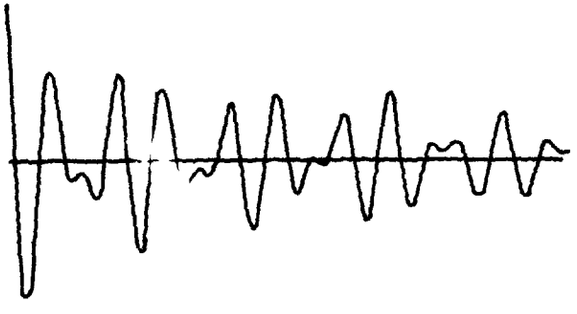

Station 5

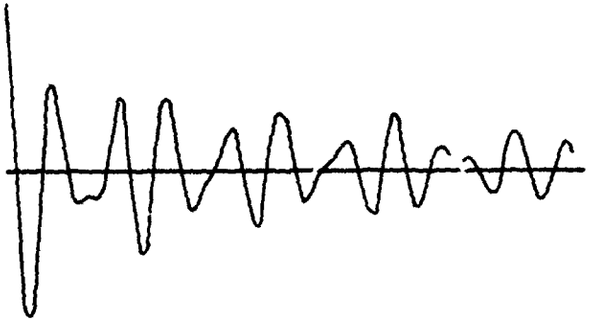

Station 7

Figure 59.- Standard signatures taken at symmetrical locations on Beam No. 2, Shaker at B.

Station 5, Standard.

Station 5, C clamp added.

Figure 60.-- Effect of adding a C clamp on gusset plate near Station 5 on field bridge.